5-13-2011

Design and Synthesis of a New Class of Self-Cross-Linked Polymer Nanogels

Siriporn Jiwpanich
University of Massachusetts Amherst

DESIGN AND SYNTHESIS OF A NEW CLASS OF SELF-CROSS-LINKED POLYMER NANOGELS

A Dissertation Presented

by

SIRIPORN JIWPANICH

Submitted to the Graduate School of the
University of Massachusetts Amherst in partial fulfillment
of the requirements for the degree of

DOCTOR OF PHILOSOPHY

May 2011

Chemistry

DESIGN AND SYNTHESIS OF A NEW CLASS OF SELF-CROSS-LINKED POLYMER NANOGELS

A Dissertation Presented

by

Siriporn Jiwpanich

Approved as to style and content by:

_____
Sankaran Thayumanavan, Chair

_____
Craig T. Martin, Member

_____
Richard W. Vachet, Member

_____
Susan C. Roberts, Member

_____
Craig T. Martin, Department Head
Chemistry Department

DEDICATION

To my parents

ACKNOWLEDGMENTS

I would like to take this opportunity to express my sincere gratitude to those who have helped and supported me to make this dissertation possible.

I am grateful to my advisor, Professor Sankaran Thayumanavan (Thai), for his training, guidance, and support throughout my doctoral degree. I appreciate the opportunity he has given me to be a part of his research group, the freedom to execute my own ideas, and his guidance to help me to develop the ability to think scientificly. I really appreciate his full effort and patience in training me to be an independent scientist. Professor Thai's guidance and support has helped me to build my confidence and has prepared me to step into my future career.

I would also like to extend my gratitude to my committee members, Professor Craig Martin, Professor Richard Vachet, and Professor Susan Roberts, for their valuable suggestions and support.

I remain grateful to Professor Mongkol Sukwattanasinitt, my former advisor at Chulalongkorn University, Thailand for his support and inspiration that has keept me following my Ph.D dream. Without his advice I would not have made it this far.

I would also like to take this opportunity to thank all former and present Thayumanavan research group members for their kind co-operation and friendship. I have enjoyed working and discussing both scientific and nonscientific topics with all of you.

I would like to acknowledge my collaborators, whom have helped me with my research: Dr. Britto Sandanaraj, who helped me to set up my first project and guided me to develop my research skills; Dr. Ja-Hyoung Ryu, Mr. Sean Bickerton, Mr. Reuben

Chacko, Dr. Byron Collins, Dr. Prakash Babu, Mr. Jiaming Zhou, a wonderful nanogel project team. It has been a great experience working with all of you. Thank you all for your tremendous help in my research work.

I would like to express my special thanks to Dr. Kothandam Krishnamoorthy, Dr. Malar Azagarsamy, Dr. Tejaswini Kale, Ms. Andrea Della Pelle, Ms. Nagamani Chikkannagari, Mr. Reuben Chacko, Mr. Bhooshan Popere, Mr. Sean Bickerton, and Mr. Krishna Reddy Raghupathi for your valuable suggestions on my publications and presentations and for discussions on my research.

I thank my class-mates at Umass-Amherst for sharing a fun and frustrating time while pursuing our Ph.D.'s together. I have had an amazing time with you guys. Thank you for your friendship and I will forever have great friends in you.

Finally, I could not have done this and be me today without the support and care of my family and friends. To my parents: your unconditional love and support keep me up and walking through this long journey. I want you to be proud of your daughter and I will bring this Ph.D. back to be yours. To Tan: I have spent a great time with you here. Thank you for your care and friendship, listening and making me smiles, being with me while I am sad and upset. You are not just a roommate or a friend, but a part of my family. To my Thai friends in Amherst: although we are a small group, we have a big friendship and always will. Thank you for sharing smiles, food, and parties that make us not feel lonely while we all are away from home. To my friends: your support and motivation are a great therapy when I almost gave up. Thank you for your friendship and being my great friends.

ABSTRACT

DESIGN AND SYNTHESIS OF A NEW CLASS OF SELF-CROSS-LINKED POLYMER NANOGELS

MAY 2011

SIRIPORN JIWPANICH

B.Sc., CHULALONGKORN UNIVERSITY

M.Sc., CHULALONGKORN UNIVERSITY

Ph.D., UNIVERSITY OF MASSACHUSETTS AMHERST

Directed by: Professor Sankaran Thayumanavan

The design and engineering of nanoscopic drug delivery vehicles that stably encapsulate lipophilic drug molecules, transport their loaded cargo to specific target sites, and release their payload in a controlled manner are of great interest in therapeutic applications, especially for cancer chemotherapy. This dissertation focuses on chemically cross-linked, water-soluble polymer nanoparticles, termed nanogels, which constitute a promising scaffold and offer the potential to circumvent encapsulation stability issues. A facile synthetic method for a new class of self-cross-linked polymer nanogels, synthesized by an intra/intermolecular disulfide cross-linking reaction in aqueous media, is described here. This simple emulsion-free method affords noncovalent lipophilic guest encapsulation and surface functionalization that may allow for targeted delivery. The encapsulation stability of lipophilic molecules sequestered within these nanoscopic containers is evaluated by a fluorescent resonance energy transfer (FRET) based method developed by our research group. We demonstrate that the encapsulation stability of

noncovalently encapsulated guest molecules in disulfide cross-linked polymer nanogels can be tuned and that guest release can be achieved in response to a biologically relevant stimulus (GSH). In addition, varied hydrophobicity in the self-cross-linked nanogels affects the lipophilic loading capacity and encapsulation stability. We reveal that optimal loading capacity is limited by encapsulation stability, where over-loading of lipophilic molecules in the nanoscopic containers may cause undersirable leakage and severely compromise the viability of such systems for drug delivery and other biological applications.

TABLE OF CONTENTS

LIST OF TABLES

LIST OF FIGURES

Figure Page

LIST OF SCHEMES

Scheme Page

LIST OF CHARTS

Chart Page

CHAPTER 1

INTRODUCTION

The engineering and manufacturing of materials at the atomic and molecular scale, so called "nanotechnology" are of great interest for several applications, especially nanomedicine.(Allen and Culis 2004; Wagner, Dullaart et al. 2006) Nanotechnology has the potential to revolutionize cancer diagnosis and therapy bringing new hope to patients. This technology can be applied to drugs that are poorly water-soluble and therefore cannot be administered via the preferred route, or in some cases, at all.

Among the current cancer therapies, including surgical intervention, radiation and chemotherapeutic drugs, chemotherapy seems to be the primary method for cancer treatment. However, the bioavailability of these drugs is limited due to their hydrophobicity which requires a specific mode of delivery and higher doses. Moreover, lack of control and specific targeting of these drugs often kills healthy cells and causes toxicity to the patient. Therefore, the development of a nanoscale targeting approach is required for delivery of chemotherapeutic agents which can selectively accumulate at the target tumor site. In this chapter, we briefly review the class of nanoscopic targeting drug delivery vehicles, particulary for cancer therapy, in term of structural design for lipophilic drug encapsulation and release.

1.1 Passive and Active Targeting Drug Delivery

Targeting mechanisms can be broadly classified into two categories, *viz*. active and passive. Passive targeting is based on the propensity of nanoscopic objects of 10-

200 nm size to extravasate into solid tumor tissues and prevent lymphatic drainage, the so-called enhanced permeation and retension (EPR) effect (Figure 1.1).(Matsumura and Maeda 1986) Early clinical data has shown that therapeutic nanoparticles can enhance efficacy in terms of improving pharmacokinetic and pharmacodynamics profiles, reducing side effects, and targeting for specific diseases.(Peer, Karp et al. 2007; Davis, Chen et al. 2008; Lee, Song et al. 2010) Thus the development of nanoparticles gains more attention, particularly for drug delivery applications which account for three-quarters of all research activities and the nanomedicine market, especially in cancer chemotherapy.(Wagner, Dullaart et al. 2006; Farokhzad and Langer 2009)

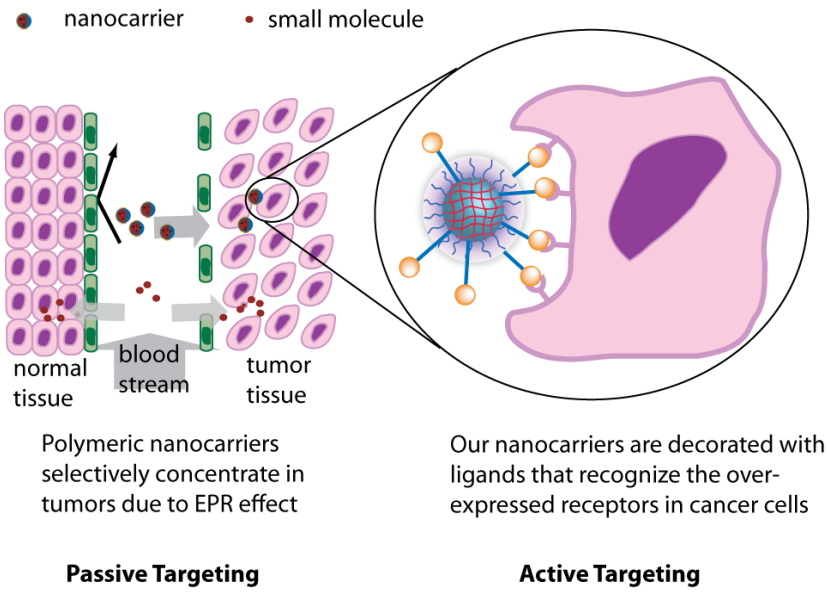

Figure 1.1: Cartoon represention of passive and active targeting mechanisms.

Although the passive targeting approach is the primary mechanism for chemotherapeutic delivery, there are still some limitations. One is that the drug may not diffuse efficiently and the random nature of the approach makes it difficult to control the drug uptake pathway. This may cause multiple-drug resistance (MDR), a situation

where the chemotherapy treatments fail due to the resistance of cancer cells towards one or more drugs.(Gottesman, Fojo et al. 2002; Ferrari 2005; Peer and Margalit 2006) MDR occurs because integral membrane proteins, known as MDR transporters, overexpressed on the surface of cancer cells can expel drugs from the cells which cause a lowering in the therapeutic effect and thus the cancer cells soon develop resistance to a variety of drugs.(Gottesman, Fojo et al. 2002)

An alternative route to achieve cancer drug delivery and avoid the MDR effect is to engineer the nanocarriers in such a way that they have specific binding to the tumor cell surfaces which can facilite the internalization of nanocontainers and diffusion of the drug into cancer cells. This can be accomplished by conjugating nanocontainers, with encapsulated cancer therapeutics, to specific ligands that are complementary to the receptors overexpressed on a tumor cell surface, so called active targeting approach (Figure 1.1). These targeting ligands enable nanoparticles to bind specifically to cell-surface receptors and can enter cells by receptor-mediated endocytosis before the drug is released. Recent works comparing non-targeting and targeting nanoparticles have shown that targeted ligands play an important role in the enhancement of cellular uptake into cancer cells.(Torchilin 2005; Bartlett, Su et al. 2007; Peer, Karp et al. 2007) For example, folate receptor-mediated cell uptake of doxorubicin-loaded liposomes into an MDR cell line has shown to be unaffected by P-glycoprotein (Pgp)-mediated drug efflux.(Goren, Horowitz et al. 2000)

1.2 Nanoscopic Drug Delivery

Nanoscopic drug delivery vehicles are nanosized materials, with 10-200 nm diameters, that can carry lipophilic drugs and release them at a specific target site. Since

the small molecule chemotherapeutics are water-insoluble and highly toxic due to the indiscriminate access to both healthy and cancerous cells, the versatile nanoscopic drug delivery vehicles, an alternative route to administer these drugs, should exhibit a few key characteristics: (*i*) the delivery vehicle should have a desirable and tunable particle size for the EPR effect; (*ii*) the nanocontainers should be able to incorporate lipophilic drug molecules and enhance the the aqueous solubility of these drugs; (*iii*) the nanocarriers should prevent the drug from degradation processes and premature release before they reach the target tumor site; (*iv*) the effective delivery vehicles should be able to cross biological barriers and release the drug into the tumor cells.(Davis, Chen et al. 2008)

To date there have been some nanoscopic drug delivery vehicles which are clinically approved and several more that are under clinical investigation and development.(Peer, Karp et al. 2007) In this chapter, we briefly review the family of nanocarriers including polymer-lipophilic drug conjuagates, metallic nanoparticles, dendrimers, liposomes, micelles, and polymeric cross-linked nonoparticles or nanogels.

1.2.1 Polymer-Drug Conjugates

The polymer-conjugated anticancer drug concept was introduced by Ringsdorf in 1975.(Ringsdorf 1975) This was considered the beginning of an era for the development of polymer therapeutics. Polymer-drug conjugates consist of a biocompatible polymeric carrier with attached low-molecular weight biologically active molecules through a bioresponsive or cleavable linker. By using this method, not only can a drug be covalently linked to the polymer backbone, but also a targeting ligand can be attached, as a guiding agent, onto the same polymer as shown in Figure 1.2. The

release of the drug can be achieved by triggering the appropriate linkers which can respond to changes in the physical and biological environments, such as temperature, pH, and the presence of enzymes or proteins at the target site.(Rodrigues, Beyer et al. 1999; Gillies, Goodwin et al. 2004; Kim, Gil et al. 2006; Schmid, Chung et al. 2007; York, Kirkland et al. 2008; Liu, Maheshwari et al. 2009; Miller, Erez et al. 2009) The polymer-drug conjugates have become a fast-growing field because they have demonstrated several advantages over the corresponding parent drugs by (*i*) enhancing the solubility of hydrophobic drugs; (*ii*) enhancing therapeutic efficacy; (*iii*) reducing the toxicity; and (*iv*) increasing plasma half-life and volume distribution.(Li and wallace 2008)

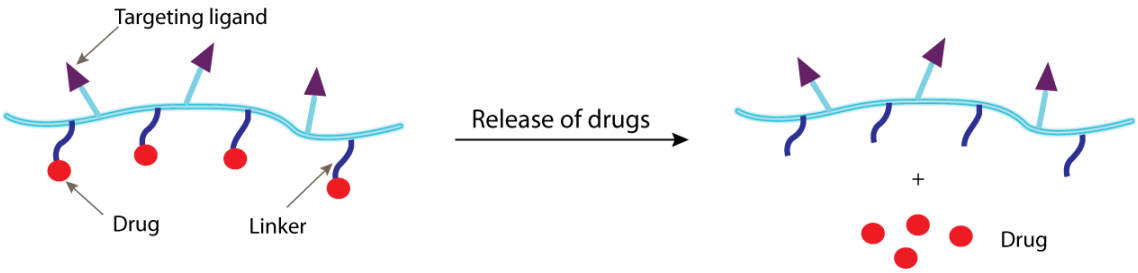

Figure 1.2: Cartoon representation of polymer-drug conjugates.

Early studies on polymer-drug conjugates by Duncan, Kopecek, and Ringdorf in the late 1970s resulted in the first polymer-drug conjugates to be used for medical treatment.(Duncan; Duncan and Kopecek 1984; Duncan 2006) Polymer-protein conjugates are the first practical use of polymer therapeutics as anticancer agents. SMANCS, a conjugate consisting of the anti-tumor protein neocarzinostatin (NCS) covalently linked to two styrene maleic anhydride (SMA) polymer chains(Iwai, Meada et al. 1984; Duncan 2006) and a PEGylated protein was introduced into clinical trial in the early 1990s.(Davis 2002; Duncan 2003; Harris and Chess 2003) To date, polymer-

protein conjugates are used routinely as anticancer therapeutics as an adjunct to chemotherapy.(Duncan 2003) Currently, more than 14 polymer-drug conjugates are in Phase I or II clinical trials, for example, anti-endothelial immunoconjugates, fusion proteins, and caplostatin, the first polymer-angiogenesis inhibitor conjugate.(Arap, Pasqualini et al. 1998; Schraa, Kok et al. 2002; Satchi-Fainaro, Puder et al. 2004; Peer, Karp et al. 2007; Sanchis, Canal et al. 2010)

Among these, the most advanced conjugate is Opaxio® (poly-*L*-glutamic acid-paclitaxel conjugate (PG-TXL)), formerly known as Xyotax® from Cell Therapeutics Inc., which is expected to reach the market in the near future.(Li and wallace 2008) In PG-TXL, paclitaxel is conjugated to a synthetic poly(*L*-glutamic acid) through its 2'-hydroxyl group via an ester linkage (Chart 1.1). The resulting conjugate is highly water soluble (>20mg/kg) and has demonstrated significant enhanced antitumor efficacy and improved safety compared with paclitaxel in preclinical studies.(Li and wallace 2008)

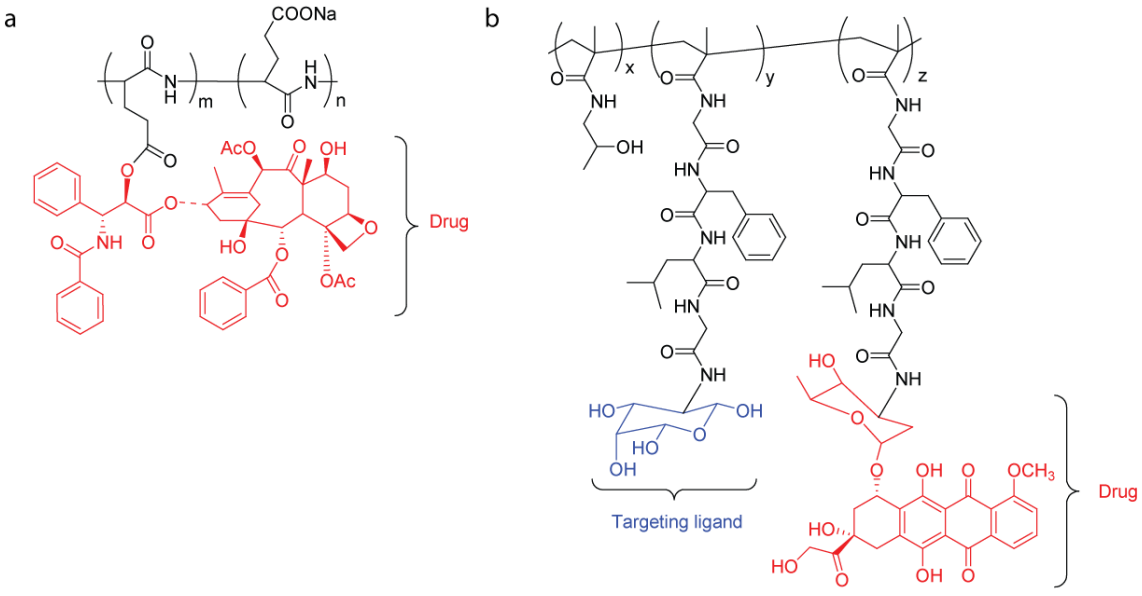

Chart 1.1: Structures of polymer-drug conjugates: a) Opaxio®; b) PK2.

HPMA copolymer-doxorubicin (Dox)-galctosamine conjugate, PK2, is the only polymer-drug conjugate based on active targeting (Chart 1.1). PK2 is a 27 kDa HMPA copolymer derivatized with 6.5% mol/wt, <2% free doxorubicin, and 2% mol/wt galactose, with efficient targeting of the asialoglycoprotein receptor selectively expressed on hepatocytes and in hepatomas.(Li and wallace 2008)

Nonetheless, the polymer-drug conjugates often have different pharmacokinetic profiles from the parent drugs, and are thus considered new chemical entities (NCEs).(Peer, Karp et al. 2007) Although there are a variety of novel drug targets and sophisticated chemistries available, only four drugs (doxorubicin, camptothecin, paclitaxel, and palatinate) and four polymers (*N*-(2-hydroxylpropyl)methacrylamide (HPMA) copolymer, poly-*L*-glutamic acid, poly(ethylene glycol) (PEG), and Dextran) have been repeatedly used to develop polymer-drug conjugates.(Duncan 2003; Peer, Karp et al. 2007) This is because significant chemistry is needed to develop an appropriate linker between the drug and the polymer backbone that can be cleaved to release the drug molecules. Another barrier is the limit of the loading capacity due to the lipophilic drug molecules attached to the polymer chain which dictate the carrier solubility.

1.2.2 Metallic Nanoparticles

Metallic nanoparticles are of great interest for nanoscopic drug delivery due to the fact that their sizes are controlled by the metal core, affording their production with near monodisperisty (Figure 1.3).(Peer, Karp et al. 2007) The surface of the metal core can be tailored by incorporating desired functionalities or ligands to facilitate the active targeting mechanism. Metallic nanoparticles, particularly gold nanoparticles have

recently been developed for cancer drug delivery.(Duncan, Kim et al. 2010) Some metal nanoparticles have been used for magnetic resonance imaging providing an opportunity to design nanocarriers which have both imaging and therapy characteristics.

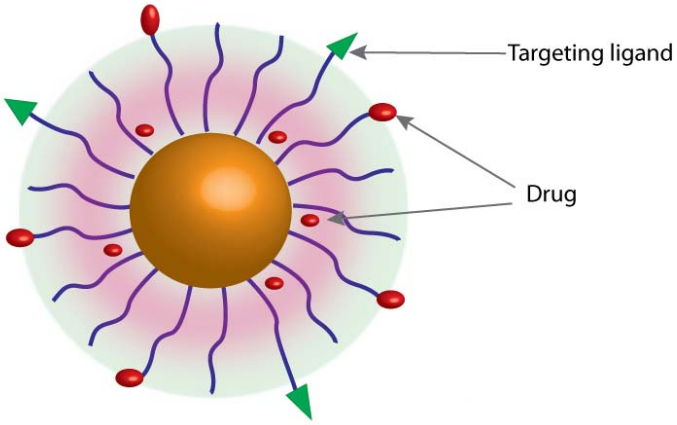

Figure 1.3: Cartoon representation of metallic nanoparticle.

Hydrophobic drugs can be loaded onto metallic nanoparticles through non-covalent interactions or covalent conjugation to the particles via cleavabale linkages similar to those described in the polymer-drug conjugation systems. The encapsulation of lipophilic drugs into the monolayer of the metallic nanoparticle can be achieved by the incorporation of appropriate ligands on the metal shell to provide hydrophobic interaction between the drug and ligands. Rotello *et al*. have reported a biocompatible gold nanoparticle with a 2.5 nm core modified with an alkanethiol interior and a tetra(ethylene glycol) (TEG) hydrophilic shell for cancer drug delivery.(Kim, Ghosh et al. 2009)

However, inorganic nanoparticles may not provide advantages over other types of nanoscopic drug deliveries for systemic targeting of individual cancer cells because

they are not biodegradable or small enough to be cleared easily, resulting in potential accumulation in the body, which may cause long-term toxicity. In addition, the drug molecules attached to the surface of the particles or loaded onto their monolayer surface limit the solubility of the drug-loaded scaffolds in aqueous media, as these drugs are lipophilic and surface functionalities dictate the solubility of these metallic nanoparticles.

1.2.3 Dendrimers

Dendrimers are synthetic, branched macromolecules that form a tree-like structure with well-controlled structural architecture that show promise in several biomedical applications.(Fréchet and Tomalia 2001) Dendrimers are considered as a new class of polymers having been first published in the late 1970s and early 1980s.(Buhleier, Wehner et al. 1978; Newkome, Yao et al. 1985; Tomalia, Dewald et al. 1985) A dendrimer is composed of focal point or core, branches or intermedediate layers, and surface groups or the periphery as shown in Figure1.4. Since dendrimer synthesis can be achieved in a stepwise fashion, they are theoretically monodisperse in size and highly reproducible. These characteristics make dendrimers interesting candidates for drug delivery scaffolds because they should also provide reproducible pharmacokinetic behavior.(Newkome, Yao et al. 1985; Tomalia, Dewald et al. 1985; Hawker and Fréchet 1990; de Brabander-van den Berg and Meijer 1993) Traditional polymer systheses result in polymers which are polydisperse making the pharmacokinetics of these polymers varied and lack control and reproducibility.

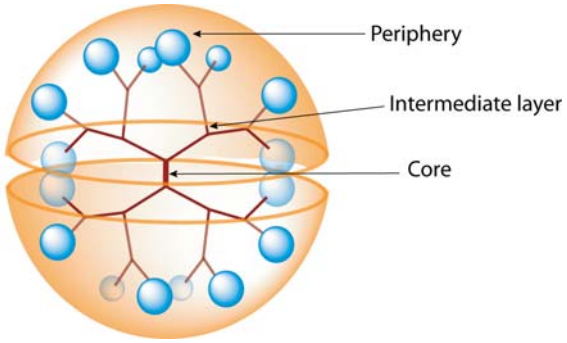

Figure 1.4: Cartoon representation of dendrimer structure.

There are several classes of dendrimers that have been reported for biological applications, *e.g.* polyamidoamines, polyamines, polyamides (polypeptides), poly(aryl ethers), polyesters, carbohydrates, and DNA.(Lee, MacKay et al. 2005) Amongst these scafolds, polyamidoamine (PAMAM) dendrimers, structure shown in Chart 1.2, are commercially available with a variety of generations and peripheral functionalities and are the most widely used dendrimer scaffolds for biological applications. However, they exhibit significant toxicity due their multiple cationic amine groups at the scaffold surface. To date, there are several classes of dendrimers that have been developed which are highly biocompatible and water soluble.(Gillies and Fréchet 2005)

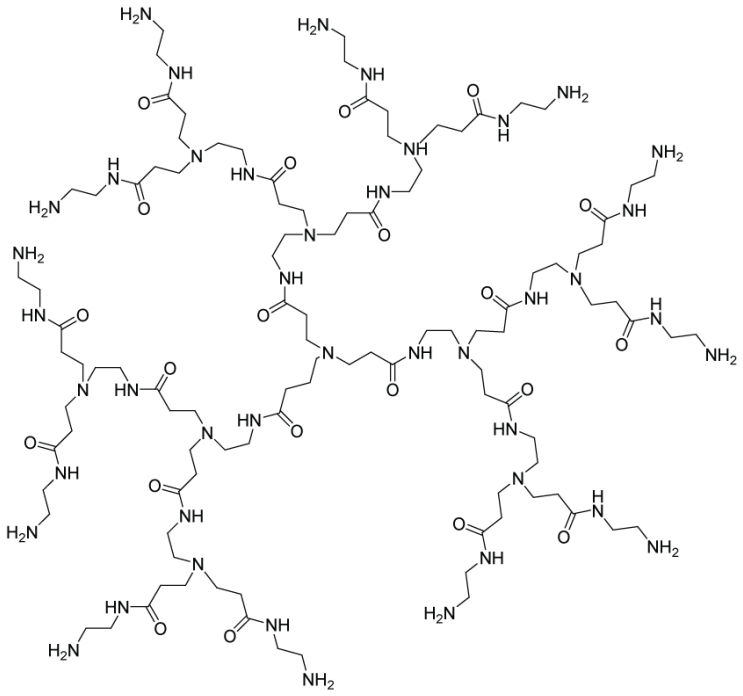

Chart 1.2: Structure of polyamidoamine (PAMAM) dendrimers.

Initial studies of dendrimers, as potential drug delivery scaffolds, focused on their use as unimolecular micelles for noncovalent encapsulation of drug molecules. Because of their highly branched structures at high molecular weighs, they show nanometer size scaffolds which are globular in shape and provide a pocket for hydrophobic molecule encapsulation. The advantage of unimolecular micelles is that their micelle structure is maintained at all concentrations (no CMC). However, it is difficult to control the release of the drugs and they have less encapsulation stability.

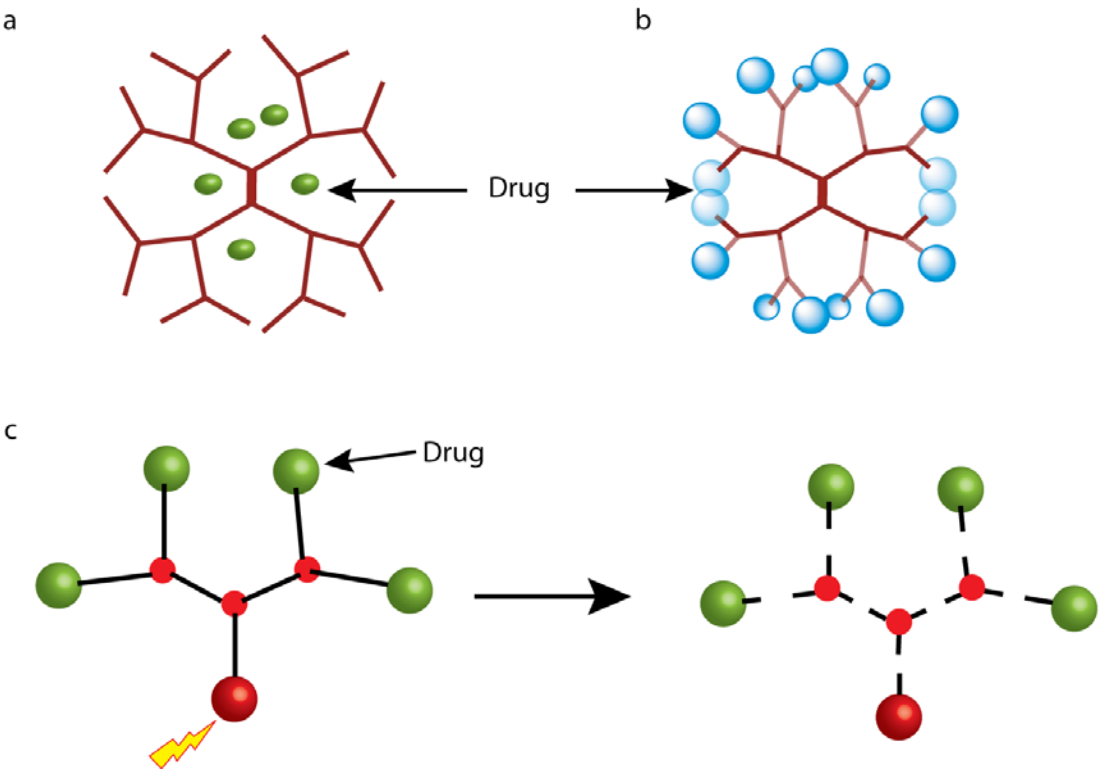

Figure 1.5: Cartoon representation of dendrimers as drug delivery scaffolds: a) unimoleculear micelle; b) drug conjugated; c) self-immolative.

An alternative approach to the development of dendrimers as drug delivery containers is to covalently link the drug molecules to the dendrimer scaffold. The stepwise syntheses of dendrimers provide scaffolds with a well-defined number of peripheral groups. The controlled multivalency of dendrimers can be used to attach several drug molecules, targeting groups, and solubilizing groups to the periphery in a well-controlled manner. The release of the drug can be controlled by incorporating degradable linkages between the drug molecule and dendrimers. For example, cisplatin, a potent anticancer drug with nonspecific toxicity and poor water solubility, was attached to the periphery of a G-4 carboxylate-terminated PAMAM dendrimer.(Malik, Evagorou et al. 1999) The dendrimer-drug conjugates show increased solubility, decreased systematic toxicity, and selective accumulation in solid tumor. PAMAM

dendrimers have also been used as antitumor targeted carriers of methotrexate.(Kukowska-Latallo, Candido et al. 2005) The amine groups at the periphery of G-5 PAMAM dendrimers were modified with acetyl groups to reduce their surface charge. The actylated PAMAM was subsequently functionalized with folate, as a target ligand, fluorescein fluorophore, and methotrexate. In vivo delivery of dendrimer-methotrexate conjugates, using multivalent targeting, results in a tenfold reduction in tumor size compared with that achieved with the same molar concentration of free systemic methotrexate.(Kukowska-Latallo, Candido et al. 2005; Hong, Leroueil et al. 2007) This work provided motivation for further pre-clinical development, and a variety of dendrimers are now under investigation for cancer treatment.

Recently, degradable dendrimers known as self-immolative, cascade-release or geometrically disassembling dendrimers have been reported. In these dendrimers, a single chemical reaction at their core or periphery initiates their complete depolymerization into small, structurally similar units.(Amir, Pessah et al. 2003; de Groot, Albrecht et al. 2003; Li, Szalai et al. 2003; Szalai, Kevwitch et al. 2003) This intelligent structural design could be a potential candidate for future delivery vehicles.

However, dendrimers are expensive and require complex synthetic methods which will bring difficulties for large-scale production. The unique properties of dendrimers could be useful in practical term, but the optimization of structure and properties to maximize drug bioavailability and targeting to the tumor cell need to be improved and further investigated.

1.2.4 Liposomes

Liposomes, nanosized lipid vesicles, first described in the 1960s, are another nanoscopic drug delivery vehicle that has shown significant promise in drug delivery technology.(Bangham, Standish et al. 1965; Gabizon 2001; Gabizon 2001; Torchilin 2005) This is because of their components which comprise of natural substances that are biocompatible, biodegradable and nontoxic. Liposomes consist of lipid bilayers with a size of ~100 nm and larger (Figure 1.6). Liposomes carrying chemotherapeutic small-molecule drugs have been approved for cancer treatment since the mid-1990s.(Peer, Karp et al. 2007) However, since liposomes have hydrophilic interiors, these assemblies are primarily used for hydrophilic drug molecules. For example, the water-soluble salt of Dox has been successfully formulated with liposomes (e.g. Doxil).(Safra, Muggia et al. 2000; Bao, Goin et al. 2004) In addition, liposomes do not provide controlled release capability and have low circulation time due to phagocytosis, a process by which phagocytes remove foreign materials.(Torchilin 2005; Peer, Karp et al. 2007)

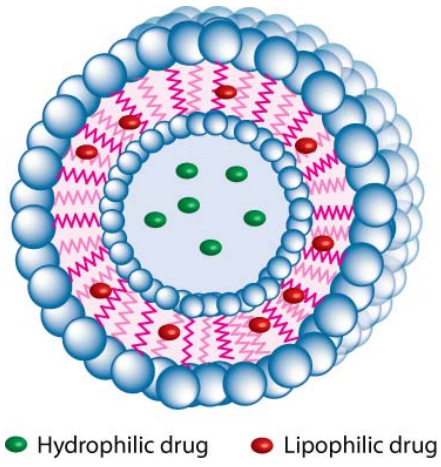

Figure 1.6: Cartoon representation of liposomes.

Cell specific targeting of liposomes was first described in 1980 and the first improved long circulating liposomes were described in 1987 and later named "Stealth liposomes".(Leserman, Barbet et al. 1980; Allen and Chonn 1987) Poly(ethylene glycol) (PEG) was first introduced in the early 1990s to modify the surface of liposomes for improved pharmacokinetics (PK) after intravenous (i.v.) administration. Subsequently, the use of polyethylene glycol (PEG) was shown to increase circulation times for liposomes.(Klibanov, Maruyama et al. 1990) However, the long circulation time of liposomes may cause extravasation of the drug in unexpected sites and lead to severe side effects. Palmar-plantar erythrodysesthesia (PPE), also called the hand-foot syndrome, is a dermatologic toxicity reaction seen with high doses of many types of chemotherapy. It is the most common clinical side effect from the PEGylated liposomal doxorubicin.(Peer, Karp et al. 2007)

Although chemotherapeutic drugs formulated with liposomes make up most of the primary delivery systems on the market, the lack of controlled release properties of encapsulated drugs, fast oxidation of some phospholipids, and high production cost need to be improved. Additionally, the liposome interior is not suitalble for encapsulating lipophilic molecules.

1.2.5 Micelles

Polymeric micelles (5-100 nm) have been of great interest as a versatile nanomedicene platform, especially for cancer therapeutic applications due to their ability to encapsulate poorly water-soluble chemotherapeutic agents in their lipophilic interior.(Kataoka, Harada et al. 2001; Torchilin 2004; Sutton, Nasongkla et al. 2007; Kale, Klaikherd et al. 2009) Micelles consist of self-assembling small molecule

surfactants or amphiphilic polymers exibiting phase separatation between hydrophobic and hydrophilic segments to form nanoscopic supramolecular core/shell structures (Figure1.7). Its hydrophobic core provides lipophilic drug encapsulation, while the hydrophilic shell provides solubility in aqueous media. Currently, five micellar formulations for anticancer therapy are under clinical evalulation, of which Genexol-PM has been FDA approved for use in patients with breast cancer. An early phase of clinical trials has shown that the cancer drug-polymer micelle formulation can enhance the aqueous solubility and prolong their in vivo half-lives with lessened systemic toxicity.(Oerlemans, Bult et al. 2010) Free doxorubicin (Dox) has an elimination phase half-life ($t_{1/2,\ \beta}$), or physiological excretion half-life, of 48 min, while the polymer micelle formulation has roughly triple the half-life, bringing it in the range of 2.3-2.8h.(Sutton, Nasongkla et al. 2007)

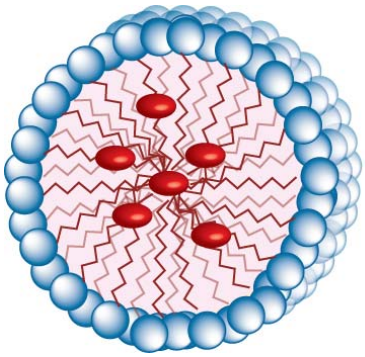

Figure 1.7: Cartoon representation of micelles.

Though, micellar assemblies formed from small molecule surfactants have inherent stability issues. Small molecule surfactants can assemble to form micelles when the concentration is above the critical micelle concentration (CMC). The assemblies formed from amphiphilic block copolymers tend to exhibit enhanced stabilities.(Gu, Zhang et al. 2008) In the late 1980s, Kazunori Kataoka and Alexander

Kabanov independently developed the used of block copolymer micelles for drug delivery. To date several micellar formulations of anticancer agents are in clinical trials. However, these still face significant complications because of a requisite concentration for assembly formation. This drastically limits the practicality of *in vivo* micelle utilization, as large dilution of injected micelles into the body can destabilize these self-assembling systems, causing undesirable release of the encapsulated drug payload before arrival at the target site.(Bae and Yin 2008) Moreover, the interaction between micelles and biological components, such as cellular membranes and blood components, can lead to release of the cargo from the micelle core at undesirable locations.(Chen, Kim et al. 2008; Chen, Kim et al. 2008) Therefore, alternate strategies are required to overcome such premature release.

1.2.6 Cross-Linked Polymer Nanoparticles

Cross-linked polymer nanoparticles or nanogels have recently been introduced as an alternative class of nanoscopic drug delivery vehicles.(Oh, Drumright et al. 2008; Kabanov and Vinogradov 2009; Vinogradov 2010) Recent studies suggest that nanogels are very promising for future biomedical applications due to their tunable chemical and three-dimensional (3D) physical structure, good mechanical properties, high water content, and biocompatibility. Nanogels are nanosized hydrogel networks that disperse in aqueous solution and are composed of hydrophilic or amphiphilic polymer matrices that are cross-linked by a physical or chemical cross-linking agent (Figure 1.8).(Kabanov and Vinogradov 2009) Like hydrogels, nanogels are three-dimensional (3D) biocompatible material with high water content. These 3D structures allow the

entrapment of large amount of bioactive molecules with high encapsulation stability in their networks.(Jiwpanich, Ryu et al. 2010)

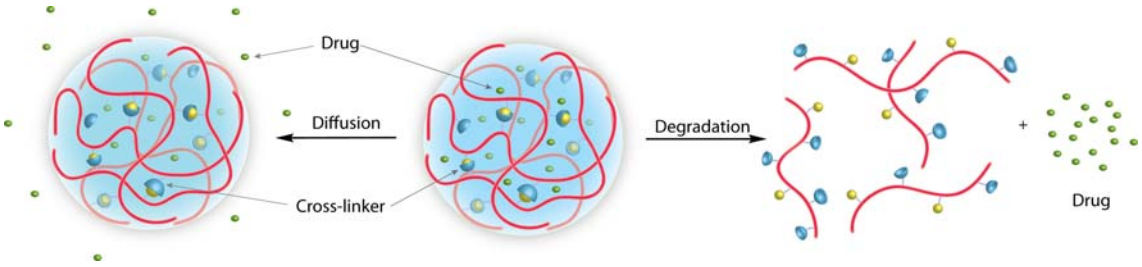

Figure 1.8: Cartoon representation of nanogels and the mechanism of drug release.

The polymeric cross-linked nanoparticles, first introduced by Sunamoto *et al.* in 1993, were nanosized swollen aggregates of cholesterol-modified polysaccharide (pullulan) for delivery of insulin.(Akiyoshi, deguchi et al. 1993) Nonetheless, the term "nanogel" was first introduced by Kabanov and Vinogradov to define cross-linked bifunctional networks of cationic and neutral polymers such as the branched PEG-cross-linked-PEI made from polyethylenenimine (PEI) and poly(ethylene glycol) (PEG) for delivery of polynucleotides.(Vinogradov, Bronich et al. 2002; Kabanov and Vinogradov 2009)

Nanogels are very promising in drug delivery applications due to their large loading capacity with high encapsulation stability and responsiveness to environment factors, for example, ionic strength, pH, temperature, and the presence of enzymes or proteins.(Kabanov and Vinogradov 2009) Loading of biological agents can be achieved by electrostatic, van der Waals and/or hydrophobic interactions between the encapsulated agents and the polymer matrix. As a result, the nanogels collapse forming stable nanoparticles, in which biological/drug compounds are entrapped. In addition, the large surface area of nanogels can be tailored with targeting ligands to enhance active

targeted nanocarrier characteristics. In order to control the release of therapeutics over a desired period of time, as well as enable the removal of the empty device after drug release, (bio)degradable linkages such as esters, peptides, acetals, disulfides, and hydrazones can be introduced into cross-linked networks.(Kabanov and Vinogradov 2009; Oh, Bencherif et al. 2009)

Although the early developments of nanogels were aimed at the transport of biomacromolecules, recently significant progress has been reported for the delivery of small therapeutic agents. For example, N-hexylcarbamoyl-5-fluorouracil, an anticancer prodrug of 5-fluorouracil (5-FU), encapsulated in poly(N-isopropylacrylamide)-co-poly(N-vinylpyrrolidone) (PNIPAAm/VP) nanogels coated with polysorbate 80 showed enhanced therapeutic efficacy against parasites as well as reduced hepatotoxicity and nephrotoxicity compared to the free drug.(Tyagi, Lala et al. 2005; Soni, Babber et al. 2006)

Since nanogels are relatively new to the area of nanoscopic drug delivery, the synthetic methodologies for their preparation still need to be developed. The classical preparations, microemulsion and inverse microemulsion methods, do not facilitate the nanogels to be both water-soluble and encapsulate lipophilic guest molecules simultaneously.(Oh, Siegwart et al. 2007; Oh, Tang et al. 2007; Bachelder, Beaudette et al. 2008; Sisson, Steinhiber et al. 2009; Ryu, Jiwpanich et al. 2010) Furthermore, present and future nanogel applications require a high degree of control over several properties. These properties include stability for prolonged circulation in the blood stream, novel functionality for further bioconjugation, controlled particle size with

uniform diameter, and biodegradability for sustained release of the drug for a desired period of time and facile removal of empty devices.

1.3 Summary and Dissertation Overview

In this chapter, we have discussed the classical nanoscopic drug delivery vehicles for cancer therapy using their nanosize characteristics to transport lipophilic drugs through cancer cells by passive targeting through EPR effect. The drug-loaded nanoscopic carriers we described above can be classified into two categories: covalent incorporation of drugs onto nanoscale scaffolds and noncovalent encapsulation of drugs into nanoscale assemblies. To avoid the modification of parent drugs, which can alter their therapeutic properties, we focus on the noncovalent encapsulation approach. We have also discussed the cross-linked nanoscopic carriers which provide high encapsulation stability and are considered promising nanoscopic drug delivery vehicles.

This dissertation describes a new class of self-cross-linked polymer nanogels as promising nanoscopic drug delivery vehicles for noncovalent encapsulation of lipophilic drugs. A methodology for the preparation of self-cross-linked nanogels is described in Chapter 2. Since the cross-linked polymeric nanoparticles could provide high encapsulation stability over classical supramolecular nanoassemblies, we describe, in Chapter 3, a method development to track the noncovalent encapsulation stability using FRET based methods. In Chapter 4, we detail the tuning of encapsulation stability at maximum loading capacity of lipophilic molecules into self-cross-linked nanogels, and Chapter 5 contains general conclusions and future research directions.

1.4 References

1. Wagner, V.; Dullaart, A.; Bock, A.-K.; Zweck, A., The emerging nanomedicine landscape. *Nat. Biotechnol.* **2006,** *24*, 1211-1217.

2. Allen, T. M.; Culis, P. R., Drug discovery systems: Entering the mainstream. *Science* **2004,** *303*, 1818-1822.

3. Matsumura, Y.; Maeda, H., A new concept of macromolecular therapies in cancer chemotherapy: mechanism of tumortropic accumulation of proteins and the antitumor agent SMANCS. *Cancer Res* **1986,** *6*, 6387-6392.

4. Peer, D.; Karp, J. M.; Hong, S.; Farokhzad, O. C.; Margalit, R.; Langer, R., Nanocarriers as an emerging platform for cancer therapy. *Nat. Nanotechnol* **2007,** *2*, 751-760.

5. Davis, M. E.; Chen, Z.; Shin, D. M., Nanoparticle therapeutics: An emerging treatment modality for cancer. *Nat. Rev. Drug Discovery* **2008,** *7*, 771-782.

6. Lee, S.-M.; Song, Y.; Hong, B. J.; MacRenaris, K. W.; Mastarone, D. J.; O'Halloran, T. V.; Meade, T. J.; Nguyen, S. T., Modular polymer-caged nanobins as a theranostic platform with enhanced magnetic resonance relaxivity and pH-responsive drug release. *Angew. Chem. Int., Ed* **2010,** *49*, 9960-9964.

7. Farokhzad, O. C.; Langer, R., Impact of nanotechnology on drug delivery. *ACS Nano* **2009,** *3*, 16-20.

8. Ferrari, M., Cancer nanotechnology: Opportunities and challenges. *Nat. Rev. Cancer* **2005,** *5*, 161-171.

9. Gottesman, M. M.; Fojo, T.; Bates, S. E., Multidrug resistance in cancer: Role of ATP–dependent transporters. *Nat. Rev. Cancer* **2002,** *2*, 48-58.

10. Peer, D.; Margalit, R., Fluoxetine and reversal of multidrug resistance. *Cancer Lett.* **2006,** *237*, 180-187.

11. Bartlett, D. W.; Su, H.; Hildebrandt, I. J.; Weber, W. A.; Davis, M. E., Impact of tumor-specific targeting on the biodistribution and efficacy of siRNA nanoparticles measured by multimodality in vivo imaging. *Proc. Natl. Acad. Sci. U.S.A.* **2007,** *104*, 15549-15554.

12. Torchilin, V. P., Recent advances with liposomes as pharmaceutical carriers. *Nat. Rev. Drug Discovery* **2005,** *4*, 145-160.

13. Goren, D.; Horowitz, A. T.; Tzemach, D.; Tarshish, M.; Zalipsky, S.; Gabizon, A., Nuclear delivery of doxorubicin via folate-targeted liposomes with bypass of multidrug-resistance efflux pump. *Clin. Cancer Res.* **2000,** *6*, 1949-1957.

14. Ringsdorf, H., Structure and properties of pharmacologically active polymers. *J. Polym. Sci. Symp.* **1975,** *51*, 135-153.

15. Gillies, E. R.; Goodwin, A. P.; Fréchet, J. M. J., Acetals as pH-sensitive linkages for drug delivery. *Bioconjug. Chem.* **2004,** *15*, 1254-1263.

16. Kim, Y. S.; Gil, E. S.; Lowe, T. L., Synthesis and characterization of thermoresponsive-*co*-biodegradable linear-dendritic copolymers. *Macromolecules* **2006,** *39*, 7805-7811.

17. York, A. W.; Kirkland, S. E.; McCormick, C. L., Advances in the synthesis of amphiphilic block copolymers via RAFT polymerization: Stimuli-responsive drug and gene delivery. *Adv. Drug Deliv. Rev.* **2008,** *60*, 1018-1036.

18. Liu, S.; Maheshwari, R.; Kiick, K., Polymer-based therapeutics. *Macromolecules* **2009,** *42*, 3-13.

19. Rodrigues, P. C. A.; Beyer, U.; Schumacher, P.; Roth, T.; Fiebig, H. H.; Unger, C.; Messori, L.; Orioli, P.; Paper, D. H.; Mulhaupt, R.; Kratz, F., Acid-sensitive polyethylene glycol conjugates of doxorubicin: Preparation, in vitro efficacy and intracellular distribution. *Bioorg. Med. Chem.* **1999,** *7*, 2517-7524.

20. Schmid, B.; Chung, D.-E.; Warnecke, A.; Fichtner, I.; Kratz, F., Albumin-binding prodrugs of camptothecin and doxorubicin with an Ala-Leu-Ala-Leu-linker that are cleaved by cathepsin B: Synthesis and antitumor efficacy. *Bioconjug. Chem.* **2007,** *18*, 702-716.

21. Miller, K.; Erez, R.; Segal, E.; Shabat, D.; Satchi-Fainaro, R., Targeting bone metastases with a bispecific anticancer and antiangiogenic polymer-alendronate-taxane conjugate. *Angew. Chem. Int., Ed* **2009,** *48*, 2949-2954.

22. Li, C.; wallace, S., Polymer-drug conjugates: Recent development in clinical oncology. *Adv. Drug Deliv. Rev.* **2008,** *60*, 886-898.

23. Duncan, R., Polymer conjugates as anticancer nanomedicines. *Nat. Rev. Cancer* **2006,** *6*, 688-701.

24. Duncan, B., Drug polymer conjugates-Potential for improved chemotherapy. *Anticancer Drugs 3*, 175-210.

25. Duncan, R.; Kopecek, J., Soluble synthetic-polymers as potential-drug carriers. *Adv. Polym. Sci.* **1984,** *57*, 51-101.

26. Iwai, K.; Meada, H.; Konno, T., Use of oily contrast medium for selective drug targeting to tumour: Enhanced therapeutic effect and x-ray image. *Cancer Res.* **1984,** *44*, 2114-2121.

27. Davis, F. F., The origin of pegnology. *Adv. Drug Deliv. Rev.* **2002,** *54*, 457-458.

28. Harris, J. M.; Chess, R. B., Effect of pegylation on pharmaceuticals. *Nat. Rev. Drug Discovery* **2003,** *2*, 214-221.

29. Duncan, R., The dawning era of polymer therapeutics. *Nat. Rev. Drug Discovery* **2003,** *2*, 347-360.

30. Arap, W.; Pasqualini, R.; Ruoslahti, E., Cancer treatment by targeted drug delivery to tumor vasculature in a mouse model. *Science* **1998,** *279*, 377-380.

31. Schraa, A. J.; Kok, R. J.; Moorlag, H. E.; Bos, E. J.; Proost, J. H.; Meijer, D. K. F.; De Leu, L. F. M. H.; Molema, G., Targeting of RGD-modified proteins to tumor vasculature: A pharmacokinetic and cellular distribution study. *Int. J. Cancer* **2002,** *102*, 469-475.

32. Satchi-Fainaro, R.; Puder, M.; Davies, J. W.; Tran, H. T.; Sampson, D. A.; Greene, A. K.; Corfas, G.; Folkman, J., Targeting angiogenesis with a conjugate of HPMA copolymer and TNP-470. *Nat. Med.* **2004,** *10*, 255-261.

33. Sanchis, J.; Canal, F.; Lucas, R.; Vicent, M. J., Polymer-drug conjugates for novel melecular targets. *Nanomedicine* **2010,** *5*, 915-935.

34. Duncan, B.; Kim, C.; Rotello, V. M., Gold nanoparticle platforms as drug and biomacromolecule delivery systems. *J. Controlled Release* **2010,** *148*, 122-127.

35. Kim, C. K.; Ghosh, P.; Pagliuca, C.; Xhu, Z.-J.; Menichetti, S.; Rotello, V. M., Entrapment of hydrophobic drugs in nanoparticles monolayers with efficient release into cancer cells. *J. Am. Chem. Soc.* **2009,** *131*, 1360-1361.

36. Fréchet, J. M. J.; Tomalia, D. A., *Dendrimers and other dendritic polymers*. John Wiley & Sons: Chichester, New York, USA, 2001.

37. Buhleier, E.; Wehner, W.; Vögtle, F., "Cascade"-and-"nonskid-chain-like" syntheses of molecular cavity topologies. *Synthesis* **1978**, *2*, 155-158.

38. Tomalia, D. A.; Dewald, J.; Hall, J.; Kallos, G.; Martin, S.; Roeck, J.; Ryder, J.; Smith, P., A new class of polymers: Starburst-dendritic macromolecules. *Polym. J.* **1985,** *17*, 117-132.

39. Newkome, G. R.; Yao, Z.; Baker, G. R.; Gupta, V. K., Micelles. Part 1. Cascade molecules: A new approach to micelles. A [27]-arborol. *J. Org. Chem.* **1985,** *50*, 2003-2004.

40. de Brabander-van den Berg, E. M. M.; Meijer, E. W., Poly(propylene imine) dendrimers: Large-scale synthesis by hetereogeneously catalyzed hydrogenations. *Angew. Chem. Int., Ed.* **1993,** *32*, 1308-1311.

41. Hawker, C. J.; Fréchet, J. M. J., Preparation of polymers with controlled molecular architecture: A new convergent approach to dendritic macromolecules. *J. Am. Chem. Soc.* **1990,** *112*, 7638-7647.

42. Lee, C. C.; MacKay, J. A.; Fréchet, J. M. J.; Szoka, F. C., Designing dendrimers for biological applications. *Nat. Biotechnol.* **2005,** *23*, 1517-1526.

43. Gillies, E. R.; Fréchet, J. M. J., Dendrimers and dendritic polymers in drug delivery. *Drug Discovery Today* **2005,** *10*, 35-43.

44. Malik, N.; Evagorou, E. G.; Duncan, R., Dendrimer-platinate: A novel approach to cancer chemotherapy. *Anticancer Drugs* **1999,** *10*, 767-776.

45. Kukowska-Latallo, J. F.; Candido, K. A.; Cao, Z.; Nigavekar, S. S.; Majoros, I. J.; Thomas, T. P.; Balogh, L. P.; Khan, M. K.; Baker, J. R., Nanoparticle targeting of anticancer drug improves therapeutic response in animal model of human epithelial cancer. *Cancer Res.* **2005,** *65*, 5317-5324.

46. Hong, s.; Leroueil, P. R.; Majoros, I. J.; Orr, B. G.; Baker, J. R.; Banaszak Holl, M. M., The binding avidity of a nanoparticle-based multivalent targeted drug delivery platform. *Chem. Biol.* **2007,** *14*, 107-115.

47. Amir, R. J.; Pessah, N.; Shamis, M.; Shabat, D., Self-immolative dendrimers. *Angew. Chem. Int., Ed.* **2003,** *42*, 4494-4499.

48. Szalai, M. L.; Kevwitch, R. M.; McGrath, D. V., Geometric disassembly of dendrimers: Dendritic amplification. *J. Am. Chem. Soc.* **2003,** *125*, 15688-15689.

49. de Groot, F. M. H.; Albrecht, C.; Koekkoek, R.; Beusker, P. H.; Scheeren, H. W., "Cascade-release dendrimers" Liberate all end groups upon a single triggering event in the dendritic core. *Angew. Chem. Int., Ed.* **2003,** *42*, 4490-4494.

50. Li, S.; Szalai, M. L.; Kevwitch, R. M.; McGrath, D. V., Dendrimer disassembly by benzyl ether depolymerization. *J. Am. Chem. Soc.* **2003,** *125*, 10516-10517.

51. Bangham, A. D.; Standish, M. M.; Watkins, J. C., Diffusion of univalent ions across the lamellae of swollen phospholipids. *J. Mol. Biol.* **1965,** *13*, 238-252.

52. Gabizon, A. A., Pegylated liposomal doxorubicin: Metamorphosis of an old drug into a new form of chemotherapy. *Cancer Invest.* **2001,** *19*, 424-436.

53. Gabizon, A. A., Stealth liposomes and tumor targeting: One step further in the quest for the magic bullet. *Clin. Cancer Res.* **2001,** *7*, 223-225.

54. Safra, T.; Muggia, F.; Jeffers, S.; Tsao-Wei, D. D.; Groshen, S.; Lyass, O.; Henderson, R.; Berry, G.; Gabizon, A., Pegylated liposomal doxorubicin (doxil): Reduced clinical cardiotoxicity in patients reaching or exceeding cumulative doses of 500 mg/m^2. *Ann. Oncol.* **2000,** *11*, 1029-1033.

55. Bao, A.; Goin, B.; Klipper, R.; Negrete, G.; Phillips, W. T., Direct 99m Tc labeling of pegylated liposomal doxorubicin (Doxil) for pharmacokinetic and non-invasive imageing studies. *J. Pharcol. Exp. Ther.* **2004,** *308*, 419-425.

56. Leserman, L. D.; Barbet, J.; Kourilsky, F.; Weinstein, J. N., Targeting to cells of fluorescent liposomes covalently coupled with monoclonal antibody or protein A. *Nature* **1980,** *288*, 602-604.

57. Allen, T. M.; Chonn, A., Large unilamellar liposomes with low uptake into the reticuloendothetial system. *FEBS Lett.* **1987,** *223*, 42-46.

58. Klibanov, A. L.; Maruyama, K.; Torchilin, V. P.; Huang, L., Amphipathic polyethyleneglycols effectively prolong the circulation time of liposomes. *FEBS Lett.* **1990,** *268*, 235-237.

59. Sutton, D.; Nasongkla, N.; Blanco, E.; Gao, J., Functionalized micellar systems for cancer targeted drug delivery. *Pharm. Res.* **2007,** *24*, 1209-1046.

60. Kale, T. S.; Klaikherd, A.; Popere, B.; Thayumanavan, S., Supramolecular assemblies of amphiphilic homopolymers. *Langmuir* **2009,** *25*, 9660-9670.

61. Kataoka, K.; Harada, A.; Nagasaki, Y., Block copolymer micelles for drug delivery: Design, characterization and biological significance. *Adv. Drug Deliv. Rev.* **2001,** *47*, 113-131.

62. Torchilin, V. P., Targeted polymeric micelles for delivery of poorly soluble drugs. *Cell. Mol. Life Sci.* **2004,** *61*, 2549-2559.

63. Oerlemans, C.; Bult, W.; Bos, M.; Storm, G.; nijsen, J. F. W.; Hennink, W. E., Polymeric micelles in anticancer therapy: Targeting, imaging and triggered release. *Pharm. Res.* **2010,** *27*, 2569-2589.

64. Gu, F.; Zhang, L.; Teply, B. A.; Mann, N.; Wang, A.; Rodovic-Moreno, A. F.; Langer, R.; Farokhzad, O. C., Precise engineering of targeted nanoparticles by using self-assembled biointegrated block copolymers. *Proc. Natl. Acad. Sci. U.S.A.* **2008,** *105*, 2586-2591.

65. Bae, Y. H.; Yin, H., Stability issues of polymeric micelles. *J. Control. Release* **2008,** *131*, 2-4.

66. Chen, H.; Kim, S.; Li, L.; Wang, S.; Park, K.; Cheng, J.-X., Release of hydrophobic molecules from polymer micelles into cell membranes revealed by förster resonance energy transfer imaging. *Proc. Natl. Acad. Sci. U.S.A.* **2008,** *105*, (18), 6596-6601.

67. Chen, H.; Kim, S.; He, W.; Wang, H.; Low, P. S.; Park, K.; Cheng, J.-X., Fast release of lipophilic agents from circulating PEG-PDLLA micelles revealed by *in vivo* förster resonance energy transfer imaging. *Langmuir* **2008,** *24*, 5213-5217.

68. Vinogradov, S., Nanogels in the race for drug delivery. *Nanomedicine* **2010,** *5*, 165-168.

69. Oh, J. K.; Drumright, R.; Siegwart, D. J.; Matyjaszewski, K., The development of microgels/nanogels for drug delivery applications. *Prog. Polym. Sci.* **2008,** *33*, 448-477.

70. Kabanov, A. V.; Vinogradov, S., Nanogels as pharmaceutical carriers: Finite networks of infinite capabilities. *Angew. Chem. Int., Ed* **2009,** *48*, 5418-5429.

71. Jiwpanich, S.; Ryu, J.-H.; Bickerton, S.; Thayumanavan, S., Noncovalent encapsulation stabilities in supramolecular nanoassemblies. *J. Am. Chem. Soc.* **2010,** *132*, 10683-10685.

72. Akiyoshi, K.; deguchi, S.; Moriguchi, N.; Yamaguchi, S.; Sumamoto, J., Self-aggregates of hydrophobized polysaccharides in water: Formation and characteristics of nanoparticles. *Macromolecules* **1993,** *26*, 3062-3068.

73. Vinogradov, S.; Bronich, T. K.; Kabanov, A. V., Nanosized cationic hydrogels for drug delivery: Preparation, properties and interactions with cells. *Adv. Drug Deliv. Rev.* **2002,** *54*, 135-147.

74. Oh, J. K.; Bencherif, S. A.; Matyjaszewski, K., Atom transfer radical polymerization in inverse miniemulsion: A versatile route toward preparation and functionalization of microgels/nanogels for targetd drug delivery applications. *Polymer* **2009,** *50*, 4407-4423.

75. Soni, s.; Babber, A. K.; Sharma, R. K.; Maitra, A., Delivery of hydrophobised 5-fluorouracil derivative to brain tissue through intravenous route using surface modified nanogels. *J. Drug. Target.* **2006,** *14*, 87-95.

76. Tyagi, R.; Lala, S.; Verma, A. K.; Nandy, A. K.; Mahto, S. B.; Maitra, A.; Basu, M. K., Targeted delivery of arjunglucoside I using surface hydrophilic and hydrophobic nanocarriers to combat experimental leishmaniasis. *J. Drug. Target.* **2005,** *13*, 161-171.

77. Ryu, J.-H.; Jiwpanich, S.; Chacko, R.; Bickerton, S.; Thayumanavan, S., Surface-functionalizable polymer nanogels with facile hydrophobic guest encapsulation capabilities. *J. Am. Chem. Soc.* **2010,** *132*, 8246-8247.

78. Bachelder, E. M.; Beaudette, T. T.; Broaders, K. E.; Dashe, J.; Fréchet, J. M. J., Acetal-derivatized dextran: An acid-responsive biodegradable material for therapeutic applications. *J. Am. Chem. Soc.* **2008,** *130*, 10494-10495.

79. Oh, J. K.; Siegwart, D. J.; Lee, H.-I.; Sherwood, G.; Peteanu, L.; Hollinger, J. O.; Kataoka, K.; Matyjaszewski, K., Biodegradable nanogels prepared by atom transfer radical polymerization as potential drug delivery carriers: Synthesis, biodegradation, *in vitro* release, and bioconjugation. *J. Am. Chem. Soc.* **2007,** *129*, 5939-5945.

80. Oh, J. K.; Tang, C.; Gao, H.; Tsarevsky, N.; Matyjaszewski, K., Inverse miniemulsion ATRP: A new Method for synthesis and functionalization of well-defined water-soluble/cross-linked polymeric particles. *J. Am. Chem. Soc.* **2007,** *128*, 5578-5584.

81. Sisson, A. L.; Steinhiber, D.; Rossow, T.; Welker, P.; Licha, K.; Haag, R., Biocompatible functionalized polyglycerol microgels with cell penetrating properties. *Angew. Chem. Int., Ed* **2009,** *48*, 7540-7545.

CHAPTER 2

SELF-CROSS-LINKED POLYMER NANOGELS: A SURFACTANT-FREE HYDROPHOBIC ENCAPSULATION METHOD

2.1 Introduction

Noncovalently encapsulating hydrophobic guest molecules in a water-soluble container and then releasing them in response to a specific trigger are important goals in supramolecular chemistry, carrying clear implications in applications such as drug delivery.(Jeong, Bae et al. 1997; Allen and Culis 2004; Haag 2004; Koo, Rubinstein et al. 2005; Lee, MacKay et al. 2005; Peer, Karp et al. 2007; Bachelder, Beaudette et al. 2008; Oh, Drumright et al. 2008; Kale, Klaikherd et al. 2009) When execution of these supramolecular events is based on a nanosized host, there is even greater interest because of the potential for passive targeting of tumor tissue through the enhanced permeability and retention effect (EPR).(Baban and Seymour 1998; Maeda, Wu et al. 2000; Duncan 2003; Gillies and Fréchet 2005)

Chemically cross-linked, water-soluble polymer nanoparticles constitute a promising scaffold in therapeutic delivery applications, offering potential to circumvent stability issue.(Kakizawa, Harada et al. 1999; Aliyar, Hamilton et al. 2005; Oh, Drumright et al. 2008; Fang, Zhang et al. 2009; Kabanov and Vinogradov 2009) However, these polymeric nanoparticles or nanogels face cetain complications, as they are prepared by microemulsion or inverse microemulsion methods.(Talsma, Eabensee et al. 2006; Bachelder, Beaudette et al. 2008; Oh, Drumright et al. 2008; Sisson, Steinhiber et al. 2009) Microemulsion methods, which involve oil-in-water emulsion, utilize lipophilic monomers to produce the nanogels, which are thus generally water

insoluble. When a water-soluble polymer nanoparticle is desired, inverse microemulsion based synthesis is the preferable method. Note that the continuous phase in the inverse microemulsion (water-in-oil) method is based on a lipophilic solvent and therefore cannot be used to encapsulate hydrophobic guest molecules during nanoparticle formation. Moreover, these methods are relatively complex and require multiple purification steps to remove not only the unreacted monomer, but also the surfactant materials that were used as the emulsion stabilizer. An attractive alternative to forming polymer nanoparticles is to collapse a limited number of polymer chains. Such methods have been previously reported, but require ultrahigh dilution conditions or inverse addition conditions,(Kadlubowski, Grobelny et al. 2003; Jiang and Thayumanavan 2005) which limit capabilities for guest molecule incorporation. To overcome these issues, we develop a facile method that allows for the design and syntheses of water-soluble polymer nanoparticles under non-emulsion conditions with high lipophilic encapsulation capabilities.

A facile method, reported by us recently, allows for the design and syntheses of polymer nanoparticles under non-emulsion condition.(Ryu, Chacko et al. 2010; Ryu, Jiwpanich et al. 2010) The versatility of these polymer nanoparticles has been further demonstrated by showing that (*i*) lipophilic guests can be easily incorporated noncovalently within the nanoparticles; (*ii*) the noncovalently encapsulated guest molecules can be released in response to a biologically relevant stimulus; and (*iii*) the surfaces of these particles are functionalizable. For a stimuli-responsive functional group, we considered a disulfide bond, since these bonds are susceptible to biochemical reductants such as glutathione (GSH), thioredoxin, and peroxiredoxin.(Bernkop-

Schnürch 2005; Heffernan and Murthy 2009) We have previously reported a synthetic methodology in which a pyridyl disulfide (PDS) side chain functionality was used as a handle for incorporating thiol-based functional groups onto polymers.(Ghosh, Basu et al. 2006) The basis for this methodology is the higher reactivity of the pyridyl disulfide bonds with thiols as compared to other disulfide functionalities, which is facilitated by the release of a stable 2-thiopyridone byproduct. We envisioned taking advantage of this high reactivity of the PDS functionality to affect cross-linking in polymer chains. Our hypothesis involves the addition of a deficient amount of dithiothreitol (DTT), which is known to cleave PDS bonds with great efficiency. When a deficient amount of DTT is added, a corresponding small percentage of PDS groups will be converted to free thiols. These free thiols would then react with an equivalent amount of the remaining PDS functionalities to create disulfide bonds, which would effectively cross-link the polymer chains, independent of whether the process is intra-chain or inter-chain. We further envisioned that because the PDS functionalities are relatively hydrophobic, they would collapse in the aqueous phase. If this were the case, we hypothesized that polymer nanoparticles would be obtained upon treatment of our polymers with deficient amount of DTT, without the need for ultrahigh dilution preparative conditions (Figure 2.1). We also envisaged that the hydrophobic interior in the aggregate would provide an opportunity to encapsulate lipophilic guest molecules prior to cross-linking.

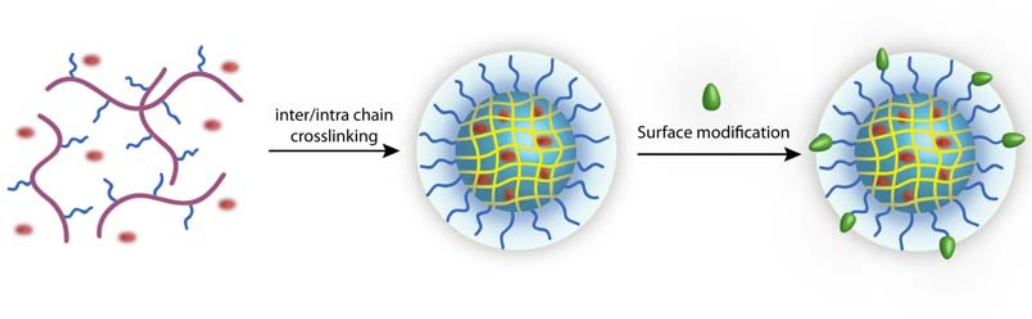

Figure 2.1: Design and synthesis of the self-cross-linked polymer nanogels.

2.2 Results and Discussion

2.2.1 Design and Synthesis

The polymer nanogel precursor is based on a random copolymer that contains oligoethyleneglycol (OEG) units and pyridyldisulfide (PDS) groups as side chain functionalities. The role of the OEG unit is to introduce a charge-neutral hydrophilic functional group, which is known to endow biocompatibility. The PDS functionality plays several key roles: (*i*) this is a lipophilic functionality and thus plays a critical role in providing a supramolecular amphiphilic nanoassembly in the aqueous phase. Note that this feature avoids the use of any additional surfactant molecules to generate the nanogel and the size of this nanoassembly dictates the size of the final polymer nanogel; (*ii*) the amphiphilic nature of the assembly and lipophilic environment afforded by the PDS functionality provides the opportunity for lipophilic guest molecules to be sequestered within these nanoassemblies prior to cross-linking. (*iii*) The PDS functionality is reactive, but specific to thiols and thus provides a mild method for disulfide cross-linking to form the nanogel. (*iv*) Since the nanogels are based on disulfide cross-linkers that can be cleaved by thiol-disulfide exchange reactions, these

nanogels also provide a pathway to trigger the release of the stably encapsulated guest molecules in response to an external stimulus.

Random co-polymer **1,** containing 30% of the oligoethyleneglycol methacrylate and 70% of the PDS-derived methacrylate, was prepared by reversible addition-fragmentation chain transfer (RAFT) polymerization. Structures of the nanogel precursors, polymer nanogels and synthetic approach are shown in Scheme 2.1.

The next step involves the conversion of these polymeric aggregates into chemically cross-linked nanogels. We hypothesized the formation of the nanogel through the following process. Addition of a deficient amount of dithiothreitol (DTT) would cause the cleavage of a well-defined percentage of the PDS groups to the corresponding thiol functionalities. These thiol functionalities will then react within the polymeric aggregates with unreacted PDS functionalities. This reaction results in disulfide cross-links within the polymeric aggregates causing the formation of the nanogels, as shown in Scheme 2.1.

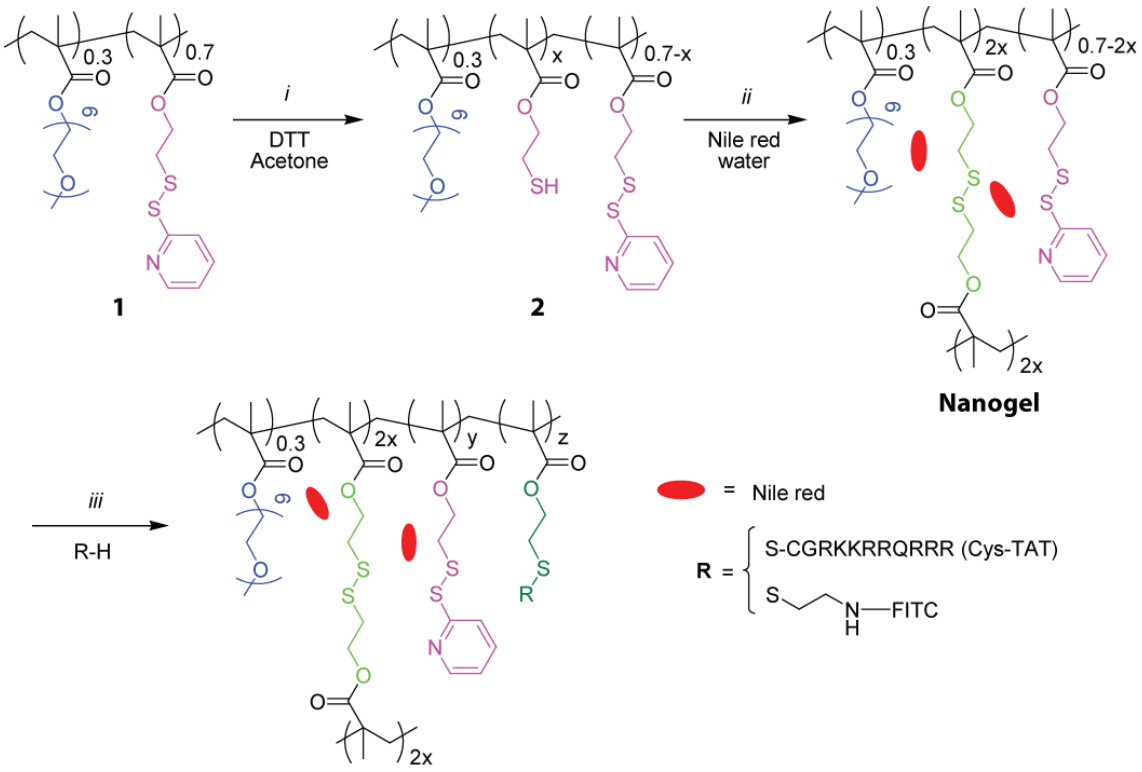

Scheme 2.1: Structures of the polymers and nanogels. (*i*) Cleavage of specific amount of PDS groups by DTT. (*ii*) Nanogel formation by inter/intrachain cross-linking. (*iii*) Surface modification of nanogels with thiol-modified Tat peptide or FITC.

Cross-linked particles were synthesized from this polymer by adding 20 mol% of DTT with respect to the number of PDS functionalities in the polymer. Note that there would be residual PDS functionalities in these gels, providing useful handles for introducing ligands on the nanogel surfaces (*vide infra*). We characterized the structures obtained from these reactions by transmission electron microscopy (TEM) and dynamic light scattering (DLS). DLS studies reveal that the structures obtained are ~190 nm in size (Figure 2.2a). TEM images shown in Figure 2.2b revealed well-defined spherical structures with slightly smaller diameters than those observed in DLS, which is attributed to the possible swelling of the nanoparticles in water.

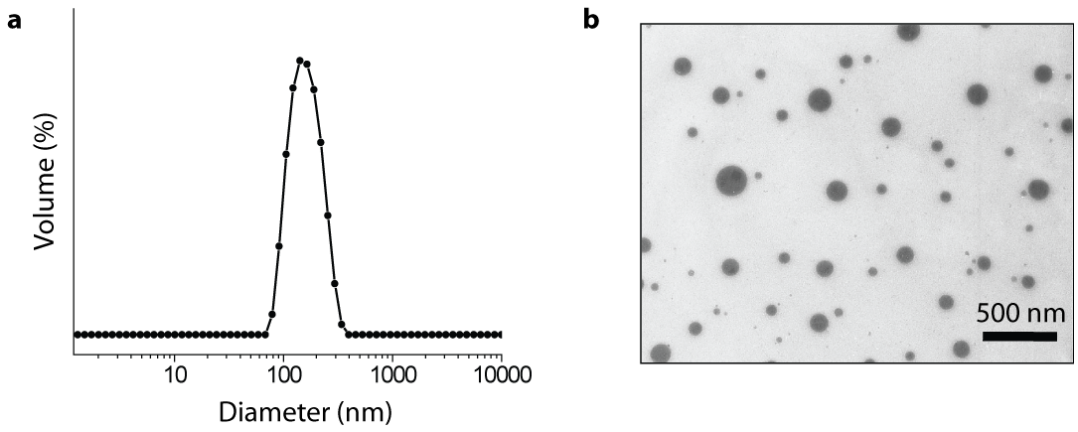

Figure 2.2: Size distribution of the nanogel (1 mg/mL) in water. (a) DLS trace. (b) TEM image.

We were interested in identifying whether the obtained particle is indeed a stable cross-linked structure and if the size of the particle is completely controlled by the size of a polymer aggregate obtained prior to the cross-linking reaction. For this purpose, we analyzed the size of the polymer assembly prior to the DTT reaction. DLS studies revealed aggregates of about 17 nm, which suggests that the particles obtained upon DTT reaction involved inter-chain cross-linking in addition to the possible intra-chain reactions. We presume that this assembly is due to the amphiphilic nature of the polymer caused by the hydrophobic PDS groups, because there were no discernible nanoassemblies when acetone alone is used as the solvent (Figure 2.3). We can control the size of the nanoparticle by varying the reaction conditions. In water, DTT cleavage and disulfide exchange reactions occurred intramolecularly in polymer aggregates and resulted in 10 nm size nanoparticles. Interestingly, after the formation of the polymer nanoparticle using the DTT reaction, the size of the assemblies in both acetone and water were identical (Figure 2.3). This illustrates the stability of the assembly and also confirms that they are formed by chemical cross-linking of the functionalities. We

calculated the water content of the nanogels based on the difference in size of the nanogels in swollen and dried state. The average size of swollen gels in water measured by DLS, and dried gels measured by TEM are 190 nm and 110 nm, respectively. Therefore, from the difference in volume between dry state and swollen state in one particle (7.0×10^5 nm^3 and 3.5×10^6 nm^3 for dried state and swelled state, respectively), we can estimate that 2.8×10^6 nm^3 volume is filled with water.

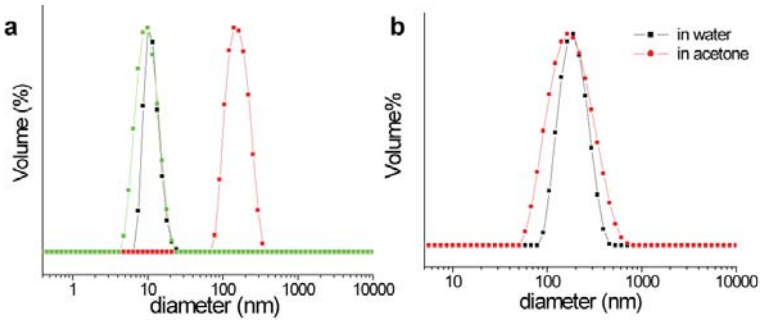

Figure 2.3: (a) Size distribution of polymers (black line) and nanoparticles prepared in water (green line) and nanogels prepared in water/acetone (red line). The concentrations are 1 mg mL^{-1} measured in water. (b) DLS of nanogel (1 mg mL^{-1}) in water and acetone showed almost same size distribution.

With our methodology, we were able to obtain two very different particle sizes by simply varying the concentration of polymers. We analyzed the sizes of polymer assemblies prior to the DTT reaction. DLS studies revealed aggregates of about 120 nm at 10 mg/mL in water, and 12 nm below 5 mg/mL. Subsequent cross-linking reaction by DTT led to nanoparticles with two different sizes (16 nm and 190 nm with 5 mg/mL and 10 mg/mL, respectively) as shown in Figure 2.4. Upon decreasing the concentration of copolymer 1 to below 0.5 wt% in water, we obtained 16 nm nanoparicles after DTT induced cross-linking. The resulting nanoparticles showed the same size (190 nm) when the solution was diluted ten times, while the polymer **1** at this concentration showed 12

nm size. This once again confirms that the obtained particles are indeed stably cross-linked structures. This suggests that we can control the size of the nanoparticles by simply tuning the reaction conditions.

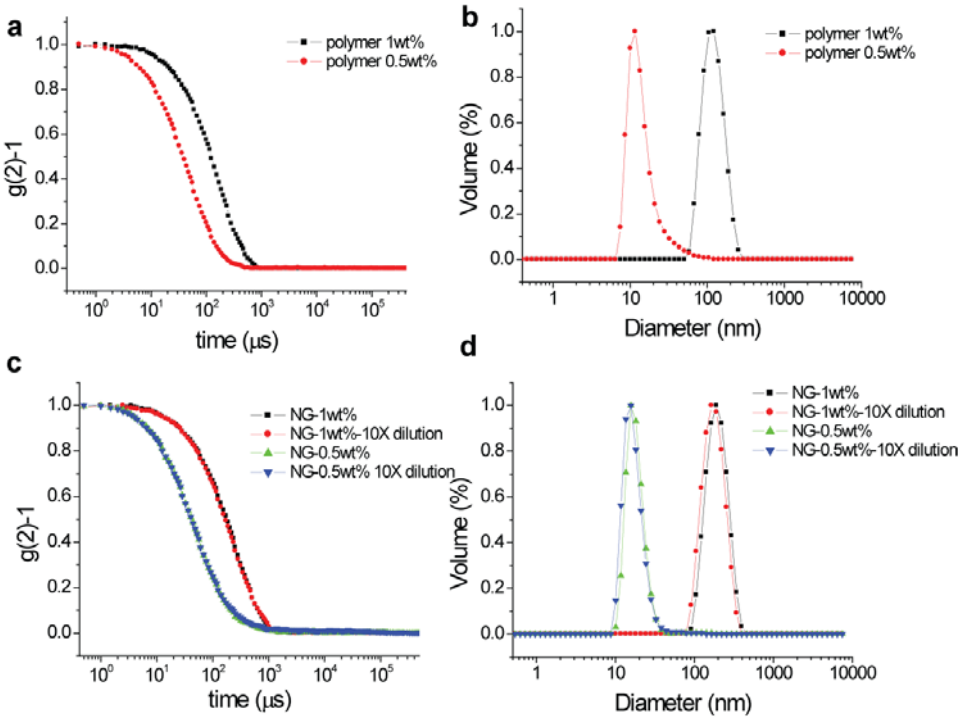

Figure 2.4: (a) Time correlation function and (b) size distribution of co-polymer 1 at different concentration (0.5 wt% and 1.0 wt%). (c) Time correlation function and (d) size distribution of nanogels which were prepared at different concentration (0.5 wt% and 1.0 wt%).

2.2.2 Guest Encapsulation and Triggered/Controlled Release

For a nanocarrier to be effective, it should be able to stably encapsulate lipophilic guest molecules and release its contents in response to a biologically relevant trigger.(Murthy, Thng et al. 2002; Jiang, Qi et al. 2007; Oh, Siegwart et al. 2007; Chan, Wong et al. 2008; Zhang, Liu et al. 2008) Disulfide bonds are particularly attractive as stimulus-sensitive functionalities in medicinal chemistry as they can be cleaved in the presence of high reducing agent concentrations. Reducing agents, such as reduced

glutathione (GSH), thioredoxin, and peroxiredoxin, are found at varying levels throughout the body. For example, GSH is found in millimolar concentrations in the cytosol, where as the extracellular concentration is only micromolar.(Bernkop-Schnürch 2005; Yang, Chen et al. 2006; Chong, Chandrawati et al. 2009; Sivakumar, Bansal et al. 2009) Therefore, a GSH-sensitive delivery vehicle can be effective in facilitating specific intracellular delivery of encapsulated molecules.(Wu and Senter 2005; Li, Lokitz et al. 2006; Bae, Mok et al. 2008; Jia, Wong et al. 2008; Bauhuber, Hozsa et al. 2009; Li, Zhu et al. 2009)

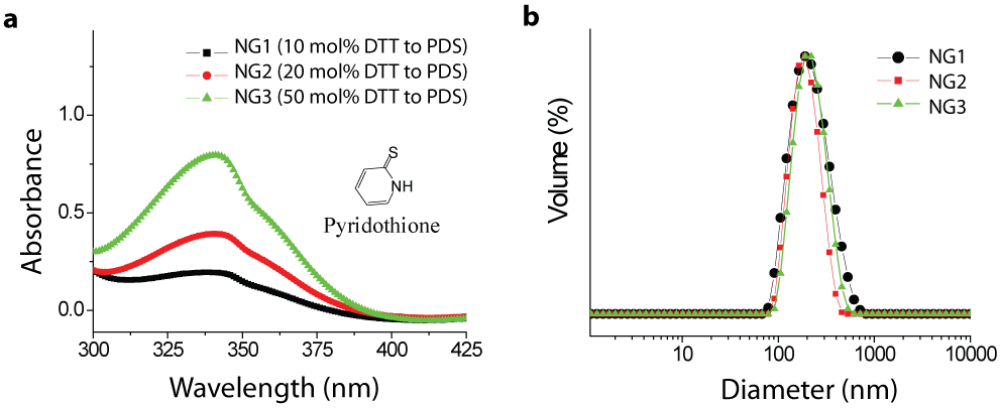

Figure 2.5: (a) Absorption spectra of pyridothione byproduct during nanogel synthesis. (b) Size distribution of nanogels (1 mg/mL) in DLS.

We hypothesized that GSH could induce the release of loaded dyes through cleavage of the disulfide cross-linking bonds and that the release kinetics could be tuned by the cross-linking density in the nanogel. To test this possibility, we prepared three different cross-linked particles by adding 10, 20 or 50 mol% (against the precursor PDS groups) of DTT to polymer **1**. The progress of the reaction was conveniently monitored by tracking the release of the pyridothione byproduct through its characteristic absorption at 343 nm. Considering the mechanism by which this addition results in

cross-linked polymer particles and the percentage of PDS functionalities in polymer **1**, this reaction should result in nanoparticles **NG1**, **NG2**, and **NG3** with 7%, 14%, and 35% cross-linking densities respectively, assuming 100% reaction efficiency. Our estimations, based on pyridothione release, indicate that the actual cross-linking densities correspond to 6%, 13%, and 25% respectively (Figure 2.5a). DLS studies reveal that the structures obtained are all about 190 nm in size (Figure 2.5b).

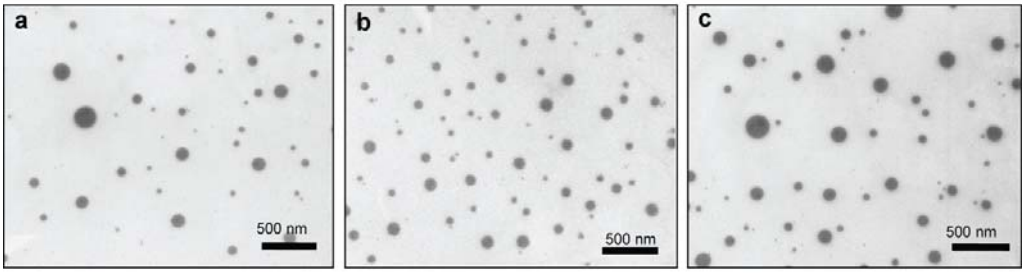

Figure 2.6: TEM images of NG1 (a), NG2 (b), and NG3 (c).

TEM images reveal well-defined spherical structures with slightly smaller diameters than those observed in DLS, which is attributed to the possible swelling of the nanoparticles in water (Figure 2.6). It is interesting to note that the sizes of all three nanogels are very similar. This suggests that the size of the assembly prior to the cross-linking reaction dictates the nanogel size and that further cross-linking occurs within that nanoassembly.

To investigate the possibility of encapsulating hydrophobic guest molecules within the interiors of these nanogels, we carried out the DTT-based cross-linking reaction in the presence of Nile red, a hydrophobic dye. Nile red is inherently insoluble in water. Therefore, the reaction was optimized using acetone as a solvent in the first steps before the addition of water during the cross-linking reaction. Isolation of the

nanoparticles and their subsequent dissolution in water retains Nile red, as discerned by the emission spectra of all three gels (Figure 2.7).

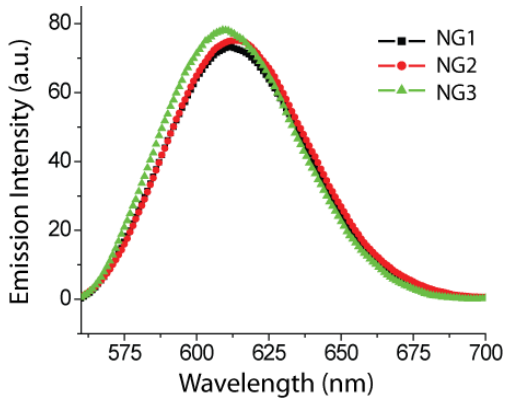

Figure 2.7: The emission spectra of Nile red sequestered in polymer nanogels.

To explore triggered release, we added GSH into nanogel solutions and investigated the release of Nile red by tracing the decrease in the hydrophobic dye's spectral emission intensity caused by its insolubility in the aqueous media. To examine the GSH-dependent dye release, Nile red loaded nanogel solutions (0.05 wt%) in pH 7.4 sodium acetate buffer solution were treated with different concentrations of GSH (10 μM and 10 mM) and the intensity of Nile red emission at 610 nm was monitored for three days.

At low GSH concentrations (10 μM), little dye release was observed for all nanogels (Figure 2.8a-c). This concentration corresponds to that commonly observed outside the cell and within the blood plasma. In contrast, high concentrations of GSH (10 mM), corresponding to those found inside the cell, induced significant dye release (Figure 2.8d-f).

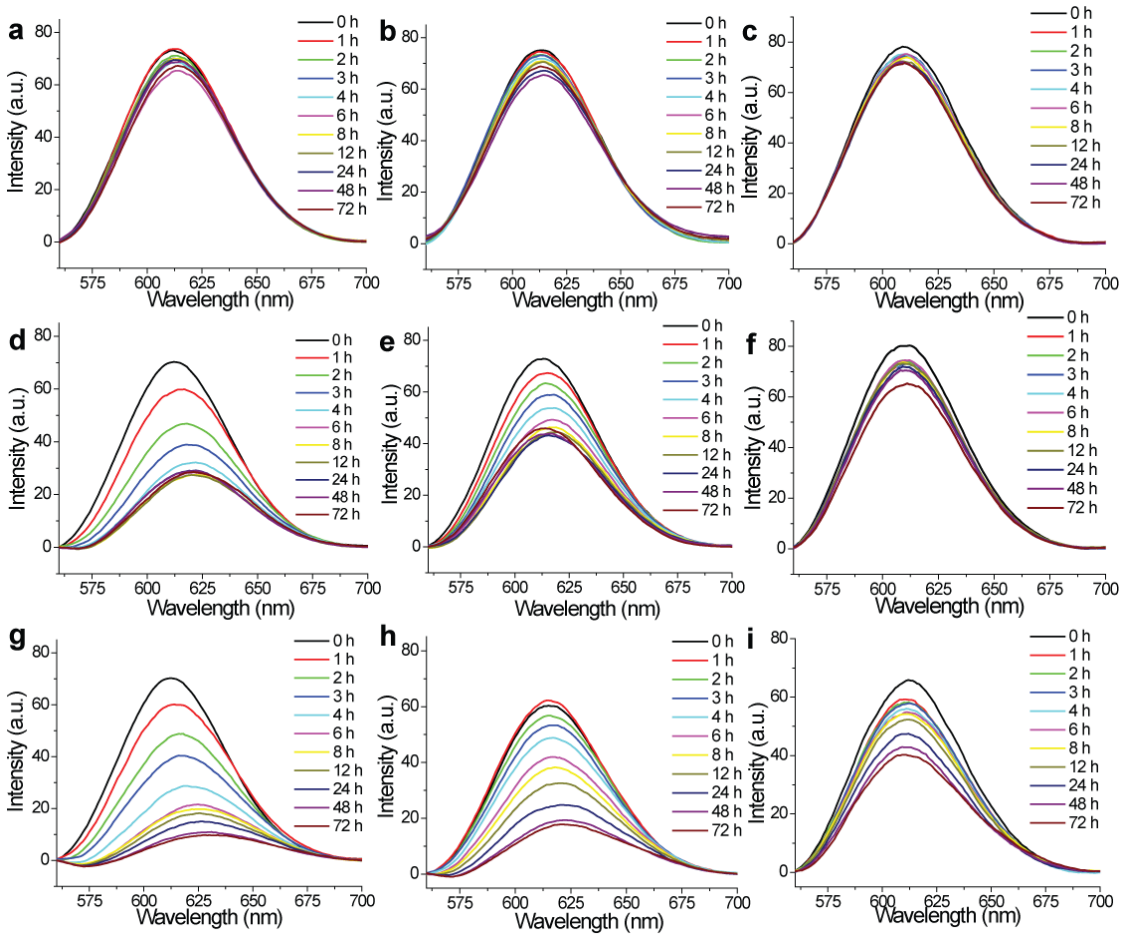

Figure 2.8: Dye release from the nanogels NG1 (a, d, g), NG2 (b, e, f), and NG3 (c, f, i) (0.05 wt%) in response to varied GSH concentrations. (a-c) 10 μM GSH and (d-f) 10 mM GSH at pH 7.4, and (g-i) 10 mM GSH at pH 5. The release only occurred at high GSH concentration. At acidic pH under 10 mM GSH, the release was faster and more gradual over time than those at neutral pH.

Cross-linking density is most likely to influence the rate of dye release from the nanogel interior. **NG1** (6% cross-linked nanogel) showed rapid release reaching a plateau after 6 h at 10 mM GSH in pH 7.4 buffer solution. **NG2** (13% cross-linked nanogel) showed slower release, reaching a maximum at 12 h; **NG3** (25% cross-linked nanogel) displayed gradual, highly sustained release for several days. Because the cellular entry of these nanogels would likely involve endocytosis, we were interested in

analyzing the release profile at lower pH. We found that the difference in the release profile of these nanogels under acidic conditions (pH 5) is very similar to that observed with pH 7 (Figure 2.8g-i). While this bodes well for endocytosis based entry into the cells, we also found the release profile at high GSH concentration to be surprising, as GSH activity is considered most efficient at neutral pH.(Moskaug, Sandvig et al. 1987) As shown in Figure 2.9, similar release profiles were observed for all three gels over several hours at both pH 5 and 7.4, clearly demonstrating that the kinetics of guest release can be controlled by cross-linking densities. Nonetheless, we observed faster release of encapsulated dyes in **NG1** and **NG2** at pH5, while there were no significant different in **NG3**. We hypothesize that the remaining of PDS groups in **NG1** and **NG2** are protonated creating charge-charge repulsions that swell the nanogel networks. The swelling of nanogels in acidic condition results in accelerating the rate of guest release.

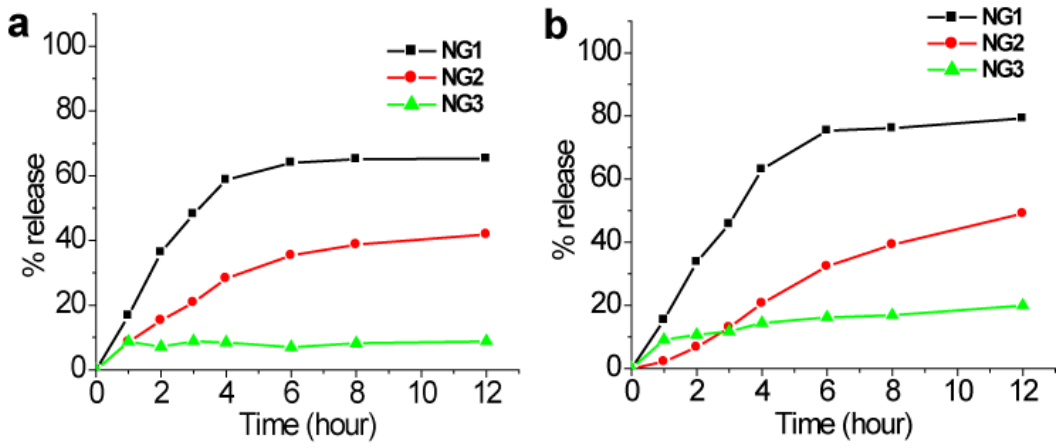

Figure 2.9: (a) Comparison of GSH-induced dye release rate from the nanogels which have different cross-linking densities at (a) pH 7.4 and (b) pH 5.

2.2.3 Cytotoxicity

We anticipated that our gels would be relatively non-toxic, because they are made from biocompatible oligoethyleneglycol components as surface displays in a

methacrylate backbone. Treatment of cells with the nanogels indeed allows high cell viability and no concentration-dependent toxicity up to a nanogel concentration of 1 mg mL^{-1} (Figure 2.10). This result indicates that the nanogel material is non-toxic and thus a potential candidate for biological applications.

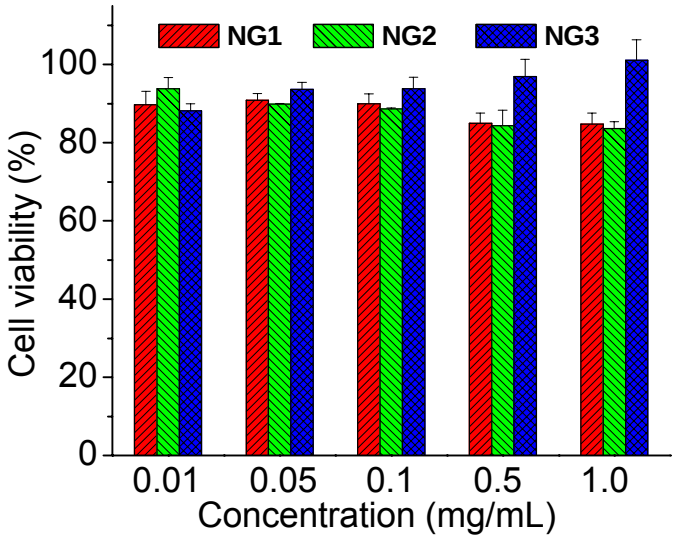

Figure 2.10: In vitro toxicity of empty nanogels with 293T cells after 24 hour incubation.

2.2.4 Surface Functionalization

We were also interested in testing our hypothesis that we can achieve surface functionalization of these nanogels by thiol-disulfide exchange reactions with the unreacted PDS groups. These PDS groups can be reacted with thiol-containing compounds, allowing for chemoselective ligand modification. To test this, nanogel solutions (1 mg mL^{-1}) were treated with either excess fluorescein isothiocyanate (FITC) or thiol-modified FITC (1 mg mL^{-1}). Figure 2.11 shows a significant difference between the two samples; while thiol-modified FITC treated nanogels exhibited very strong fluorescein emission, the bare FITC treated nanogels solution showed very little

emission, suggesting that the nanogels were covalently functionalized with thiol-modified FITC by disulfide linkage and that the observed fluorescence is not due to noncovalent surface binding of the dye molecules.

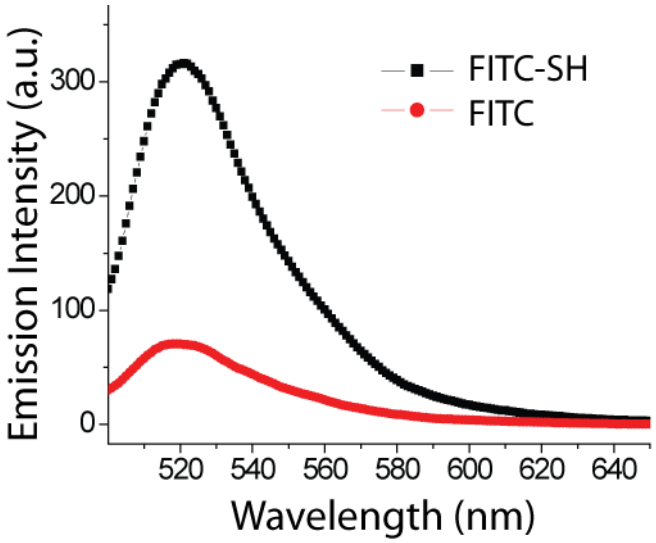

Figure 2.11: The emission spectra of nanogels (1mg/mL) treated with thiol-modified FITC (FITC-SH) and FITC.

To further investigate surface modification possibilities, nanogel solutions (0.1 mg mL^{-1}) containing the hydrophobic dye, 1,1'-dioctadecyl-3,3,3',3'-tetramethylindo-carbocyanine perchlorate (DiI), were treated with a modified cell penetrating peptide, Tat-SH (0.1 mg mL^{-1}) with a *C*-terminal cysteine, for 24 h. These solutions were then incubated with MCF-7 human breast cancer cell lines for just 2 h. The cell internalization efficiency of the unmodified nanogels (control) and Tat-SH treated nanogels were then examined by confocal microscopy.

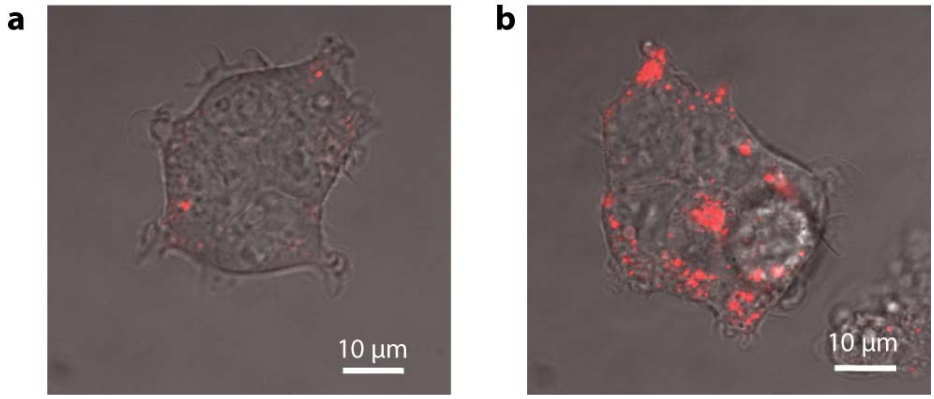

Figure 2.12: Representative confocal microscopy images of MCF-7 cells incubated with; (a) the unmodified nanogels, (b)Tat-SH treated nanogels.

As shown in Figure 2.12, the internalization of Tat-SH modified nanogels occurred much more readily than that observed with the control gels, confirming the effectiveness of using the remaining PDS groups to simply modify the nanogel surface. This presents a clear method for incorporating ligands onto the polymer nanoparticles and thus achieves specificity to pathogenic cells using chemoselective disulfide chemistry.

2.3 Summary

We have demonstrated a simple, emulsion free method for the preparation of biocompatible nanogels that provides the ability to encapsulate hydrophobic guest molecules using intra/intermolecular disulfide formation of PDS containing polymers. Since disulfide bonds are biodegradable in a reducing environment, these nanoparticles hold great potential as intracelluar drug delivery vehicles. The release of guest molecules can be induced by external stimuli. By varying the cross-linking density of the nanogels, the release kinetics of guest molecules can be controlled. Additionally, we have demonstrated that the surface of these nanoparticles can be efficiently

functionalized under mild conditions. Taken together, the nanogel formation using the self-cross-linking polymers and corresponding method of surface modification open a new avenue for enhanced cytosolic drug delivery and establish a novel approach to creating polymer nanogels for a range of biomedical applications from drug delivery to biosensing.

2.4 Experimental

2.4.1 General Methods and Procedure

2,2′-Dithiodipyridine, 2-mercaptoethanol, polyethylene glycol monomethyl ether methacrylate (MW 450), D,L-dithiothreitol (DTT), 1,1'-dioctadecyl-3,3,3',3'-tetramethyl-indocarbocyanine perchlorate (DiI), Nile red, Tat-SH, and other conventional reagents were obtained from commercial sources and were used as received unless otherwise mentioned. Polymer was synthesized with RAFT polymerization and then purified by precipitation with ethyl ether. S-dodecyl-S'-2-(2,2-dimethylacetic acid) trithiocarbonate (CTA) and pyridyl disulfide ethyl methacrylate (PDSEMA) were prepared using a previously reported procedures.(Lai, Filla et al. 2002; Ghosh, Basu et al. 2006) ^{1}H-NMR spectra were recorded on a 400 MHz Bruker NMR spectrometer using the residual proton resonance of the solvent as the internal standard. Molecular weights of the polymers were estimated by gel permeation chromatography (GPC) using PMMA standards with a refractive index detector. Dynamic light scattering (DLS) measurements were performed using a Malvern Nanozetasizer. The fluorescence spectra were obtained from a JASCO FP-6500 spectrofluorimeter. Transmission electron microscopy (TEM) images were taken using a JEOL 100CX at 100 KV.

Synthesis of pyridyl disulfide ethyl alcohol:

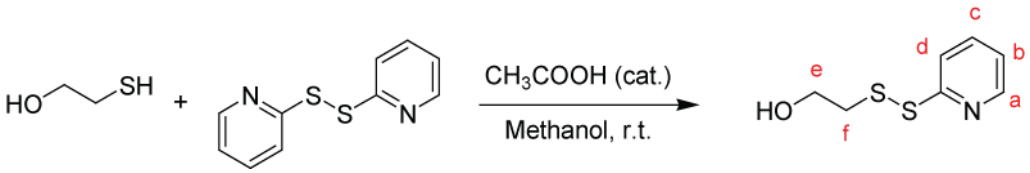

Aldrithiol-2 (20 g, 91 mol) was dissolved in 2.5 mL of methanol and then glacial acetic acid (1 mL) was added to the solution. To this mixture, a solution of mercaptoethanol (7.8 g, 99 mmol) in methanol (150 mL) was added drop-wise at ambient temperature with continuous stirring. After, the reaction mixture was stirring at room temperature for additional 3 hours, solvent was removed to get the yellow oil crude product which was purified by flash column chromatography by using silica gel as stationary phase and mixture of ethyl acetate:hexane (40:60) to afford the desired product as colorless oil. Yield: 68 % ^{1}H NMR (400 MHz, $CDCl_3$) δ 8.54 (m, 1H, a), 7.63 (m, 1H, b), 7.42 (m, 1H,c), 7.18 (m, 1H, d), 3.83 (t, 2H, e), 2.97 (t, 2H, f).

Synthesis of pyridyl disulfide ethyl methacrylate:

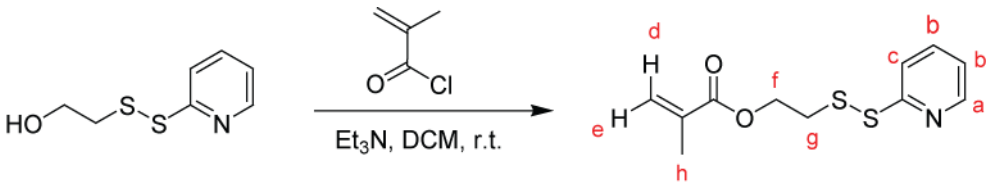

Pyridyl disulfide ethyl alcohol (11 g, 59 mmol) in dichloromethane (250 mL) was added triethylamine (8.3 g, 82 mmol), and then the mixture was cooled in an ice-bath. To this cold mixture, a solution of methacryloyl chloride (8.6 g, 82 mmol) was added drop-wise with continuous stirring. After the mixture was stirring at ambient temperature for 6 hours, the mixture solution was extracted with water and wash with brine. The organic layer was collected, dried over anhydrous Na_2SO_4 and concentrated. The yellow oil crude product was purified by column chromatography using silica gel and mixture of ethyl acetate:hexane (20:80). Yield: 66% ^{1}H NMR (400 MHz, $CDCl_3$) δ 8.47 (m, 1H, a), 7.63 (m, 2H, b), 7.08 (m, 1H,c), 6.12 (d, 1H, d), 5.58 (d, 1H, e), 4.39 (t, 2H, f), 3.08 (t, 2H, g), 1.93 (s, 3H, h). ^{13}C NMR (100 MHz, $CDCl_3$) δ 167.1, 159.8, 149.7, 137.1, 136.0, 126.1, 120.9, 119.8, 62.4, 37.4, 18.3.

Synthesis of random copolymer (1):

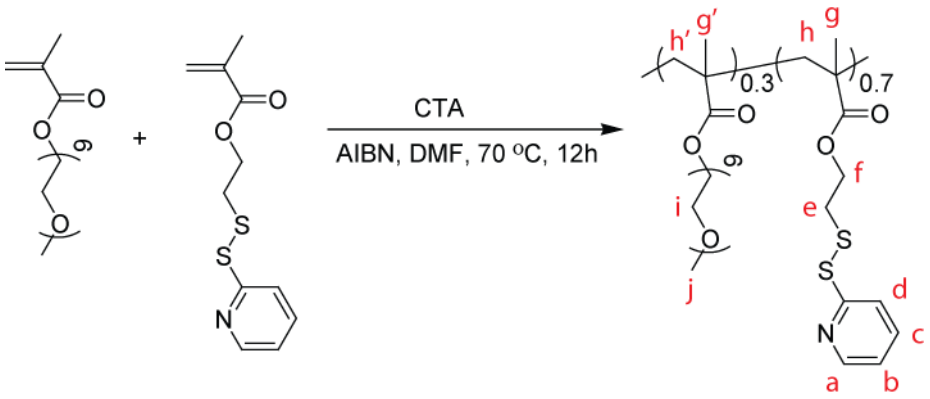

A mixture of S-dodecyl-S'-2-(2,2-dimethylacetic acid) trithiocarbonate (CTA) (90 mg, 0.3 mmol), PDSEMA (5 g, 20 mmol), polyethylene glycol monomethyl ether methacrylate (4 g, 8 mmol) and AIBN (10 mg, 0.06 mmol) were dissolved in DMF (10 mL) and degassed by performing three freeze-pump-thaw cycles. The reaction mixture was sealed and then put into a pre-heated oil bath at 70 °C for 12h. The resultant mixture was dissolved in dichloromethane (5 mL) and precipitated in hexane (200 mL). To remove unreactive monomers, the precipitate was further dissolved in dichloromethane (5 mL) and re-precipitated in ethyl ether (200 mL) to yield purified random copolymer as a waxy liquid. Yield: 78%. GPC (THF) M_n: 24.7 K. PDI: 1.6. ^{1}H NMR (400 MHz, $CDCl_3$) δ: 8.40 (a), 7.62 (c, d), 7.05 (b), 4.16-4.02 (i, f), 3.58-3.48 (i), 3.31 (j), 2.97 (e), 2.04-1.65 (h, h'), 1.24-0.72 (g, g'). The molar ratio between the two blocks was determined by integrating the methoxy proton in the polyethylene glycol unit and the aromatic proton in the pyridine and found to be 3:7 (PEO:PDSEMA).

Synthesis of thiol-modified FITC:

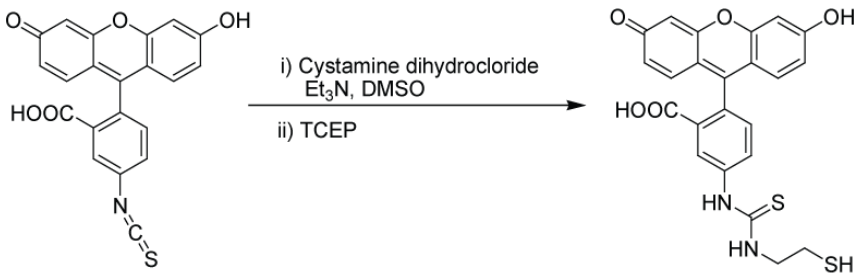

A mixture of FITC (10 mg, 0.03 mmol), cystamine dihydrochloride (6 mg, 0.03 mmol) and triethylamine (TECP) (13 mg, 0.13 mmol) was dissolved in DMSO (400 µL) and stirred for 4 h. To this reaction mixture was added tris(2-carboxyethyl)phosphine hydrochloride (9 mg, 0.03 mmol) and stirred for 1 h. The resultant mixture was precipitated in ethyl ether and washed with water. The crude product was used for nanogel surface modification without further purification.

Synthesis of nanogel containing nile red:

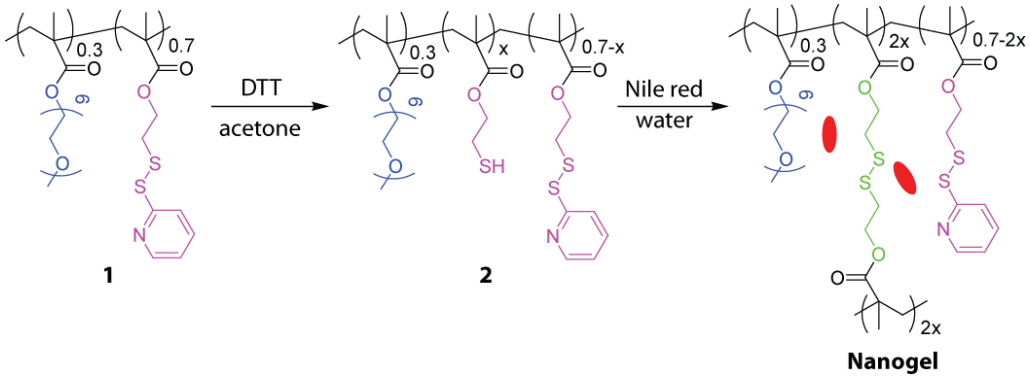

The polymer **1** (10 mg) and Nile red (2 mg) were dissolved in 200 µL of acetone and measured amount of DTT (4 µmol, 20 mol% against PDS groups) was added. After stirring for 10 min, 1 mL of deionized water was added and the mixture solution was stirred overnight at room temperature, open to the atmosphere allowing the organic solvent to evaporate. Excess insoluble Nile red was removed by filtration and

pyridothione was removed from the nanogel solution by ultrafiltration (triplicate) using a membrane with a molecular weight cutoff of 10,000 g mol^{-1} (Amicon Ultra cell-10K).

Cell culture:

The cell viability of the nanogels was tested against 293T cells. This experiment has done by Mr. Reuben Chacko. 293T cells were cultured in T75 cell culture flasks using Dulbecco's Modified Eagle Medium/Nutrient Mixture F-12 (DMEM/F12) with 10% fetal bovine serum (FBS) supplement. The cells were seeded at 10,000 cells/well/200 µL in a 96 well plate and allowed to grow for 24 hours under incubation at 37 ^{o}C and 5% CO_2. These cells were then treated with nanogels of different concentrations and were incubated for another 24 hours. Cell viability was measured using the Alamar Blue assay with each data point measured in triplicate. Fluorescence measurements were made using the plate reader SpectraMax M5 by setting the excitation wavelength at 560 nm and monitoring emission at 590 nm on a black well plate.

Surface modification:

This experiment has done by Mr. Reuben Chacko. FITC or thiol-modified FITC (1 mg) was dissolved in 100 µL of DMF and then 2 mL of nanogel (1 mg/mL) in water was added. The mixture solution was stirred overnight at room temperature. Non-conjugated or physically adsorbed dye molecules were removed by ultrafiltration (thrice) using a membrane with a molecular weight cutoff of 10,000 g/mol. For Tat peptide modification, 10 µL of nanogel (1mg/mL) which contains 1% DiI molecules was added to 90 µL of phosphate pH 5 buffer. To this solution, 10 µL of Tat peptide solution (1 mg/mL) was added. After stirring overnight, 100 µL of this solution was

added to MCF-7 cells, which were grown in coverslip-bottomed Petri dishes, to make a total of 2 mL of culture medium. Cells were incubated with surface modified nanogels and control nanogels for 2 h before confocal imaging.

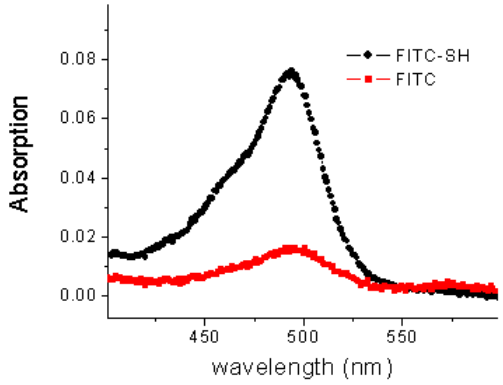

Figure 2.13. The absorption spectra of nanogel (0.5 mg mL^{-1}) treated with thiol-modified FITC (FITC-SH) and with FITC. To estimate the number of FITC molecules on the nanogel surface, the absorption of FITC at 492 nm wavelength was compared in each nanogel treated with FITC-SH and FITC. Based on the calculation of FITC molar concentration by extinction coefficient and assuming that the nanogel density is around 1.00, the number of FITC molecules on the nanogel surface was determined to be approximately three thousand molecules per particle.

Laser scanning confocal microscopy:

The laser confocal experiment was performed by Mr. Reuben Chacko. MCF-7 cells were cultured in T75 cell culture flask containing DMEM/F12 with 10% FBS supplement. 50,000 cells in 2mL of culture medium were seeded in coverslip-bottomed Petri dishes and allowed to grow for 3 days at 37 ^{o}C in a 5% CO_2 incubator. These cells were treated with 100 µL of nanogels and incubated at 37 ^{o}C for 2 h before observing them by confocal microscopy.

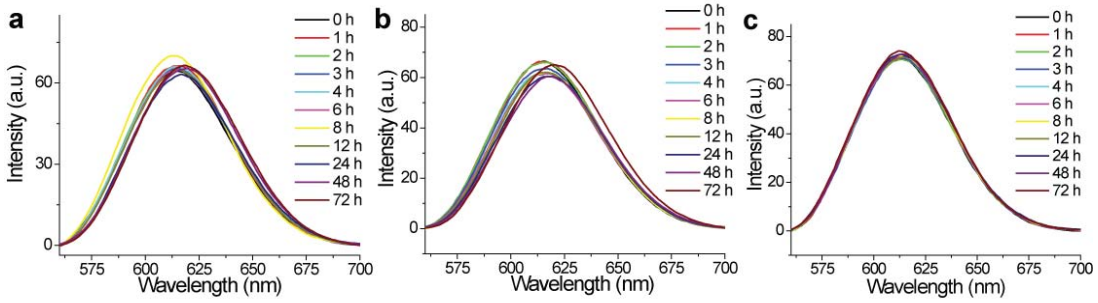

Figure 2.14. **Dye release from** NG1 **(a),** NG2 **(b), and** NG3 **(c) (0.05 wt%) in 10 µM GSH at pH 5.**

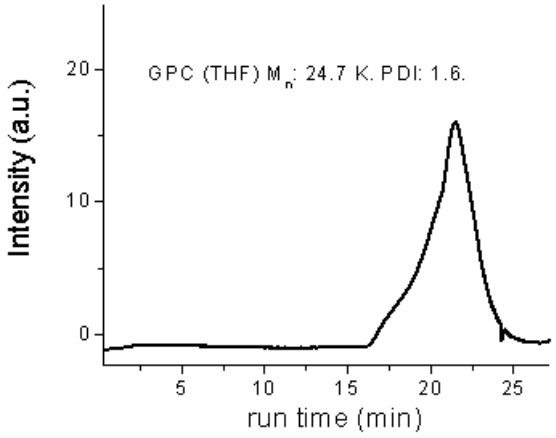

Figure 2.15: GPC trace of the polymer **1.**

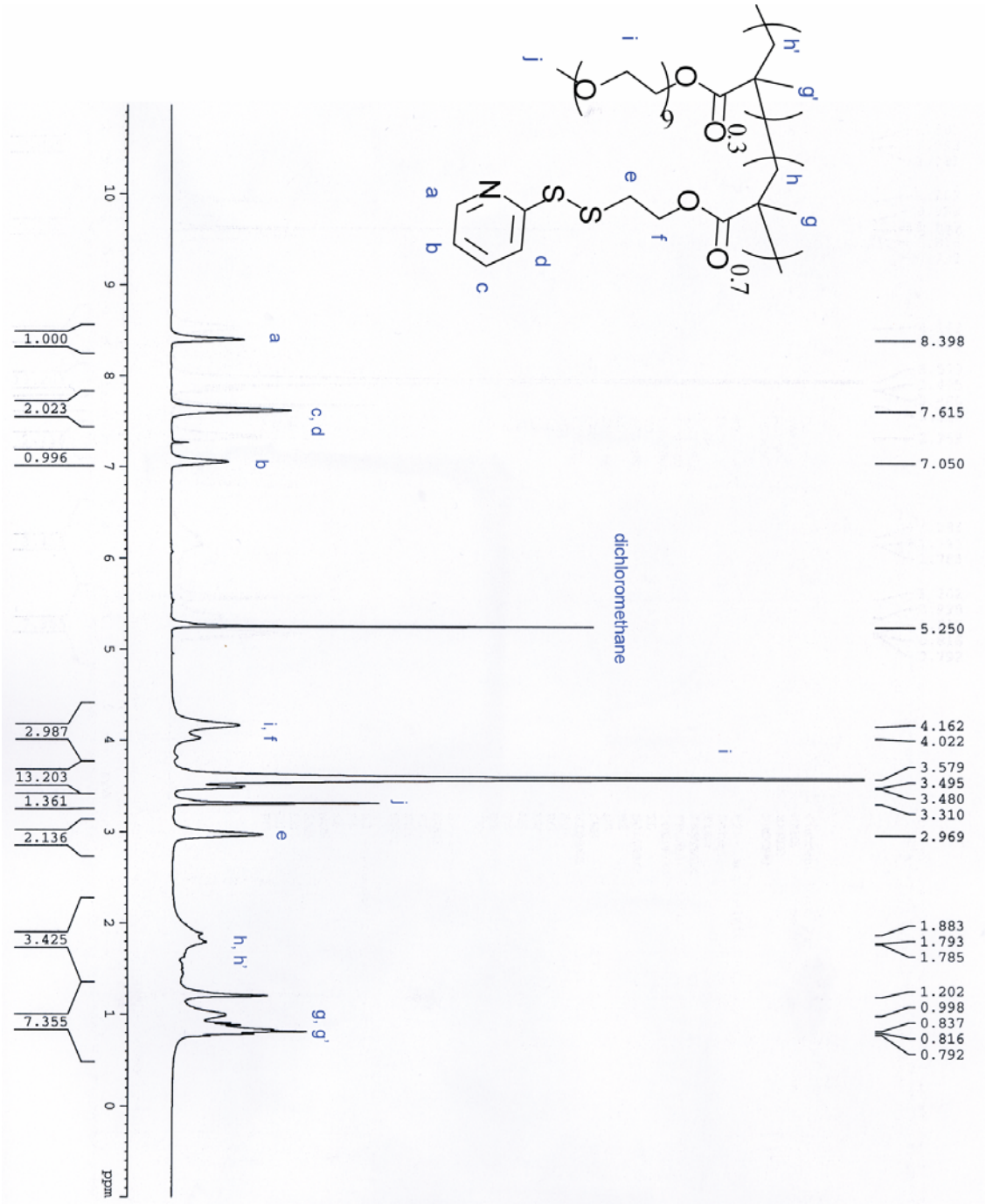

Figure 2.16: ^{1}H-NMR of the polymer 1**.**

2.5 References

1. Peer, D.; Karp, J. M.; Hong, S.; Farokhzad, O. C.; Margalit, R.; Langer, R., Nanocarriers as an emerging platform for cancer therapy. *Nat. Nanotechnol* **2007,** *2*, 751-760.

2. Haag, R., Supramolecular drug-delivery systems based on polymeric core–shell architectures. *Angew. Chem. Int., Ed.* **2004,** *43*, 278-282.

3. Allen, T. M.; Culis, P. R., Drug discovery systems: Entering the mainstream. *Science* **2004,** *303*, 1818-1822.

4. Kale, T. S.; Klaikherd, A.; Popere, B.; Thayumanavan, S., Supramolecular assemblies of amphiphilic homopolymers. *Langmuir* **2009,** *25*, 9660-9670.

5. Koo, O. M.; Rubinstein, I.; Onyuksel, H., Role of nanotechnology in targeted drug delivery and imaging: A concise review. *Nanomedicine: NBM* **2005,** *1*, 193-212.

6. Oh, J. K.; Drumright, R.; Siegwart, D. J.; Matyjaszewski, K., The development of microgels/nanogels for drug delivery applications. *Prog. Polym. Sci.* **2008,** *33*, 448-477.

7. Bachelder, E. M.; Beaudette, T. T.; Broaders, K. E.; Dashe, J.; Fréchet, J. M. J., Acetal-derivatized dextran: an acid-responsive biodegradable material for therapeutic applications. *J. Am. Chem. Soc.* **2008,** *130*, 10494-10495.

8. Lee, C. C.; MacKay, J. A.; Fréchet, J. M. J.; Szoka, F. C., Designing dendrimers for biological applications. *Nat. Biotechnol.* **2005,** *23*, 1517-1526.

9. Jeong, B.; Bae, Y. H.; Lee, D. S.; Kim, S. W., Biodegradable block copolymers as injectable drug-delivery systems. *Nature* **1997,** *388*, 860-862.

10. Maeda, H.; Wu, J.; Sawa, T.; Matsumura, Y.; Hori, K., Tumor vascular permeability and the EPR effect in macromolecular therapeutics: A review. *J. Controlled Release* **2000,** *65*, 271-284.

11. Baban, D. F.; Seymour, L. W., Control of tumour vascular permeability. *Adv. Drug Delivery Rev.* **1998,** *34*, 109-119.

12. Duncan, R., The dawning era of polymer therapeutics. *Nat. Rev. Drug Discovery* **2003,** *2*, 347-360.

13. Gillies, E. R.; Fréchet, J. M. J., Dendrimers and dendritic polymers in drug delivery. *Drug Discovery Today* **2005,** *10*, 35-43.

14. Kabanov, A. V.; Vinogradov, S., Nanogels as pharmaceutical carriers: Finite networks of infinite capabilities. *Angew. Chem. Int., Ed* **2009,** *48*, 5418-5429.

15. Kakizawa, Y.; Harada, A.; Kataoka, K., Environment-sensitive stabilization of core−shell structured polyion complex micelle by reversible cross-linking of the core through disulfide Bond. *J. Am. Chem. Soc.* **1999,** *121*, 11247-11248.

16. Aliyar, H. A.; Hamilton, P. D.; Remsen, E. E.; Ravi, N., Synthesis of polyacrylamide nanogels by intramolecular disulfide cross-linking. *J. Bioactive Compat. Polym.* **2005,** *20*, 169-181.

17. Fang, H.; Zhang, K.; Shen, G.; Wooley, K. L.; Taylor, J. A., Cationic shell-cross-linked knedel-like (cSCK) nanoparticles for highly efficient PNA delivery. *Mol. Pharmaceutics* **2009,** *6*, 615-626.

18. Sisson, A. L.; Steinhiber, D.; Rossow, T.; Welker, P.; Licha, K.; Haag, R., Biocompatible functionalized polyglycerol microgels with cell penetrating properties. *Angew. Chem. Int., Ed* **2009,** *48*, 7540-7545.

19. Talsma, S. S.; Eabensee, J.; Murthy, N.; Williams, I. R., Development and *in vitro* validation of a targeted delivery vehicle for DNA vaccines. *J. Controlled Release* **2006,** *112*, 271-279.

20. Kadlubowski, S.; Grobelny, J.; Olejniczak, W.; Cichomski, M.; Ulanski, P., Pulses of fast electrons as a tool to synthesize poly(acrylic acid) nanogels. Intramolecular cross-linking of linear polymer chains in additive-free aqueous solution. *Macromolecules* **2003,** *36*, 2484-2492.

21. Jiang, J.; Thayumanavan, S., Synthesis and characterization of amine-functionalized polystyrene nanoparticles. *Macromolecules* **2005,** *38*, 5886-5891.

22. Ryu, J.-H.; Jiwpanich, S.; Chacko, R.; Bickerton, S.; Thayumanavan, S., Surface-functionalizable polymer nanogels with facile hydrophobic guest encapsulation capabilities. *J. Am. Chem. Soc.* **2010,** *132*, 8246-8247.

23. Ryu, J.-H.; Chacko, R. T.; Jiwpanich, S.; Bickerton, S.; Babu, R. P.; Thayumanavan, S., Self-cross-linked polymer nanogels: A versatile nanoscopic drug delivery platform. *J. Am. Chem. Soc.* **2010,** *132*, 17227-17235.

24. Heffernan, M. J.; Murthy, N., Disulfide-crosslinked polyion micelles for delivery of protein therapeutics. *Ann. Biomed. Eng.* **2009,** *37*, 1993-2002.

25. Bernkop-Schnürch, A., Thiomers: A new generation of mucoadhesive polymers. *Adv. Drug Deliv. Rev.* **2005,** *57*, 1569-1582.

26. Ghosh, S.; Basu, S.; Thayumanavan, S., Simultaneous and reversible functionalization of copolymers for biological applications. *Macromolecules* **2006,** *39*, 5595-5597.

27. Murthy, N.; Thng, Y. X.; Schuck, S.; Xu, M. C.; Fréchet, J. M. J., A novel strategy for encapsulation and release of proteins: Hydrogels and microgels with acid-labile acetal cross-linkers. *J. Am. Chem. Soc.* **2002,** *124*, 12398-12399.

28. Chan, Y.; Wong, T.; Byrne, F.; Kavallaris, M.; Bulmus, V., Acid-labile core cross-linked micelles for pH-rriggered release of antitumor drugs. *Biomacromolecules* **2008,** *9*, 1826-1836.

29. Oh, J. K.; Siegwart, D. J.; Matyjaszewski, K., Synthesis and biodegradation of nanogels as delivery carriers for carbohydrate drugs. *Biomacromolecules* **2007,** *8*, 3326-3331.

30. Zhang, L.; Liu, W.; Lin, L.; Chen, D.; Stenzel, M. H., Degradable disulfide core-cross-linked micelles as a drug delivery system prepared from vinyl functionalized nucleosides via the RAFT process. *Biomacromolecules* **2008,** *9*, 3321-3331.

31. Jiang, J.; Qi, B.; Lepage, M.; Zhao, Y., Polymer micelles stabilization on demand through reversible photo-cross-linking. *Macromolecules* **2007,** *40*, 790-792.

32. Sivakumar, S.; Bansal, V.; Cortez, C.; Chong, S.-F.; Zelikin, A. N.; Caruso, F., Degradable, surfactant-free, monodisperse polymer-encapsulated emulsions as anticancer drug carriers. *Adv. Mater.* **2009,** *21*, 1820-1824.

33. Yang, J.; Chen, H.; Vlahov, I. R.; Cheng, J.-X.; Low, P. S., Evaluation of disulfide reduction during receptor-mediated endocytosis by using FRET imaging. *Proc. Natl. Acad. Sci. U.S.A.* **2006,** *103*, 13872-13877.

34. Chong, S.-F.; Chandrawati, R.; Städler, B.; Park, J.; Cho, J.; Wang, Y.; Jia, Z.; Bulmus, V.; Davis, T. P.; Zelikin, A. N.; Caruso, F., Stabilization of polymer-hydrogel capsules via thiol–disulfide exchange. *Small* **2009,** *5*, 2601-2610.

35. Jia, Z.; Wong, L.; Davis, T. P.; Bulmus, V., One-pot conversion of RAFT-generated multifunctional block copolymers of HPMA to doxorubicin conjugated acid- and reductant-sensitive crosslinked micelles. *Biomacromolecules* **2008,** *9*, 3106-3113.

36. Li, Y.; Lokitz, B. S.; Armes, S. P.; McCormick, C. L., Synthesis of reversible shell cross-linked micelles for controlled release of bioactive agents. *Macromolecules* **2006,** *39*, 2726-2728.

37. Bauhuber, S.; Hozsa, C.; Breunig, M.; Cöpferich, A., Delivery of nucleic acids via disulfide-based carrier systems. *Adv. Mater.* **2009,** *21*, 3286-3306.

38. Wu, A. M.; Senter, P. D., Arming antibodies: Prospects and challenges for immunoconjugates. *Nat. Biotechnol.* **2005,** *23*, 1137-1146.

39. Bae, K. H.; Mok, H.; Park, T. G., Synthesis, characterization, and intracellular delivery of reducible heparin nanogels for apoptotic cell death. *Biomaterials* **2008,** *29*, 3376-3383.

40. Li, Y.-L.; Zhu, L.; Liu, Z.; Cheng, R.; Meng, F.; Cui, J.-H.; Ji, S.-J.; Zhong, Z., Reversibly stabilized multifunctional dextran nanoparticles efficiently deliver doxorubicin into the nuclei of cancer cells. *Angew. Chem. Int., Ed* **2009,** *48*, 9914-9918.

41. Moskaug, J. O.; Sandvig, K.; Olsnes, S., Cell-mediated reduction of the interfragment disulfide in nicked diphtheria toxin. *J. Biol. Chem.* **1987,** *262*, 10339-10345.

42. Lai, J. t.; Filla, D.; Shea, R., Functional polymers from novel carboxyl-terminated trithiocarbonates as highly efficient RAFT agents. *Macromolecules* **2002,** *35*, 6754-6756.

CHAPTER 3

NONCOVALENT ENCAPSULATION STABILITIES IN SUPRAMOLECULAR NANOASSEMBLIES

3.1 Introduction

The complications faced in the administration of insoluble and toxic hydrophobic drugs to target sites have spurred tremendous interest in the field of delivery vehicle design.(Allen and Culis 2004; Farokhzad and Langer 2009) Of the many factors considered in such design, the encapsulation stability of the delivery container is critical.(Savić, Eisenberg et al. 2006; Chen, Kim et al. 2008; Chen, Kim et al. 2008) Encapsulation of a hydrophobic molecule in aqueous media itself is just an indicator of the thermodynamic distribution of the molecules between the container and the bulk solvent. This does not provide indications on the stability of encapsulation in terms of the dynamics of guest exchange with the bulk media. Understanding the dynamics of interchange between the bulk solvent and the nanocontainer is crucial, as this carries clear implications to the potential leakage of encapsulated guest molecules from the vehicles as they pass through a biological system. Thus, an analysis of this process is necessary for optimization of the design and construction of drug delivery carriers.

To probe the stability of encapsulation, we describe here the dynamics of encapsulated guest interchange in nanocarriers using Fluorescence Resonance Energy Transfer (FRET) as a tool. We then utilize this method to investigate the stability of encapsulation in a new class of polymer nanogels and compare it with that observed in classical amphiphilic nanoassemblies.(Jiwpanich, Ryu et al. 2010)

A lipophilic FRET pair, 3,3'-dioctadecyloxacarbocyanine (DiO, donor) and 1,1'-dioctadecyl-3,3,3',3'-tetramethylindocarbocyanine perchlorate (DiI, acceptor), were used for this purpose. These two dye molecules were independently sequestered in nanocarriers. When the solutions containing the dye molecules were mixed, two limiting scenarios are possible (Figure 3.1). If the dye molecules are stably encapsulated and do not exchange the guest molecules with the bulk solvent environment, then the two dye molecules will continue to be in two separate nanocontainers. If this is the case, no FRET will be observed since the distance between the two dye molecules is much higher than their Förster radius. However, if there is a significant exchange of the guest molecules between the container interior and the bulk solvent when the two solutions are mixed, it is likely that the dye molecules will equilibrate between the two containers due to the indistinguishable nature of all nanocarriers in solution. The resulting equilibration will cause DiI and DiO molecules to occupy the same container, leading to increased FRET. Thus, tracing the evolution of FRET in such systems provides insight into the dynamics of guest interchange and potential carrier leakage.

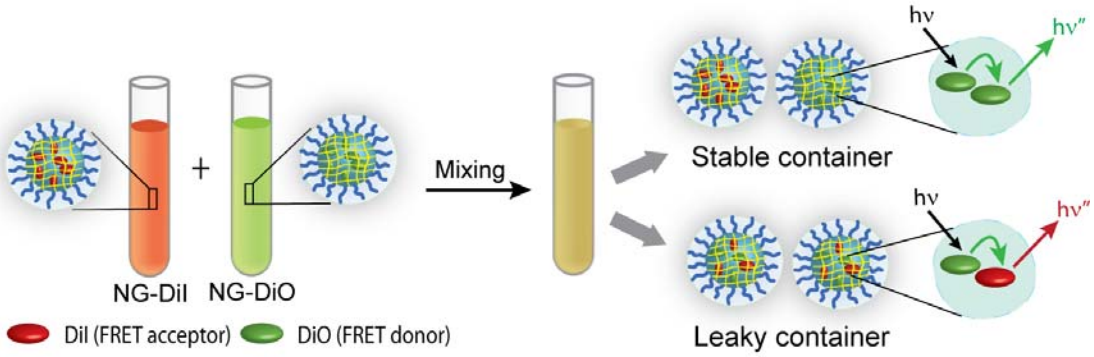

Figure 3.1: Mixed nanogels encapsulating DiI/DiO and their FRET behavior.

3.2 Results and Discussion

3.2.1 Design and Synthesis

We sought to investigate the versatility of such an approach using cross-linked polymeric nanogels. The reason for this choice is the assertion that variations in cross-linking densities provide a method for tuning encapsulation stabilities and thus an opportunity to test our FRET-based strategy. Understandably, this feature also renders nanogels to be of great interest for controlled release applications in the area of pharmaceutical and biomedical research.(Byrne, Park et al. 2002; Kopeček 2002; Hamidi, Azadi et al. 2008; Kabanov and Vinogradov 2009) Generating water-soluble polymeric nanogels that encapsulate lipophilic molecules can be cumbersome. However, we have recently introduced a new emulsion-free method for nanogel preparation in aqueous solution described in Chapter 2 that also provides for facile hydrophobic guest encapsulation (Figure 1b).(Ryu, Chacko et al. 2010; Ryu, Jiwpanich et al. 2010)

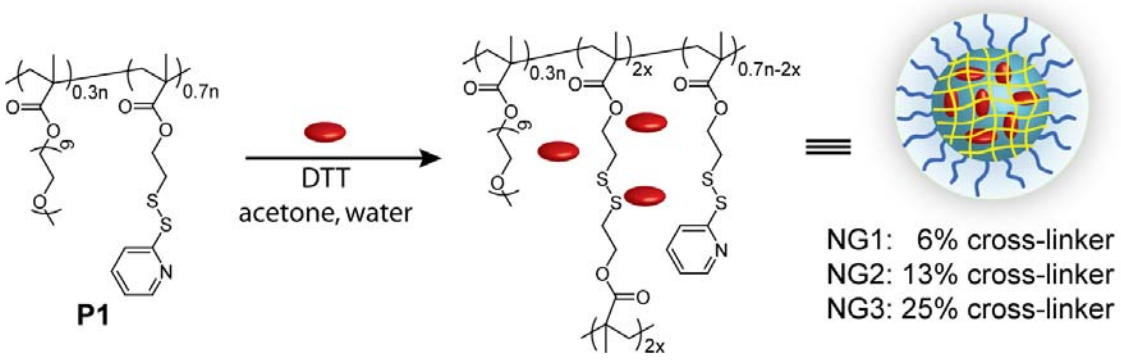

Scheme 3.1: Synthesis of nanogels containing hydrophobic guest molecules.

To probe the guest exchange dynamics, aqueous solutions of **NG1** (6% crosslinked; ~200 nm in size) containing 1 wt% DiO or 1 wt% DiI were prepared by *in*

situ loading (Scheme 3.1). The two solutions containing the separate dyes, referred as NG1-DiO and NG1-DiI, were then mixed in water. Fluorescence from the DiO excitation (450 nm) was monitored over time. The evolution of FRET was obtained by tracing the decrease in the donor (DiO) emission and concurrent increase in acceptor's (DiI). The results show that there is a gradual equilibration of the dye molecules over a 48 hour period (Figure 3.2). Interestingly, the thermodynamic distribution of the dye molecule significantly favors the nanogel interior, as discerned by the overall concentration of the otherwise insoluble dyes in the aqueous phase.[6] Thus, the continuous interchange of the dyes among the nanocarriers is responsible for observed enhancement in FRET.

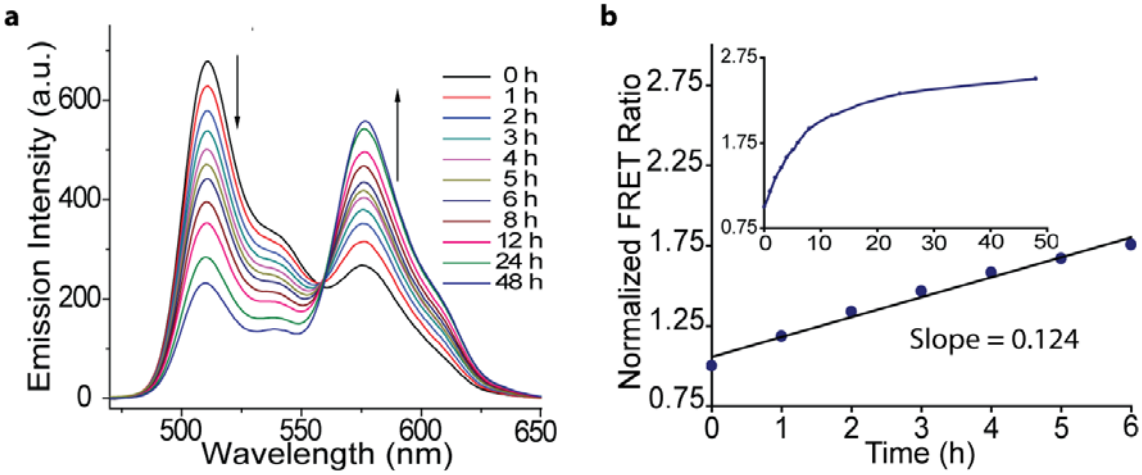

Figure 3.2: (a) Fluorescence emission spectra of mixed NG1 encapsulating DiI/DiO. (b) Plot of FRET ratio *vs* time.

The FRET ratio $I_a/(I_d+I_a)$, where I_a and I_d are the fluorescence intensities of the acceptor (DiI) and the donor (DiO) respectively, was plotted against time (Figure 3.2). The slope of the linear fit is related to the dynamics of the guest exchange and we

define this as the leakage coefficient (Λ), which was found to be about 0.124 h^{-1} for the first six hours in **NG1** (Figure 3.2).

3.2.2 Tuning Encapsulation Stability

We envisaged that cross-linking density could be used to tune the rate of exchange/leakage. The preparation method indeed allows for control over the degree of cross-linking.(Ryu, Chacko et al. 2010; Ryu, Jiwpanich et al. 2010) Accordingly, nanogels **NG1**, **NG2**, and **NG3**, with cross-linking densities of 6%, 13%, and 25% respectively, with encapsulated DiI and DiO were prepared. DLS studies reveal that the structures obtained are all about 200 nm in size (Figure 3.3)

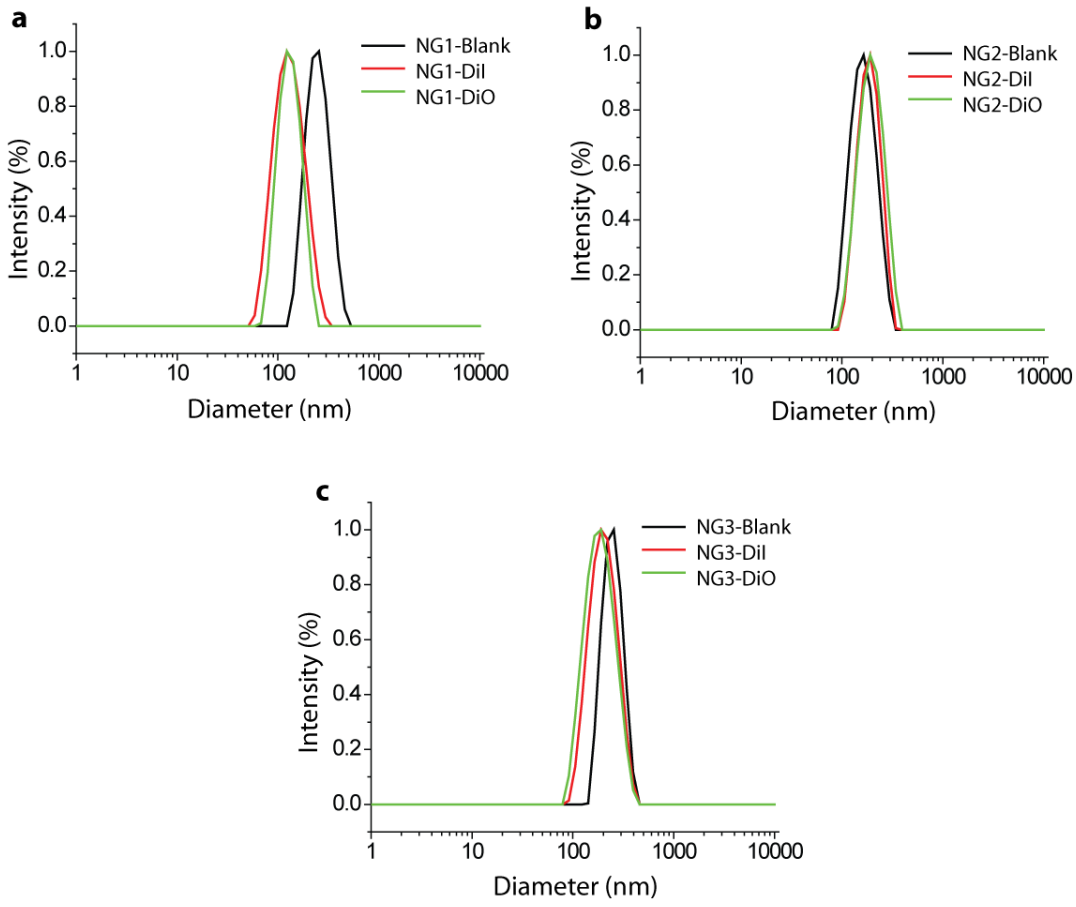

Figure 3.3: DLS traces of nanogels (a) NG1, (b) NG2, (c) NG3.

Dynamics of guest interchange were monitored and the FRET ratios were plotted against time. The leakage coefficient (Λ) in supramolecular nanoassemblies was calculated as shown in Table 3.1. **NG2** and **NG3** exhibited minimal exchange over 6 hours at an Λ of 0.011 h^{-1} or below, compared to 0.124 h^{-1} for **NG1** (Figures 3.4). These results suggest that degree of cross-linking is effective in tuning guest exchange dynamics. Since the precursor polymer **P1** itself is capable of encapsulating DiO and DiI, we were interested in evaluating the exchange dynamics before and after cross-linking. **P1** exhibited a Λ of 0.739 after mixing, indicating rapid guest interchange as compared to the cross-linked nanogels (Figure 3.4).

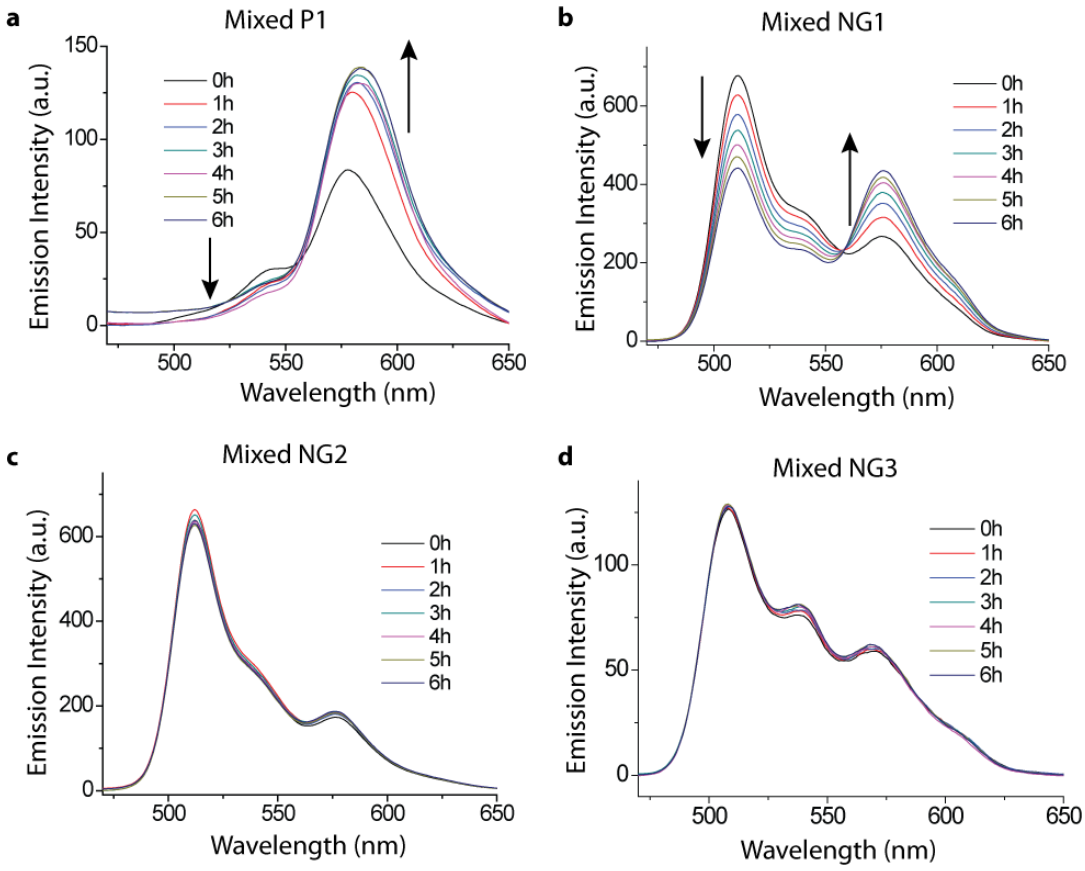

Figure 3.4: FRET behavior of mixed nanocontainers encapsulating DiI/DiO: (a) P1, (b) NG1, (c) NG2, (d) NG3.

3.2.3 Encapsulation Stability of Supramolecular Nanoassemblies

The key motivation in developing these experiments is to develop a screening method for probing exchange dynamics, and thus the potential, of drug delivery vehicles. Therefore, we were interested in investigating the guest exchange characteristics of other supramolecular assemblies that are known to encapsulate lipophilic guest molecules (Chart 3.1).

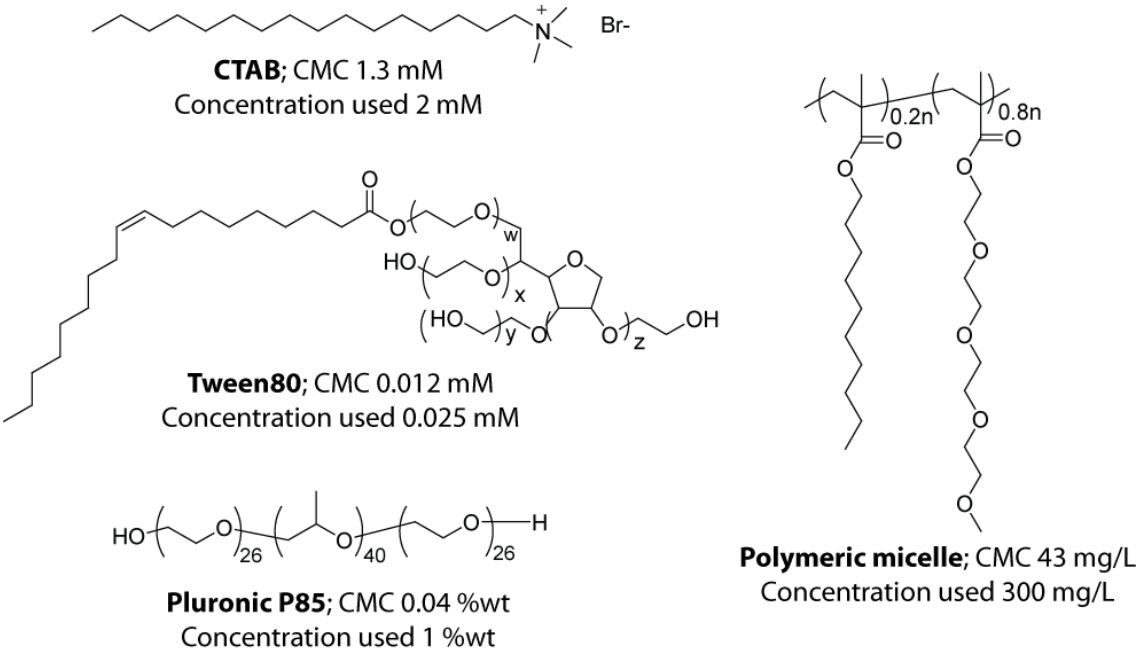

Chart 3.1: Structures of surfactants.

The simplest supramolecular assembly that encapsulates lipophilic guest molecules involves small molecule surfactant-based micelles (Chart 3.1).(Kabanov, Nazarova et al. 1995; Savriar, Ghosh et al. 2008; Ryu, Roy et al. 2010) Accordingly, we encapsulated DiO and DiI in CTAB (cetyl trimethylammonium bromide) and Tween80 micelles and carried out the FRET experiments. Complete equilibration of the dye molecules was observed instantaneously upon mixing the DiO and DiI based micelles with the FRET ratios of 0.850 and 0.501 respectively (Figure 3.5).

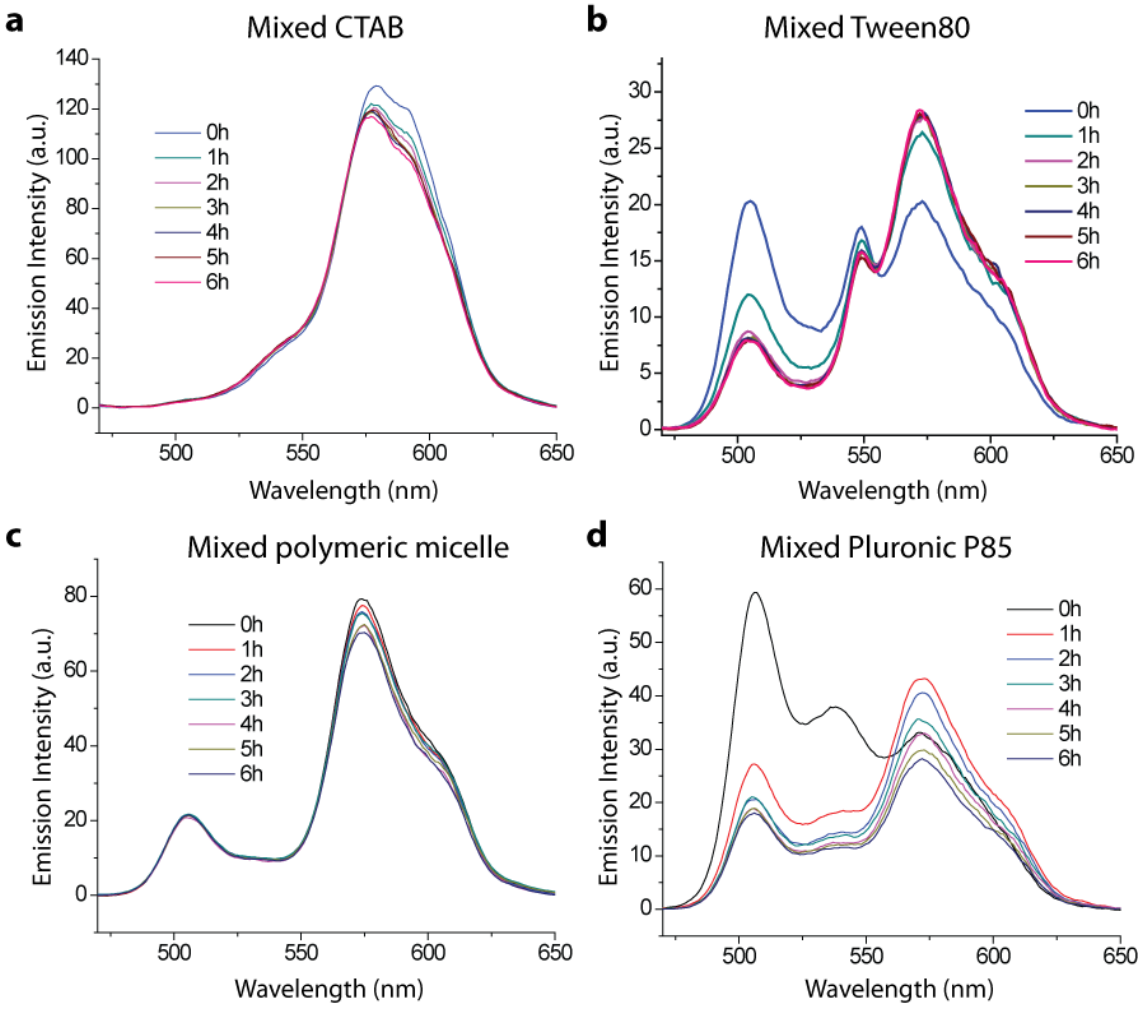

Figure 3.5: Fluorescence spectra (λex = 450 nm) of mixed containers encapsulating DiI and DiO; (a) CTAB, (b) Tween80, (c) Amphiphilic random copolymer, (d) Block copolymer Pluronic P85.

Since the nanogels are based on polymers, we also investigated other polymer-based nanoassemblies. We measured the guest exchange dynamics of an amphiphilic random copolymer (structure shown in Chart 3.1).(Ryu, Roy et al. 2010) The guest exchange rate in these assemblies was found to be 0.788 (Figure 3.5). Similarly, the encapsulation stability of pluronic block copolymer micellar assemblies,(Kabanov, Batrakova et al. 2002; Sharma and Bhatia 2004; Batrakova and Kabanov 2008) which are widely used in biomedical applications, exhibited an Λ of 0.358 (Figure 3.5). This is

slower than assemblies based on small molecule surfactants and random copolymers, but faster than the nanogels.

Table 3.1: Leakage coefficient (Λ) in supramolecular nanoassemblies.

Supramolecular nanoassemblies	Leakage coefficient (Λ), h^{-1}
NG1	0.124
NG2	0.011
NG3	0.005
P1	0.739
CTAB	0.850
Tween80	0.501
Random copolymer micelles	0.788
Pluronic® P85	0.358

3.2.4 Triggering Release by External Stimului (GSH)

The results above suggest that the crosslinked polymer nanogels exhibit high encapsulation stability and the leakage dynamics can be tuned by varying the crosslinking density. While encapsulation stability is important, a practical delivery vehicle must also be able to release its contents in response to a biologically-relevant stimulus. As the nanogels consist of biodegradable disulfide crosslinkers, the release of encapsulated molecules can be potentially triggered upon exposure to reducing agents.

To test this possibility, we utilized **NG2** that exhibited very stable encapsulation. Glutathione (GSH, 10 mM), a disulfide reducing agent present at higher concentrations inside cells, was added to the solution containing NG2-DiO and NG2-DiI after 2.5 h. Significant increase of the FRET ratio was observed at this point (Figure 3a and 3b). This is presumably caused by dye leakage upon cleavage of the disulfide crosslinkers due to the presence of GSH, which loosens the gel and reduces encapsulation stability.

Moreover, significant decreases in the emission intensities of the individual dyes indicate that the GSH reaction reduces the distribution coefficient of these dyes as well (Figure 3.11). These results, combined with experiments with **NG3**, confirm that the dynamics of guest interchange can be controlled by crosslinking density and that drug release can be externally triggered (Figure 3.6).

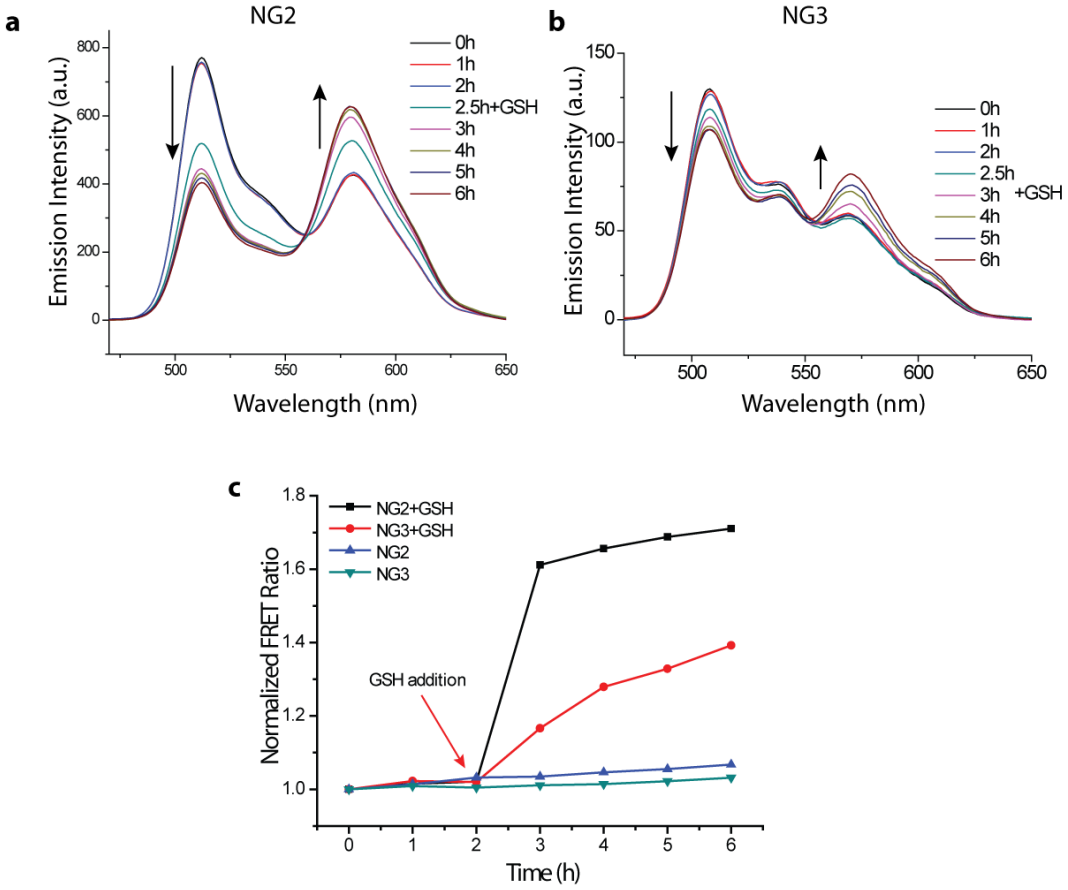

Figure 3.6: Release of dye from mixed nanogels encapsulating DiI/DiO with the addition of GSH (10 mM) at 2.5 h: (a) NG2, (b) NG3, (c) dynamics of dye exchange in the presence/absence of GSH (10 mM).

3.3 Summary

In summary, we have developed on a FRET-based method to monitor the guest exchange dynamics in water-soluble nanoassemblies, which provides insight into the

leakage characteristics of these nanocontainers. We have thus defined a leakage coefficient parameter, Λ, from the FRET experiments and analyzed this value for a variety of nanoassemblies. We find that the guest exchange is slower in crosslinked polymer nanogels and that this can be conveniently tuned by altering the degree of crosslinking. We have also investigated the relative guest exchange rates in other amphiphilic nanoassemblies. We find that while pluronic block copolymers exhibit higher encapsulation stabilities compared to small molecules and random copolymers, they do not compare to those offered by crosslinked polymer nanogels. In addition, we show that the stably encapsulated guests in the nanogels can be released in response to an external trigger. The dyes employed model the hydrophobic nature of efficacious drug molecules that commonly face solubility issues during administration. Thus, understanding the dynamics of encapsulated guest exchange between nanocarriers, using this method, provides a useful starting point for evaluating viable drug delivery vehicles. Moreover, the exchange dynamics provide information on the possibility of utilizing a vehicle to deliver multiple drugs in separate containers with timed release. These FRET-based studies also highlight the advantages of the newly developed polymeric nanogels in drug delivery applications.

3.4 Experimental

Materials and Methods

All chemicals and solvents were purchased from commercial sources and were used as received, unless otherwise mentioned. Pluronic block copolymer P85 (lot no. WPDF512B) was provided as a gift by the BASF corporation (Mount Olive, NJ). Polymer **P1** was synthesized by RAFT polymerization and then purified by

precipitation. S-dodecyl-S'-2-(2,2-dimethylacetic acid) trithiocarbonate and pyridyldisulfide ethylmethacrylate (PDSEMA) was prepared using a previously reported procedure.(Lai, Filla et al. 2002; Ghosh, Basu et al. 2006) ^{1}H-NMR spectra were recorded on a 400 MHz Bruker NMR spectrometer using the residual proton resonance of the solvent as the internal standard. Chemical shifts are reported in parts per million (ppm). Molecular weights of the polymers were estimated by gel permeation chromatography (GPC) using PMMA standard with a refractive index detector. Dynamic light scattering (DLS) measurements were performed using a Malvern Nanozetasizer. UV-visible absorption spectra were recorded on a Varian (model EL 01125047) spectrophotometer. The fluorescence spectra were obtained from a JASCO FP-6500 spectrofluorimeter. Transmission electron microscopy (TEM) images were taken using a JEOL 100CX at 100 KV.

Synthesis of random copolymer (P1):

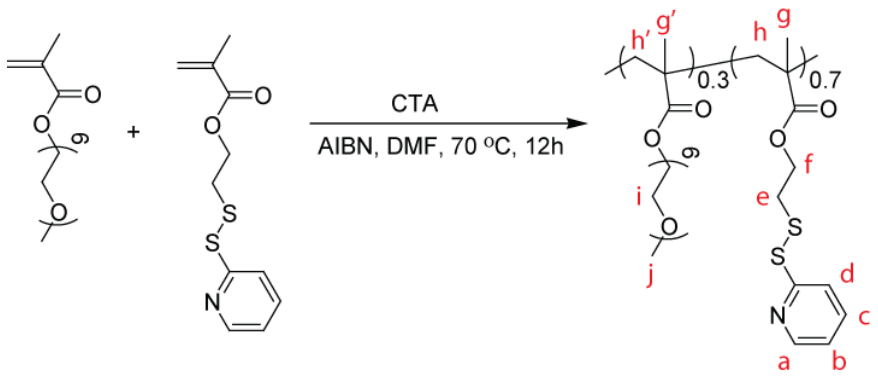

The polymer (**P1**) was synthesized by similar method which is published elsewhere.(Ryu, Jiwpanich et al. 2010) Briefly, a mixture of S-dodecyl-S'-2-(2,2-dimethylacetic acid) trithiocarbonate (90 mg, 0.3 mmol), PDSEMA (5 g, 20 mmol), polyethylene glycol monomethyl ether methacrylate (Mw 450) (4g, 8 mmol) and AIBN (10 mg, 0.06 mmol) were dissolved in DMF (10 mL) and degassed by performing three freeze-pump-thaw cycles. The reaction mixture was sealed and then transferred into a pre-heated oil bath at 70 °C for 12 h. The resultant mixture was dissolved in dichloromethane (5 mL) and precipitated in hexane (200 mL). To remove unreacted monomers, the precipitate was further dissolved in dichloromethane (5 mL) and reprecipitated in ether (200 mL) to yield the random copolymer as a waxy substance. Yield: 78%. GPC (THF) M_n: 24.7 K. PDI: 1.6. ^{1}H NMR (400 MHz, $CDCl_3$) δ: 8.40 (a), 7.62 (c, d), 7.05 (b), 4.16-4.02 (i, f), 3.58-3.48 (i), 3.31 (j), 2.97 (e), 2.04-1.65 (h, h'), 1.24-0.72 (g, g'). The molar ratio between the two blocks was determined by integrating the methoxy proton in the polyethylene glycol unit and the aromatic proton in the pyridine and found to be 3:7 (PEO:PDSEMA). The molar ratio between the two blocks was determined by integrating the methoxy proton in the polyethylene glycol unit and the aromatic proton in the pyridine and found to be 3:7 (PEO:PDSEMA).

Synthesis of nanogels contaning DiI/DiO:

The polymer (2 mg) and DiI or DiO (0.02 mg) were dissolved in 200 µL of acetone and a measured amount of DTT (0.4 µmol, 0.8 µmol and 2.0 µmol for 10 mol%, 20 mol% and 50 mol% against PDS groups, respectively) was added. The solution color changed to yellow, indicative of the production of pyridinethione byproduct of PDS cleavage. After stirring for 10 min, 1 mL of deionized water was added and the mixed solution was stirred overnight at room temperature, open to the atmosphere allowing the organic solvent to evaporate. Insoluble DiI/DiO was removed by filtration and pyridinethione was removed from the nanogel solution by extensive dialysis using a membrane with a molecular weight cutoff of 10,000 g/mol.

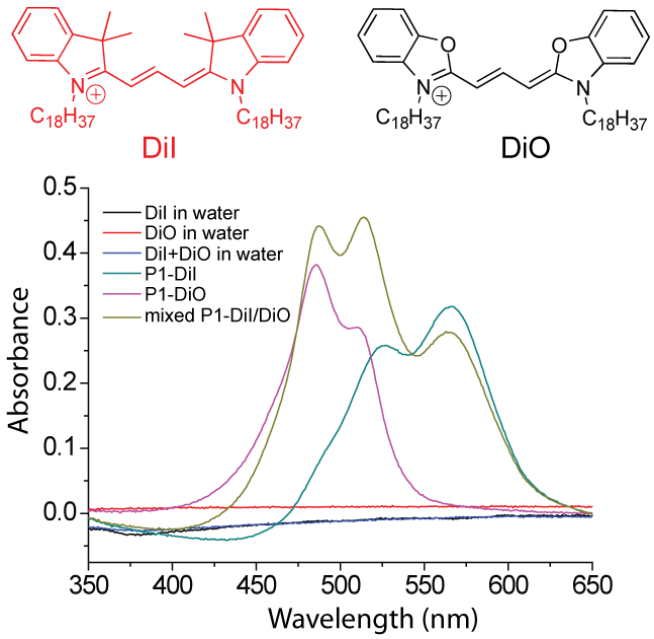

Figure 3.7: Absorption spectra of DiI/DiO in water and in polymer solution.

DLS measurement:

Dynamic light scattering (DLS) measurements were performed using a Malvern Nanozetasizer. The light source was solid-stat laser system, operating at 514 nm. The nanogels in deionized water (1mg/mL) was kept constant at 25 °C throughout the experiment. Dust was eliminated by filtering the solution through 0.45 µm filter. All the measurements were done at a correlation time of 30 seconds.

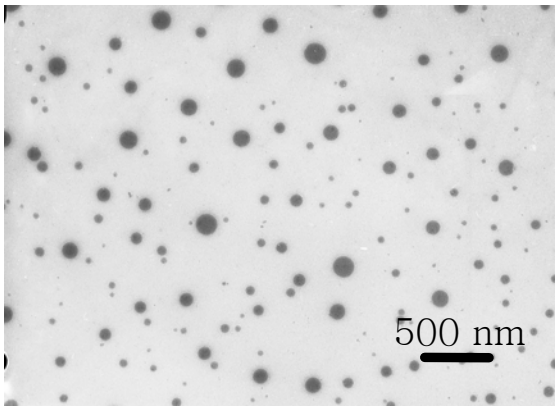

Figure 3.8: TEM image of nanogel (NG2).

Micelle encapsulated dye (DiI/DiO) preparation:

A stock solution of dye (3 mg/mL) in acetone was taken (13 µL) in a vial and the solvent was evaporated by a mild blow of argon gas. To this vial, a 2 mL solution of the surfactant (concentration well above CMC: CTAB = 2 mM; tween80 =0.03 mM, polymer micelle = 300 mg/L; Pluronic P85 = 1%wt) was added and the solution was sonicated for 30 minutes to encapsulate the dye. Insoluble DiI/DiO was removed by filtering the solution through 0.45 µm filter.

Nanogel encapsulated dye mixing:

A solution of nanogel containing DiI (100 µL) was mixed with a solution of nanogel containing DiO (100 µL) in a cuvette, and then milliQ water (800 µL) was added to adjust the volume. The fluorescence intensity was recorded at 450 nm excitation wavelength.

Nanogel encapsulated dye mixing in the presence of GSH:

A solution of nanogel containing DiI (100 µL) was mixed with a solution of nanogel containing DiO (100 µL), and milliQ water (800 µL) in a cuvette. GSH (3 mg) was added to the mixed solution at 2.5 hours of mixing. The fluorescence intensity was recorded at 450 nm excitation wavelength at time interval.

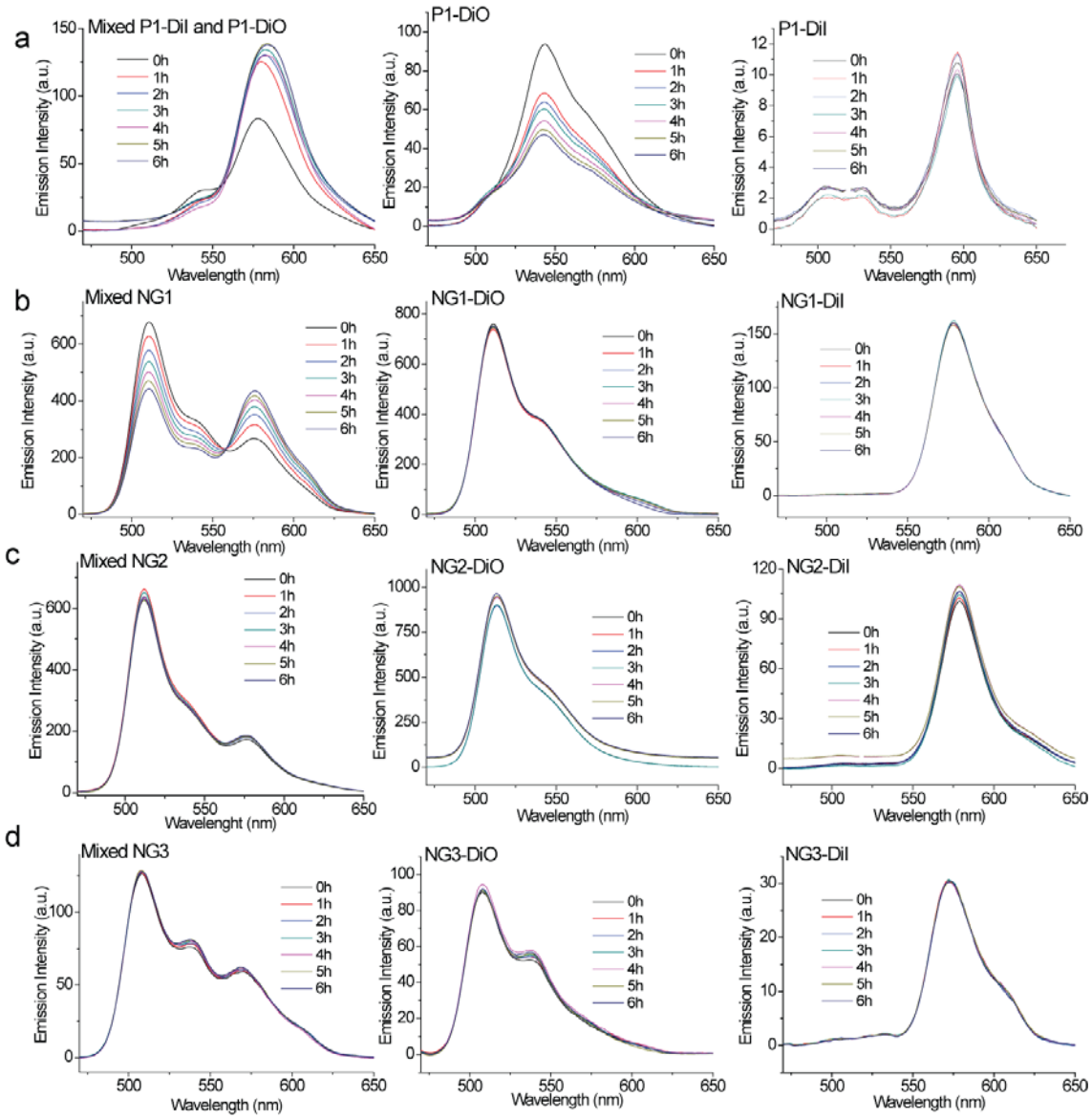

Figure 3.9: Fluorescence spectra (λ_{ex} = 450 nm) of mixed nanogels (left), nanogel containing DiO (middle) and nanogel containing DiI (right); (a) non-crosslinked polymer (P1), (b) NG1, (c) NG2, and (d) NG3.

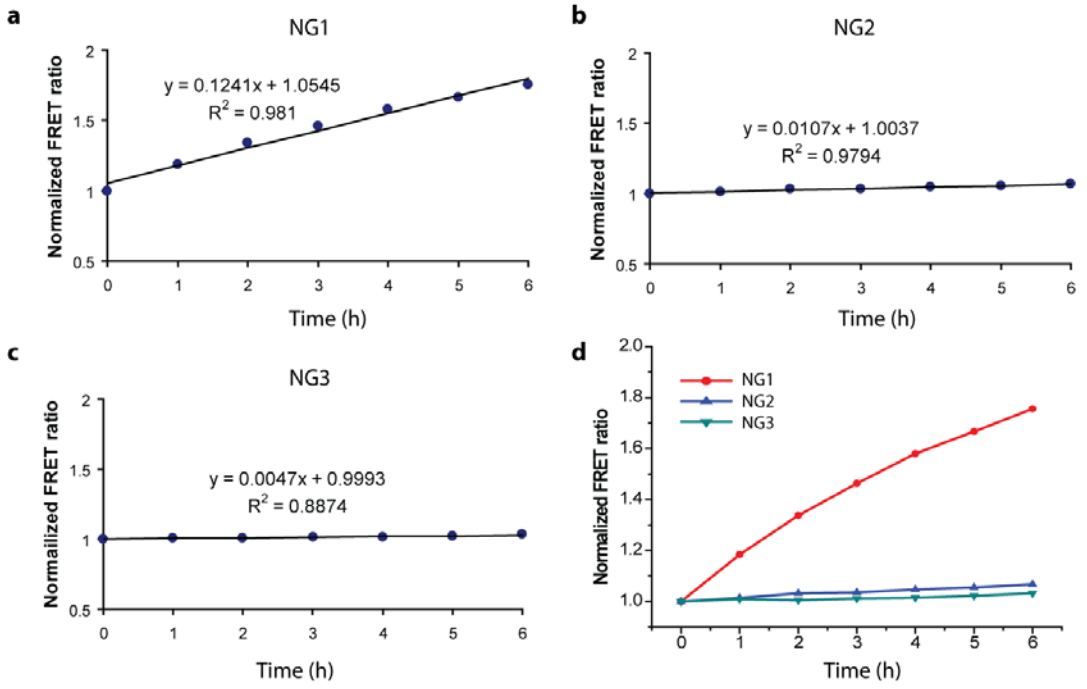

Figure 3.10: Plot of normalized FRET ratio *vs* time of (a) NG1, (b) NG2, (c) NG3, (d) comparing the dynamics of leakage/interchange of NG1, NG2, and NG3.

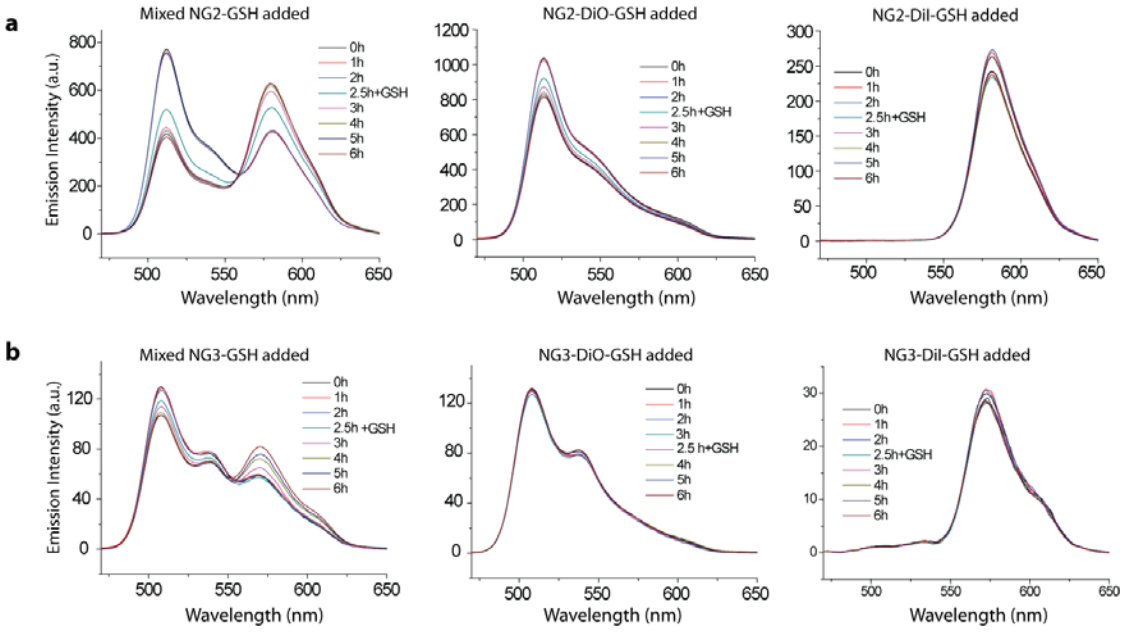

Figure 3.11: Fluorescence spectra (λ_{ex} = 450 nm) of mixed nanogels (left), nanogel containing DiO (middle) and nanogel containing DiI (right) with GSH (10 mM) added at 2.5h; (a) NG2, and (b) NG3.

Micelle encapsulated dye mixing:

A solution of micelle containing DiI (0.5 mL) was added to a solution of micelle containing DiO (0.5 mL). The fluorescence intensity was recorded at 450 nm excitation wavelength.

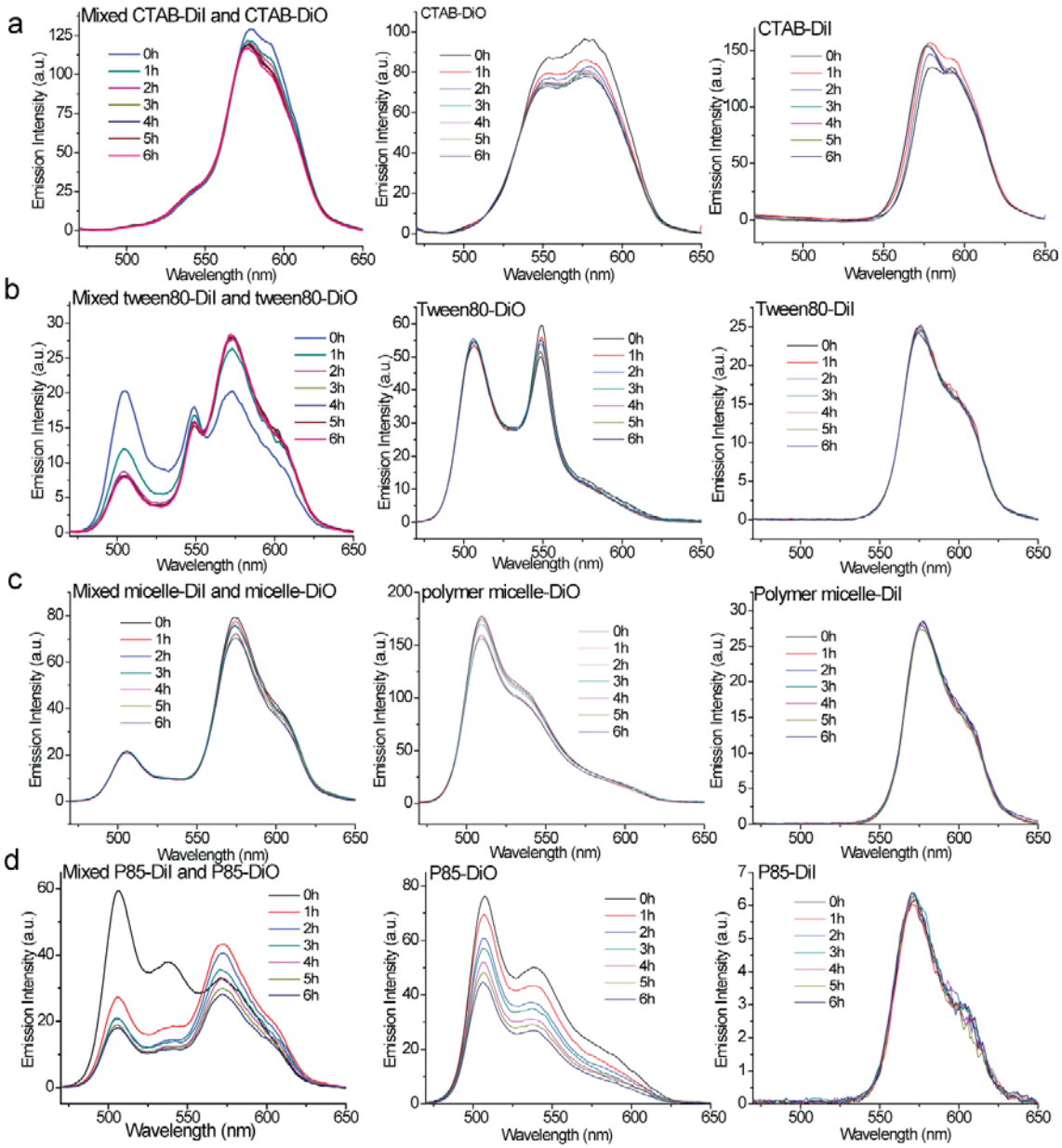

Figure 3.12: Fluorescence spectra (λex = 450 nm) of mixed micelle containing DiI and DiO (left), micelle containg DiO (middle), and micelle containing DiI (right); (a) CTAB, (b) Tween80, (c) Amphiphilic random copolymers, and (d) Pluronic P85.

3.5 References

1. Farokhzad, O. C.; Langer, R., Impact of nanotechnology on drug delivery. *ACS Nano* **2009,** *3*, 16-20.

2. Allen, T. M.; Culis, P. R., Drug discovery systems: Entering the mainstream. *Science* **2004,** *303*, 1818-1822.

3. Savić, R.; Eisenberg, A.; Maysinger, D., Block copolymer micelles as delivery vehicles of hydrophobic drugs: Micelle–cell interactions. *J. Drug. Target.* **2006,** *14*, 343-355.

4. Chen, H.; Kim, S.; Li, L.; Wang, S.; Park, K.; Cheng, J.-X., Release of hydrophobic molecules from polymer micelles into cell membranes revealed by förster resonance energy transfer imaging. *Proc. Natl. Acad. Sci. U.S.A.* **2008,** *105*, 6596-6601.

5. Chen, H.; Kim, S.; He, W.; Wang, H.; Low, P. S.; Park, K.; Cheng, J.-X., Fast release of lipophilic agents from circulating PEG-PDLLA micelles revealed by *in vivo* förster resonance energy transfer imaging. *Langmuir* **2008,** *24*, 5213-5217.

6. Jiwpanich, S.; Ryu, J.-H.; Bickerton, S.; Thayumanavan, S., Noncovalent encapsulation stabilities in supramolecular nanoassemblies. *J. Am. Chem. Soc.* **2010,** *132*, 10683-10685.

7. Byrne, M. E.; Park, K.; Peppas, N. A., Molecular imprinting within hydrogels. *Adv. Drug Deliv. Rev.* **2002,** *54*, 149-161.

8. Kabanov, A. V.; Vinogradov, S., Nanogels as pharmaceutical carriers: Finite networks of infinite capabilities. *Angew. Chem. Int. Ed* **2009,** *48*, 5418-5429.

9. Kopeček, J., Polymer chemistry: Swell gels. *Nature* **2002,** *417*, 388-391.

10. Hamidi, M.; Azadi, A.; Rafiei, P., Hydrogel nanoparticles in drug delivery. *Adv. Drug Deliv. Rev.* **2008,** *60*, 1638-1649.

11. Ryu, J.-H.; Jiwpanich, S.; Chacko, R.; Bickerton, S.; Thayumanavan, S., Surface-functionalizable polymer nanogels with facile hydrophobic guest encapsulation capabilities. *J. Am. Chem. Soc.* **2010,** *132*, 8246-8247.

12. Ryu, J.-H.; Chacko, R. T.; Jiwpanich, S.; Bickerton, S.; Babu, R. P.; Thayumanavan, S., Self-cross-linked polymer nanogels: A versatile nanoscopic drug delivery platform. *J. Am. Chem. Soc.* **2010,** *132*, 17227-17235.

13. Savriar, E. N.; Ghosh, S.; González, D. C.; Thayumanavan, S., Disassembly of noncovalent amphiphilic polymers with proteins and utility in pattern sensing. *J. Am. Chem. Soc.* **2008,** *130*, 5416-5417.

14. Ryu, J.-H.; Roy, R.; Ventura, J.; Thayumanavan, S., Redox-sensitive diassembly of amphiphilic copolymer based micelles. *Langmuir* **2010,** *26*, 7086-7092.

15. Kabanov, A. V.; Nazarova, I. R.; Astafieva, I. V.; Batrakova, E. V.; Alakhov, V. Y.; Yaroslavov, A. A.; Kabanov, V. A., Micelle formation and solubilization of fluorescent probes in poly(oxyethylene-b-oxypropylene-b-oxyethylene) solutions. *Macromolecules* **1995,** *28*, 2303-2314.

16. Batrakova, E. V.; Kabanov, A. V., Pluronic block copolymers: Evaluation of drug delivery concept from inert nanocarriers to biological response modifiers. *J. Controlled Release* **2008,** *130*, 98-106.

17. Kabanov, A. V.; Batrakova, E. V.; Alakhov, Y., Pluronic® block copolymers for overcoming drug resistance in cancer. *Adv. Drug Deliv. Rev.* **2002,** *54*, 759-779.

18. Sharma, P. K.; Bhatia, S. R., Effect of anti-inflammatories on pluronic® F127: Micellar assembly, gelation and partitioning. *Int. J. Pharm.* **2004,** *278*, 361-377.

19. Ghosh, S.; Basu, S.; Thayumanavan, S., Simultaneous and reversible functionalization of copolymers for biological applications. *Macromolecules* **2006,** *39*, 5595-5597.

20. Lai, J. t.; Filla, D.; Shea, R., Functional polymers from novel carboxyl-terminated trithiocarbonates as highly efficient RAFT agents. *Macromolecules* **2002,** *35*, 6754-6756.

CHAPTER 4

TUNING LOADING CAPACITY AND ENCAPSULATION STABILITY

4.1 Introduction

Nearly one-third of newly discovered drug compounds are highly insoluble in water.(Lipinski 2000) However, designing water-soluble, nanoscopic drug delivery vehicles to non-covalently encapsulate such lipophilic molecules and stably transfer them to target sites still stands as a significant challenge.(Allen and Culis 2004; Torchilin 2004; Farokhzad and Langer 2009) For drugs administered orally or through systemic injection, this challenge must be overcome, as low aqueous solubility severely limits bioavailability and causes non-specific accumulation in healthy tissues that gives rise to adverse side effects.(Lipinski, Lombardo et al. 2001; Savić, Eisenberg et al. 2006)

Self-assembling polymer micelles are one promising scaffold for lipophilic drug formulation due to their core-shell structure that allows for the sequestration of lipophilic molecules into a hydrophobic core that is surrounded by a water-soluble corona.(Kabanov, Nazarova et al. 1995; Torchilin 2004; Matsumura 2008; Kale, Klaikherd et al. 2009) However, polymer micelles exhibit inherent stability issues derived from their concentration-dependent stabilities.(Bae and Yin 2008; Jiwpanich, Ryu et al. 2010) The requisite concentration for micelle formation (CMC) severely limits the potential for the use of micelles *in vivo*, as mass dilution during biodistribution will cause gradual disintegration of the assemblies into their polymer constituents.(Chen, Kim et al. 2008; Kim, Shi et al. 2010) Additionally, interactions

between micelles and biological components will likely compromise the integrity of the self-assembling particles, resulting in undesirable release of encapsulated guest molecules at off-target sites.(Chen, Kim et al. 2008) Furthermore, as discussed in Chapter 3, the encapsulation stability of hydrophobic compounds sequestered in micellar assemblies has been shown to be relatively poor.(Jiwpanich, Ryu et al. 2010)

The chemically cross-linked counterparts of polymer micelles, polymer nanogels, offer the potential to overcome these issues.(Hamidi, Azadi et al. 2008; Oh, Drumright et al. 2008; Kabanov and Vinogradov 2009; Raemdonck, Demeester et al. 2009; Ryu, Chacko et al. 2010; Vinogradov 2010) We have described in Chapter 2 that our synthetic method for self-cross-linked polymer nanogels provides an alternative carrier scaffold that affords the noncovalent trapping of lipophilic molecules in aqueous media with high encapsulation stability.(Jiwpanich, Ryu et al. 2010; Ryu, Chacko et al. 2010; Ryu, Jiwpanich et al. 2010) In this Chapter, we are particularly interested in optimizing our cross-linked polymer nanogel system for the solubilization of lipophilic guests by tuning the hydrophobicity of the nanogel network. We describe the effect of varying the lipophilic content of the polymer nanogels on observed loading capacities and encapsulation stabilities. We hypothesized that increasing hydrophobicity in nanogel interior would enhance the loading capacity and efficiency for lipophilic molecules.

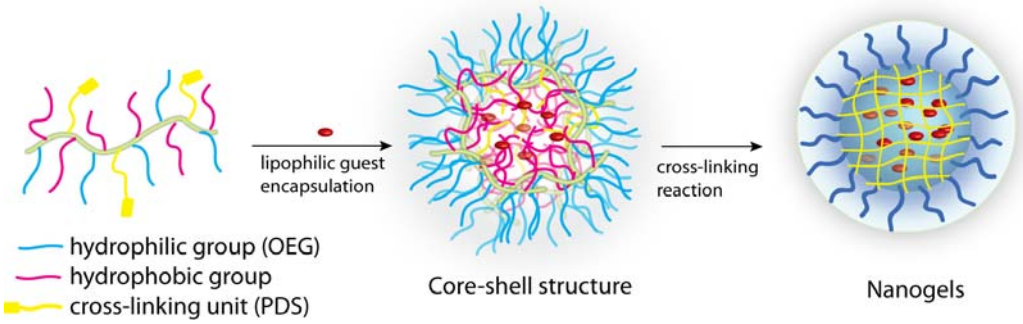

Figure 4.1: Cartoon representation of self-cross-linked nanogels with lipophilic guest encapsulation.

The nanogel delivery system we have discussed in Chapters 2 and 3 is based on random copolymers that contain oligoethyleneglycol (OEG) and pyridyldisulfide (PDS) units. In order to vary the hydrophobicity inside the cores of the self-cross-linked nanogel networks, the polymer precursor will be modified with lipophilic alkyl groups as additional side chain functionalities (Figure 4.1). The consequences of the induced changes in the hydrophobic-lipophilic balance (HLB) of the polymer aggregates, and thus the obtained nanogel carriers, to loading capacity and encapsulation stability is investigated using the FRET based method described in Chapter 3. We expected that: (*i*) the use of a random copolymer containing hydrophilic and lipophilic functionalities as a nanogel precursor will allow for aggregate formation prior to cross-linking; (*ii*) increasing the contribution of the hydrophobic alkyl component will provide enhanced lipophilic guest encapsulation capacity; (*iii*) the encapsulation stability of lipophilic guest molecules trapped inside the cross-linked nanogel networks can be tuned by varying the hydrophobicity of the precursor polymers.

4.2 Results and Discussion

4.2.1 Design and Synthesis

In order to test the effect of varying hydrophobicity on the various parameters of lipophilic encapsulation in our self-cross-linked nanogel system, amphiphilic random copolymer precursors with varying hydrophobic content were synthesized. Drawing from our previously explored PEG-PDS copolymer, which used the contained PDS side chains as a handle for the cross-linking of the nanogel structure, polymer precursors for these studies were designed to contain a constant amount of the PDS functionality that was determined sufficient to achieve to self-cross-linking reaction. The OEG units were again included as water soluble, biocompatible functionalities and constituted the major hydrophilic content of the precursor polymers. To achieve precursor polymers with variable hydrophobic content, lipophilic alkyl chain functionalities were added to the OEG-PDS composition. The relative hydrophobicities of the precursor polymers were varied in two different manners: (*i*) by varying the length of the alkyl chain contained in the incorporated comonomer and (*ii*) by altering the ratio of comonomers containing a constant length alkyl chain to those containing the hydrophilic OEG group. The synthesized polymer structures are shown in Chart 4.1. Both sets of polymer nanogel precursors were prepared by reversible addition-fragmentation chain transfer (RAFT) polymerization.

For the first series, four polymers (**P1**-**P4**) were prepared to contain 50% of the OEG methacrylate, 20% of the PDS-derived methacrylate, and 30% of alkyl methacrylate. Within this polymer series, the alkyl chain (denoted by R in Chart 4.1a)

length is varied to generate polymers **P1** (R = butyl), **P2** (R = hexyl), **P3** (R = octyl), and **P4** (R = decyl).

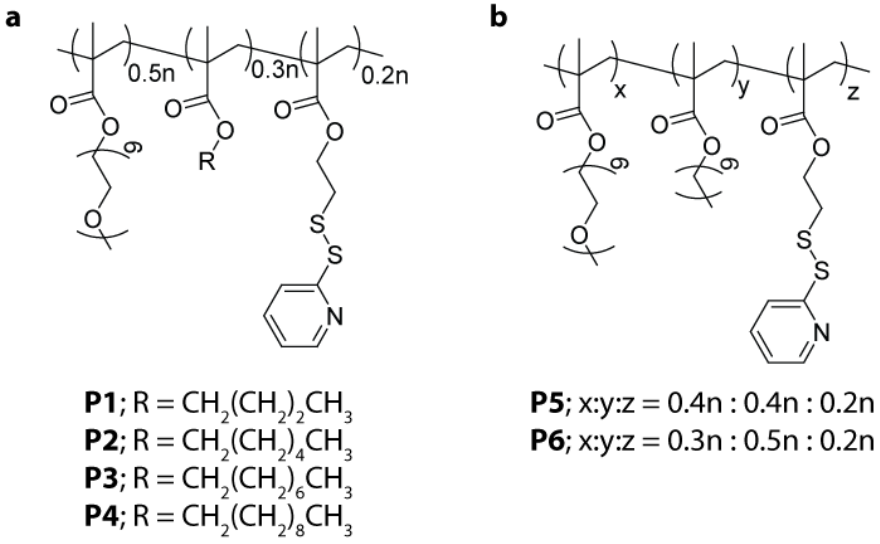

Chart 4.1: Structures of polymer precursors.

For the second series, two additional polymers **(P5-P6)** were prepared with varying percentages of the incorporated alkyl-containing comonomer. For this purpose, we chose the decylmethacrylate comonomer as the lipophilic side chain and varied the ratio of this hydrophobic commoner to OEG while keeping the PDS monomer at a constant 20 mol%. Combining polymer **P4** from the first series with polymers **P5** and **P6**, a series was generated in which the ratio of OEG methacrylate to decylmethacrylate to PDS methacrylate was made to equal 50%:30%:20%, 40%:40%:20% and 30%:50%:20%, respectively.

Since polymers **P1-P6** contain both hydrophobic alkyl groups and hydrophilic OEG side chain units, these polymers were observed to exhibit core-shell like structures, similar to those observed with micellar assemblies, when they were allowed to self-assemble in aqueous solution. Such aggregation of the amphiphilic random

copolymers generated assemblies with lipophilic cores that could accommodate the sequestration of lipophilic guest molecules in water. Using the procedure described in Chapter 3, two FRET pair dye molecules (DiI and DiO) were independently loaded into the cores of these polymer aggregates. Subsequent addition of the reducing agent, DTT (0.5 equivalents with respect to PDS groups in the precursor polymer), activated the intra/interchain disulfide bond formation that has been shown to generate the cross-linked polymer nanogel structure (Scheme 4.1). Polymer nanogels, **NG1-NG6**, were prepared from the polymer precursors, **P1-P6**, respectively. Performing this preparation in the presence of either DiI or DiO allowed these lipophilic dyes to efficiently accumulate within the hydrophobic cores of the formed polymer aggregates, achieving noncovalent encapsulation within the obtained water soluble nanogel carriers after crosslinking.

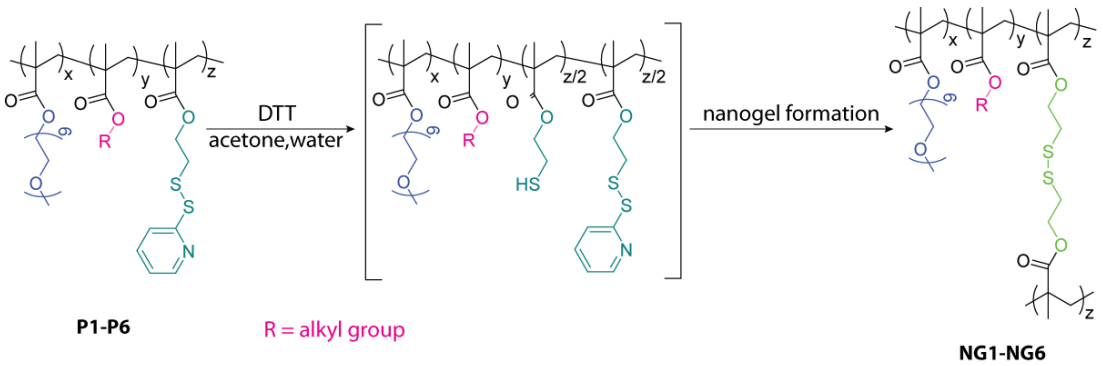

Scheme 4.1: Synthesis of the self-cross-linked polymer nanogels from precursor polymers containing OEG, PDS and hydrophobic alkyl groups.

We investigated the aggregation sizes of polymers **P1-P6** in water prior to cross-linking by dynamic light scattering (DLS), as it was hypothesized that the sizes of these assemblies would dictate the sizes of the obtained nanogels (**NG1-NG6**). Solutions of polymers **P1-P6** (10 $mg.mL^{-1}$) in water displayed assembly sizes with diameters

centered at around 10 nm by volume based DLS measurement (Figure 4.2a). The nanogels formed from these polymer precursors exhibited similar sizes to those observed for their corresponding aggregates with the exception of the butylmethacrylate containing **NG1,** which showed a larger size centered at around 200 nm diameter (Figure 4.2b). It is hypothesized that this discrepancy may be due to a lack of stable polymer aggregation exhibited by **P1**. Polymer **P1** contains 30% of the butylmethacrylate side chain, which is the shortest lipophilic side chain used in the present work. Considering the contribution to the overall aggregate HLB from the 50% of hydrophilic OEG segments, it is likely that this butyl chain does not sufficiently stabilize the observed 10 nm polymer aggregate. Such instability increases the probability of interaggregate cross-linking occurring during the DTT initiated reaction, resulting in a larger polymer nanogel than those formed from the more stabilized aggregates of polymers **P2-P6**.

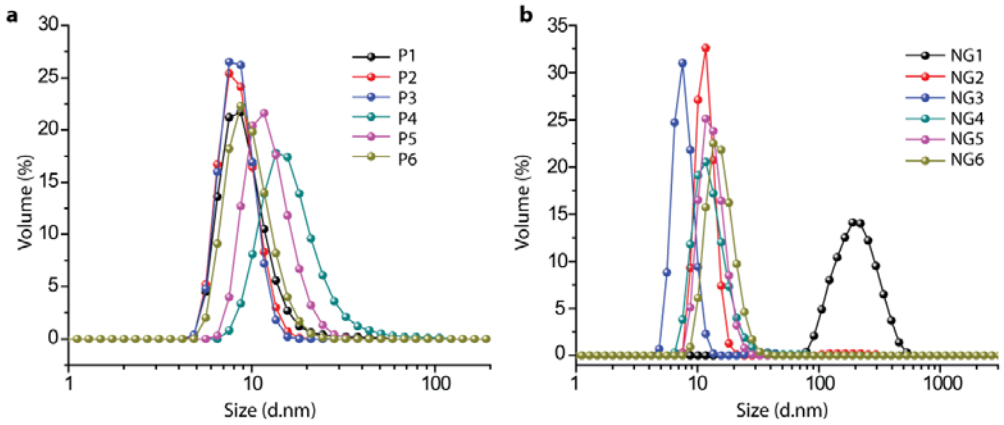

Figure 4.2: Size distributions in water by volume based DLS for a) polymer aggregates of P1-P6 (10 mg.mL^{-1}) and b) self-cross-linked polymer nanogels, NG1-NG6.

4.2.2 Hydrophobic Effect on Loading Capacity

Dominated by the hydrophobic effect and polymer-drug miscibility, loading in polymer micelles has been shown to be highly dependent on HLB, with enhanced loading observed when the length or density of the hydrophobic block is increased.(Li, Danquah et al. 2010) Considering this fact, we were interested in tuning the loading capacity for lipophilic guest molecules in our polymer nanogel system by varying the hydrophobic content of our nanogel constructs. To investigate this possibility, the polymer series **P1-P6** described above was synthesized. Nanogels, **NG1-NG6**, were prepared from these polymers using the DTT initiated crosslinking reaction in the presence of either DiI or DiO to afford noncovalent encapsulation of one of the FRET pair dyes within the nanogel interior. Polymer nanogels, **NG1**-**NG4**, were separately loaded *in situ* with DiI and DiO using 2 wt% of the lipophilic dyes. After filtering off unencapsulated dye molecules and removing the pyridothione crosslinking reaction byproduct by dialysis, the extent of guest encapsulation in solution of mixed DiI and DiO samples was measured by UV-Vis spectroscopy. The absorption spectra (solid lines) of these dye loaded nanogels, shown in Figure 4.3, reveal a clear trend of increasing dye encapsulation as the length of the lipophilic alkyl chain is increased from butyl (**NG1**) to decyl (**NG4**). This is attributed to the increasingly hydrophobic environment created by these alkyl chains within the nanogel cores that can favorably accommodate liphophilic guests.

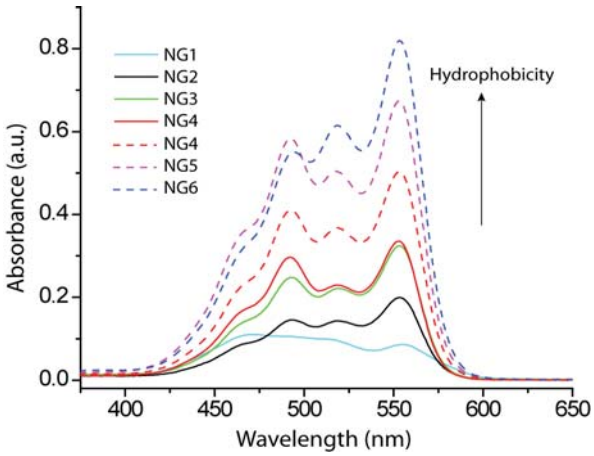

Figure 4.3: Hydrophobic effect of cross-linked polymer nanogels on loading capacity: 2 wt% of dye feeding solution (solid line); 10 wt% of dye feeding (broken line).

While this trend is rather clear, two questions may be raised from these spectra. The first is the clear difference in spectrum shape of the dye pair encapsulated in **NG1** from that observed in with all other nanogel solutions. While the exact cause of this discrepancy is unclear, we expect that it is an effect of a very different core environment in this nanogel structure; a combination of the loose packing of the short butyl chain and the larger size (~200 nm) of the nanogels makes the interior of **NG1** relatively hydrophilic as compared to the rest of the series, a feature which likely alters the absorbance characteristics of the encapsulated dye molecules.

Second is the similarity in absorbance of the dyes encapsulated within the decyl containing **NG4** and those encapsulated within the octyl containing **NG3**. This suggests that these two polymers display similar loading with an equal feed amount of dye. However, we hypothesize that this 2 wt% dye feeding, while above the 100% loading efficiency thresholds of **NG1-NG3**, was at a point where the loading efficiency of **NG4** was near 100%. In this case, the apparent loading capacity of **NG4** may have been limited by the feeding dye concentration. We tested this hypothesis by increasing the

feed concentration of dye from 2 wt% to 10 wt%. The enhanced dye encapsulation observed with **NG4** (broken red line) confirms that 2 wt% is well below the dye amount that this nanogel can absorb with nearly perfect loading efficiency and that more dye can be encapsulated (with less than 100% efficiency) when higher dye concentration is used during preparation.

We were also interested in investigating the hydrophobic effect on loading capacity with the **NG4-NG6** series, in which the nanogel hydrophobicity was varied by altering the ratio of decyl chains to OEG units. Dye loaded **NG4-NG6** were prepared by *in situ* loading of 10 wt% DiI or DiO during the DTT crosslinking reaction. The obtained nanogels, all of constant crosslinking degree, contain OEG:decyl ratios of 50:30 (**NG4**), 40:40 (**NG5**) and 30:50 (**NG6**). Analysis of the spectra shown in Figure 4.3 (broken lines), reveals increasing dye encapsulation as the relative percentage of the decylmathecrylate monomer in the precursor polymer is increased. Similar to the effect of increasing the length of the alkyl chain, increasing the amount of decyl chains within the polymer enhances the hydrophobicity of the interior of the formed aggregates and creates an increasingly preferential nanogel core for the encapsulation of lipophilic guest molecules. Interestingly, **NG4** in this series exhibited much higher encapsulation than its counterpart in the first series, suggesting that 2 wt% was well below its maximal loading capacity.

4.2.3 Hydrophobic Effect on Encapsulation Stability

Having demonstrated that the loading capacity for lipophilic guest molecules can be tuned in our nanogel system by introducing hydrophobic variations into the precursor polymers, we were next interested in investigating the consequences that such

variations would have on the encapsulation stabilities in the prepared nanogel carriers. For this purpose, we have used our FRET based method described in Chapter 3 to quantitatively compare the encapsulation stabilities exhibited by dye loaded nanogels, **NG1-NG6**. The same nanogel samples used for the analysis of loading capacities were used in these experiments. Nanogel samples containing encapsulated DiI were mixed with those containing DiO and the evolution of FRET between the dye pair, indicated by concomitant decrease in donor (DiO) intensity at 505 nm and increase in acceptor (DiI) intensity at 568 nm, was followed over a 24 hour period.

It was hypothesized that the by increasing the hydrophobicity of the nanogel core through variations to the precursor polymer we would be able to enhance not only the loading capacities of the obtained carriers, but also the encapsulation stability of lipophilic guests sequestered within the nanoassemblies. This was based on the thought that an increasingly hydrophobic core would provide a better environment for the solubilization of lipophilic guests, enhancing the ability of the nanogel to hold on to its guest molecules and limiting exchange with the aqueous bulk environment.

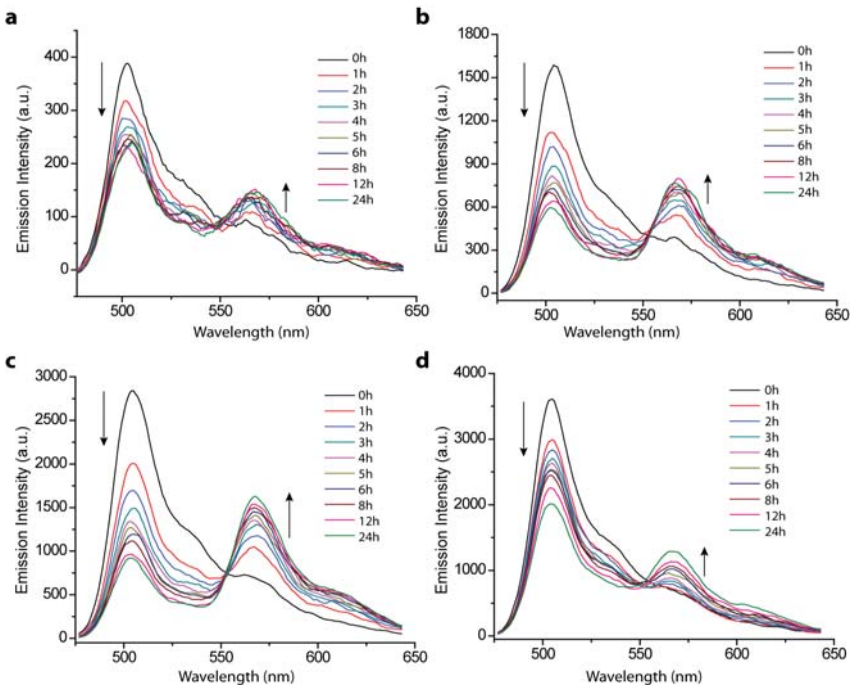

Figure 4.4: Fluorescence spectra (λ_{ex} = 450 nm) of mixed nanogels containing DiI and DiO prepared with 2 wt% dye loading: a) NG1, b) NG2, c) NG3, and d) NG4.

This was first tested with the **NG1-NG4** series, which was prepared with 2 wt% feeding of the dyes. The time-dependent FRET evolution for these nanogels is plotted in Figure 4.4. Interestingly, the recorded FRET development behaviors did not support our originally proposed hypothesis. In fact, analysis of **NG1-NG3** indicates the exact opposite trend, with a more rapid rate of FRET evolution being observed as the length of the incorporated alkyl chain increases from butyl to hexyl to octyl (Figure 4.4 a, b, c). However, it is also noted from these plots that the FRET evolution for the decyl containing **NG4** (Figure 4.4d) deviates from this trend. As this **NG4** sample was previously shown to be well below its maximal loading capacity, an alternate hypothesis, taking into account the observed effects on both encapsulation capacity and stability, was formulated to explain this behavior.

It was demonstrated in the previous section that the capacity for lipophilic encapsulation is enhanced as the length of the alkyl chain within the polymer nanogel is increased. The amphiphilic nature of the precursor polymer is thought to induce formation of a micelle-type aggregate, in which the majority of hydrophobic content is buried within the core of the self-assembling construct. If this is the case, a likely feature of lipophilic encapsulation in these systems is that initially sequestered guest molecules accumulate deep within the core and gradually move out towards the assembly periphery as core volume is filled. The extent of such peripheral loading in this system will necessarily be dependent on the nature (length and density) of the hydrophobic units dispersed throughout the random compolymer network and the amount of dye used during the nanogel preparation. Thus, as the length of the alkyl chain is increased from **NG1** to **NG4**, the observed increase in loading capacity could be due, in part, to an enhanced ability to load lipophilic dye molecules closer to the nanogel surface. However, it is also a reasonable assumption that these peripherally loaded dye molecules will be those that are least stably encapsulated and most easily exchange with the bulk environment. This would explain why enhanced loading observed going from **NG1** to **NG3** translates to faster FRET evolution and less stable encapsulation. It would also rectify the apparent aberration with **NG4**, as the majority of the 2 wt% dye used is likely stably encapsulated within the core of this nanogel, which is below its maximal capacity, and does not leak out into the aqueous exterior.

To test this hypothesis, we investigated the encapsulation stability of the **NG4-NG6** series prepared using 10 wt% of DiI and DiO. According to the new hypothesis, we expected to observe faster rates of FRET exchange with greater dye loading caused

by an increasing relative amount of the decyl unit in nanogels **NG4** to **NG6**. We were gratified to observe that this was indeed the case. **NG4**, containing a 50:30 ratio of OEG to decyl chain, exhibited the lowest dye encapsulation with the 10 wt% feeding but also displayed gradually increasing FRET over the tested 24 hour period (Figure 4.5a). **NG5**, with a ratio of 40:40, encapsulated an intermediate amount of dye and exhibitied much faster FRET development (Figure 4.5b). Finally, **NG6**, containing a 30:50 ratio, encapsulated the highest amount of dye and displayed a very rapid burst of FRET evolution, with the majority of exchange occurring within the first three hours of the experiment (Figure 4.5c).

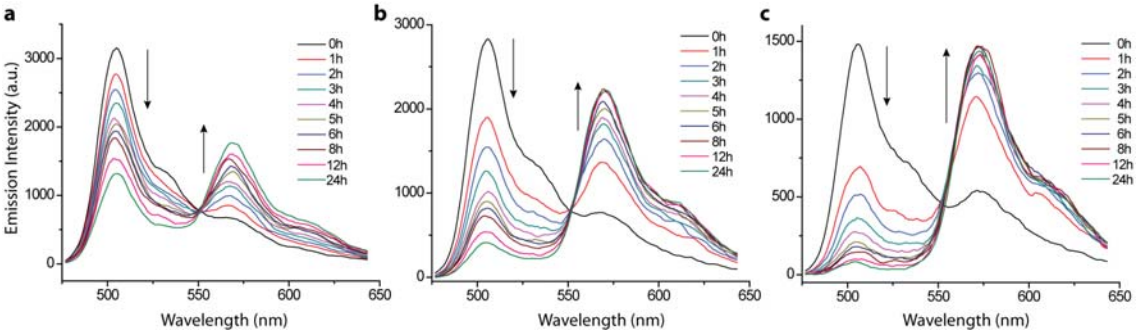

Figure 4.5: Fluorescence spectra (λex = 450 nm) of mixed nanogels encapsulated DiI and DiO prepared with 10% dye loading; a) NG4, b) NG5, and c) NG6.

The apparent inverse relationship between loading amount and encapsulation stability is clearly seen in the plots of FRET ratio *vs.* time for the **NG1-NG4** and **NG4-NG6** series (Figure 4.6). The FRET ratio $I_a/(I_d+I_a)$, where I_a and I_d are the fluorescence intensities of the acceptor (DiI) and the donor (DiO), respectively, is a used as a quantitative comparison of the extents of dye leakage observed for each nanogel sample. As described in Chapter 3, the development of FRET between the independently sequestered DiO and DiI molecules is dependent on leakage from the nanocarrier in which they were originally encapsulated and subsequent uptake by a

different container in the aqueous solution. This will cause increasing accumulation of both DiO and DiI within their Förster radius in the cores of the same nanocarrier, leading to increased energy transfer between the two dyes. While the data reported in this section supports the hypothesis of loading dependent encapsulation stability, there exists an alternate explanation that must be addressed.

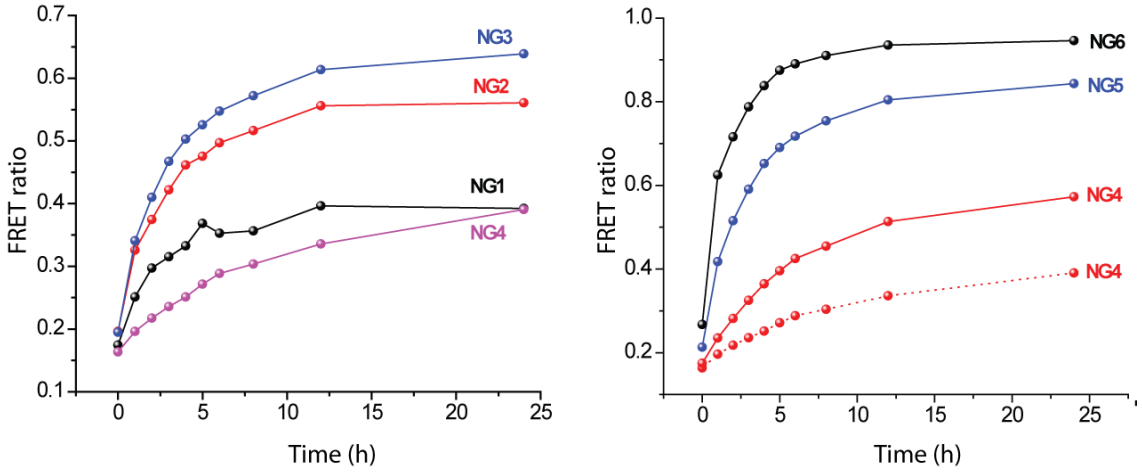

Figure 4.6: Plot of FRET ratio *vs* time; a) chain length variation prepared from 2 wt% dye stock solution, b) alkyl group percentage variation prepared from 10 wt% (solid link) and 2 wt% (dot line) of dye stock solution.

The observed development of FRET using this method is dependent on the relative rates of two distinct events. The first is the leakage of dye molecules from the interior of the originally encapsulating nanogel into the aqueous exterior. The second is the re-encapsulation of leaked dye molecules into the interior of some nanogel present in solution. While increasing the hydrophobicity of the nanogel material has been shown to limit the first process, it is also possible that it has an effect on the second process. Specifically, increasing hydrophobicity of the nanogel could enhance its ability to sequester leaked dye molecules from the aqueous environment. The fact that no significant changes in either dye's absorbance were observed with any sample over the

lifetime of the experiment (Figure 4.7) suggests that this is not the case. However, it could be that the increasingly hydrophobic nanogels tend to re-encapsulate within their core, causing close proximity of the sequestered dyes, whereas lower hydrophobicity only affords uptake from the exterior along the surface of the nanogel.

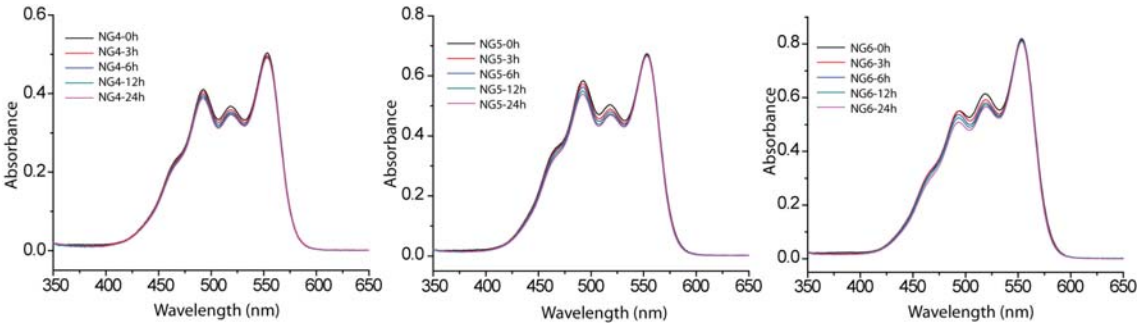

Figure 4.7: Absorbance of mixed nanogels encapsulated DiI and DiO prepared with 10% dye loading; a) NG4, b) NG5, and c) NG6**.**

4.2.4 Correlating Loading Capacity and Encapsulation Stability

To distinguish between these two possibilities, an additional experiment using nanogels **NG4-NG6**, which were loaded with a normalized amount of DiI and DiO well below the maximal loading capacities of these decyl containing gels, was performed. The nanogel samples were prepared using 1 wt% of the two dyes. UV-vis absorbance spectra taken of the purified samples (Figure 4.8) reveal an equal level of encapsulation in all three nanogels, which was calculated to correspond to nearly 100% encapsulation efficiency.

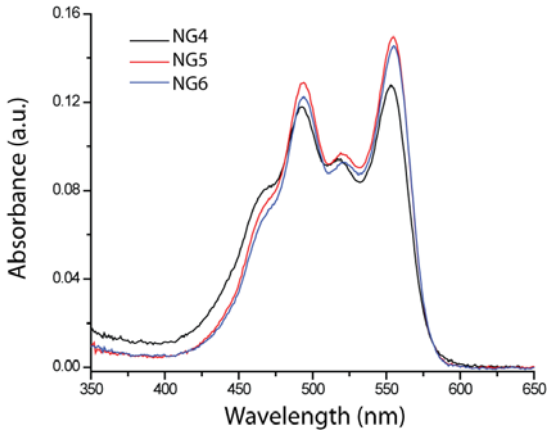

Figure 4.8: Dye encapsulation in samples of mixed NG4-NG6 prepared using 1wt% of both DiI and DiO.

The DiI and DiO containing samples were mixed and the FRET development for these normalized loading nanogels was monitored. This experiment was performed to test the hypothesis of loading dependent encapsulation stability. With all tested samples being normalized to a dye amount well below their maximal encapsulation capacity, we expected the true effect of increasing nanogel hydrophobicity on encapsulation stability to determine the rate of guest exchange. Thus, if our hypothesis were true, we expected that the enhanced lipophilicity of the nanogel core provided by an increasing number of decyl chains in the precursor polymer would allow for more stable guest encapsulation, preventing exchange with the bulk exterior and limiting the development of FRET. If the alternate possibility were true, any leakage from the more hydrophobic samples would lead to an increase in FRET due to the enhaced abilities of these nanogels to uptake leaked guests from the aqueous exterior.

The plots of FRET development observed for **NG4-NG6** (Figure 4.9) support the first case, revealing decreased FRET development over time as the percentage of decyl group within the nanogel is increased. **NG4**, containing 30% of the decyl unit, displays a gradual, sustained increase in FRET over the tested 72 hour period (Figure

4.9a). **NG5**, containing 40% of the decyl chain, displays enhanced encapsulation stability, only beginning to show FRET development at 24 hours after mixing (Figure 4.9b). Finally, the 50% decyl containing **NG6** displays superior encapsulation stability, with no observed FRET development over the tested 72 hour period (Figure 4.9c). These results clearly demonstrate the effect of increasing hydrophobicity on the encapsulation stability exhibited by our nanogel carriers. Specifically, at less than maximal loading capacity, introducing hydrophobic groups into the nanogel scaffold can be used to greatly enhance the encapsulation stabilities of these nanoscopic carriers.

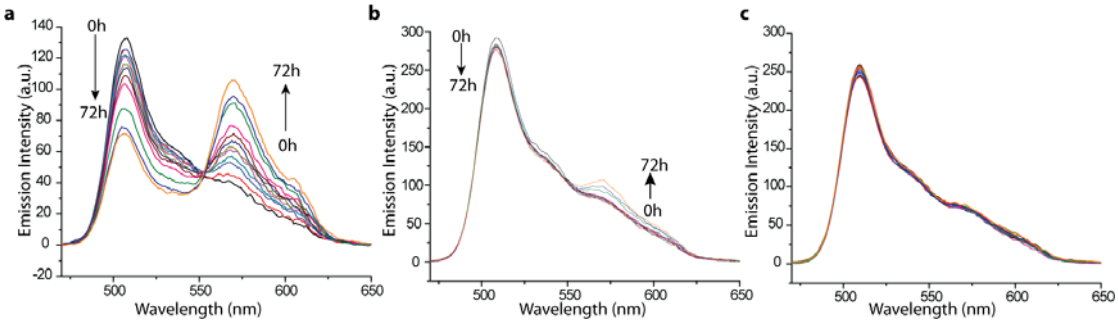

Figure 4.9: Fluorescence spectra (λex = 450 nm) of mixed nanogels encapsulated DiI and DiO prepared with 1 wt% dye loading; a) NG4, b) NG5, and c) NG6.

4.3 Summary

In this Chapter, we have examined the effect of hydrophobic composition on the container properties of our nanogel system, specifically in reagrds to loading capacity and encapsulation stability. Modifying the previously explored PEG-PDS copolymer to contain hydrophobic alkyl groups, two series of random copolymers were generated. The hydrophobicity of the first series, **NG1-NG4**, was varied by altering the length of the alkyl chain incorporated into the precursor polymers from butyl to decyl with two carbon increments. The hydrophobicity of the second series, **NG4-NG6**, was

varied by targeting OEG:decyl ratios within the polymers of 50:30, 40:40 and 30:50 while keeping the PDS unit at a constant 20%.

By carrying out the DTT initiated crosslinking reaction in the presence of the lipophilic dyes, DiI or DiO, we were able to achieve *in* situ loading within the interiors of the formed nanogels. The loading capacity and efficiency was shown to be directly dependent on the hydrophobicity of the nanogel composition. Specifically, the loading capacities of these nanogel carriers can be enhanced by increasing the hydrophobic content of the structures, either through size or density of the incorporated lipophilic functionalities.

Nonetheless, encapsulation stability at maximal loading was observed to decrease as the hydrophobicity within the nanogels increased. Enhanced loading in a more hydrophobic nanogel is due, in part, to increased peripheral loading of the dye molecules. As a result, highly hydrophobic nanogels that were loaded with dye well below their maximal loading capacities were able to hold on to their encapsulated guests molecules with enhanced stabilities.

These results provide crucial insight into the optimization of loading paramters for this nanogel system and other nanoscopic delivery vehicles. Notably, this work suggests that loading capacity and encapsulation stability cannot be maximized simultaneously, with an optimal balance occurring well below the maximal loading capacity of a given nanocarrier. As one of the major focuses in the future development of nanoparticle enabled drug delivery systems is the improvement of loading capacity, this trade off must be taken as a crucial consideration. It should be noted that the nanogels employed in this study were designed to explore the structure-property

relationship between scaffold hydrophobicity and container ability. Emphatically, these nanogels were not optimized for the loading capacities or efficiencies required for any biologically relevant applications. Nonetheless, we believe that the observed loading depedent encapsulation stability behavior is a basic property of the nanoscopic vehicle and its implications will translate to other carrier scaffolds. The reported FRET based system is a rather robust method, capable of detecting guest molecule leakage in cases where UV-vis, simple fluorescence, and traditional FRET based experiments yield a false impression of *in vitro* encapsulation stability. This method may be widely employed to determine an optimal balance of stable lipophilic guest molecule loading for nanoscopic drug delivery vehicles.

4.4 Experimental

Materials and Methods

All chemicals and solvents were purchased from commercial sources and were used as received, unless otherwise mentioned. Polymers **P1-P6** were synthesized by RAFT polymerization and purified by precipitation. S-dodecyl-S'-2-(2,2-dimethylacetic acid) trithiocarbonate and pyridyldisulfide ethylmethacrylate (PDSEMA) were prepared using previously reported procedures.(Lai, Filla et al. 2002; Ghosh, Basu et al. 2006) ^{1}H-NMR spectra were recorded on a 400 MHz Bruker NMR spectrometer using the residual proton resonance of the solvent as the internal standard. Chemical shifts are reported in parts per million (ppm). Molecular weights of the polymers were estimated by gel permeation chromatography (GPC) using a PMMA standard with a refractive index detector. Dynamic light scattering (DLS) measurements were performed using a Malvern Nanozetasizer. UV-visible absorption spectra were recorded on a Varian

(model EL 01125047) spectrophotometer. The fluorescence spectra were obtained using a combination of PTI and JASCO FP-6500 spectrofluorimeters.

General procedure for Syntheses of random copolymers:

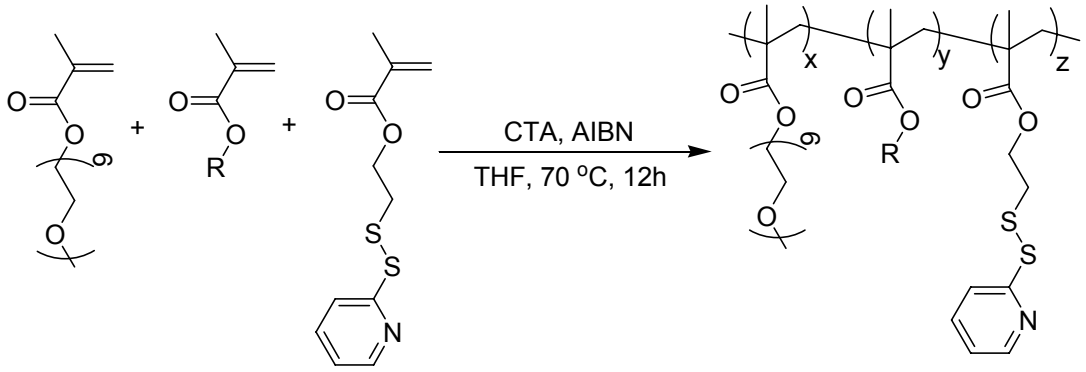

Briefly, a mixture of S-dodecyl-S'-2-(2,2-dimethylacetic acid) trithiocarbonate (CTA), PDSEMA, poly(ethylene glycol) methyl ether methacrylate (PEGMA, Mw 475), the alkyl chain derived methacrylate monomer and AIBN were dissolved in THF and degassed by performing three freeze-pump-thaw cycles. The reaction mixture was sealed and transferred into a pre-heated oil bath at 70 °C for 12 h. The resultant mixture was dissolved in dichloromethane (0.1 mL) and precipitated in hexane (5 mL). To remove unreacted monomers, the precipitate was further dissolved in dichloromethane (0.1 mL) and reprecipitated in ether (5 mL) to yield the random copolymer as a pale yellow, waxy substance.

Synthesis of P1:

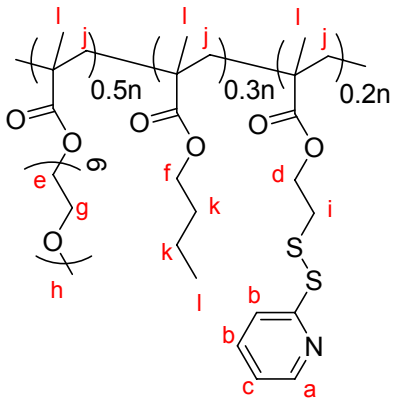

According to general procedure for synthesis of random copolymers, a mixture of CTA (14.0 mg, 0.04 mmol), PDSEMA (200 mg, 0.78 mmol), PEGMA (930 mg, 1.9 mmol), butylmethacrylate (170 mg, 1.2 mmol) and AIBN (1.3 mg, 7.8 µmol) were polymerized in THF (2.6 mL). GPC (THF) *Mn*: 55K. PDI: 2.2. ^{1}H NMR (400 MHz, $CDCl_3$) δ 8.44 (a), 7.66 (b), 7.10 (c), 4.20 (d), 4.05 (e), 3.89 (f), 3.60 (g), 3.34 (h), 3.00 (i), 2.04-1.80 (j), 1.80-1.22 (k), 1.01-0.78 (l). The molar ratio between the three blocks was determined by integrating the methoxy proton in the polyethylene glycol unit, methoxy proton in alkyl derived methacrylate, and the aromatic proton in the pyridine and found to be 5:3:2 (PEO:ButylMA:PDSEMA).

Synthesis of P2:

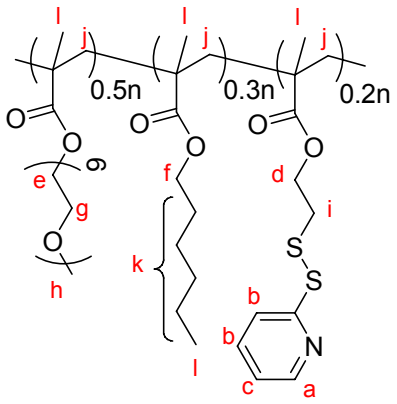

According to general procedure for synthesis of random copolymers, a mixture of CTA (14.0 mg, 0.04 mmol), PDSEMA (200 mg, 0.78 mmol), PEGMA (930 mg, 1.9 mmol), hexylmethacrylate (200 mg, 1.2 mmol) and AIBN (1.3 mg, 7.8 µmol) were polymerized in THF (2.7 mL). GPC (THF) *Mn*: 38K. PDI: 1.5. ^{1}H NMR (400 MHz, $CDCl_3$) δ 8.48 (a), 7.70 (b), 7.13 (c), 4.22 (d), 4.08 (e), 3.91 (f), 3.64 (g), 3.37 (h), 3.04 (i), 2.10-1.60 (j), 1.40-1.20 (k), 1.10-0.78 (l). The molar ratio between the three blocks was determined by integrating the methoxy proton in the polyethylene glycol unit, methoxy proton in alkyl derived methacrylate, and the aromatic proton in the pyridine and found to be 5:3:2 (PEO:HexylMA:PDSEMA).

Synthesis of P3:

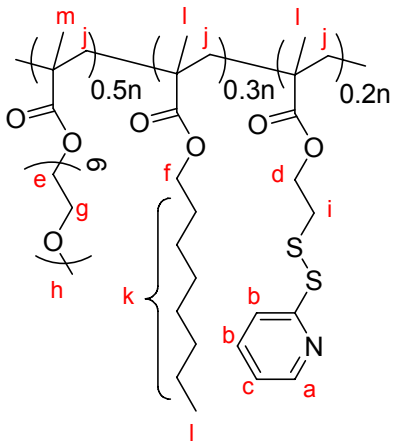

According to general procedure for synthesis of random copolymers, a mixture of CTA (14.0 mg, 0.04 mmol), PDSEMA (200 mg, 0.78 mmol), PEGMA (930 mg, 1.9 mmol), octylmethacrylate (230 mg, 1.2 mmol) and AIBN (1.3 mg, 7.8 µmol) were polymerized in THF (2.7 mL). GPC (THF) *Mn*: 41K. PDI: 1.4. ^{1}H NMR (400 MHz, $CDCl_3$) δ 8.48 (a), 7.70 (b), 7.13 (c), 4.22 (d), 4.08 (e), 3.91 (f), 3.64 (g), 3.37 (h), 3.04 (i), 2.10-1.60 (j), 1.40-1.20 (k), 1.20-0.78 (l). The molar ratio between the three blocks was determined by integrating the methoxy proton in the polyethylene glycol unit, methoxy proton in alkyl derived methacrylate, and the aromatic proton in the pyridine and found to be 5:3:2 (PEO:OctylMA:PDSEMA).

Synthesis of P4:

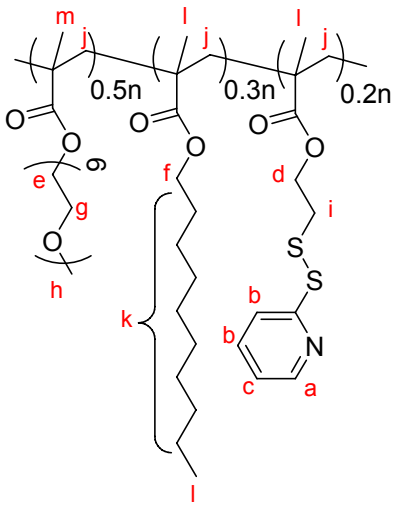

According to general procedure for synthesis of random copolymers, a mixture of CTA (14.0 mg, 0.04 mmol), PDSEMA (200 mg, 0.78 mmol), PEGMA (930 mg, 1.9 mmol), decylmethacrylate (270 mg, 1.2 mmol) and AIBN (1.3 mg, 7.8 µmol) were polymerized in THF (2.8 mL). GPC (THF) *Mn*: 49K. PDI: 2.1. ^{1}H NMR (400 MHz, $CDCl_3$) δ 8.45 (a), 7.66 (b), 7.10 (c), 4.19 (d), 4.05 (e), 3.88 (f), 3.61 (g), 3.35 (h), 3.04 (i), 2.10-1.60 (j), 1.50-1.20 (k), 1.10-0.70 (l). The molar ratio between the three blocks was determined by integrating the methoxy proton in the polyethylene glycol unit, methoxy proton in alkyl derived methacrylate, and the aromatic proton in the pyridine and found to be 5:3:2 (PEO:DecylMA:PDSEMA).

Synthesis of P5:

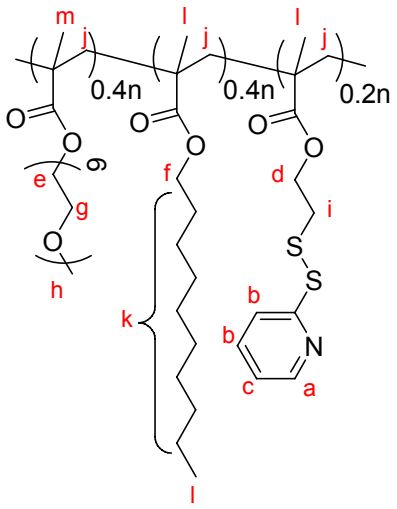

According to general procedure for synthesis of random copolymers, a mixture of CTA (14.0 mg, 0.04 mmol), PDSEMA (200 mg, 0.78 mmol), PEGMA (740 mg, 1.6 mmol), declmethacrylate (350 mg, 1.6 mmol) and AIBN (1.3 mg, 7.8 µmol) were polymerized in THF (2.6 mL). GPC (THF) *Mn*: 42K. PDI: 2.0. ^{1}H NMR (400 MHz, $CDCl_3$)δ 8.43 (a), 7.65 (b), 7.09 (c), 4.18 (d), 4.04 (e), 3.72 (f), 3.70 (g), 3.33 (h), 3.04 (i), 2.10-1.55 (j,k), 1.48-1.20 (k), 1.10-0.70 (l). The molar ratio between the three blocks was determined by integrating the methoxy proton in the polyethylene glycol unit, methoxy proton in alkyl derived methacrylate, and the aromatic proton in the pyridine and found to be 4:4:2 (PEO:DecylMA:PDSEMA).

Synthesis of P6:

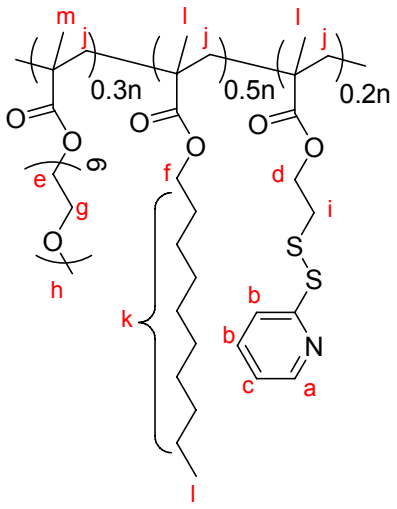

According to general procedure for synthesis of random copolymers, a mixture of CTA (14.0 mg, 0.04 mmol), PDSEMA (200 mg, 0.78 mmol), PEGMA (560 mg, 1.2 mmol), decylmethacrylate (440 mg, 2.0 mmol) and AIBN (1.3 mg, 7.8 µmol) were polymerized in THF (2.4 mL). GPC (THF) *Mn*: 52K. PDI: 2.2. ^{1}H NMR (400 MHz, $CDCl_3$)δ 8.45 (a), 7.65 (b), 7.09 (c), 4.19 (d), 4.05 (e), 3.88 (f), 3.61 (g), 3.34 (h), 3.00 (i), 2.10-1.50 (j,k), 1.40-1.20 (k), 1.10-0.80 (l). The molar ratio between the three blocks was determined by integrating the methoxy proton in the polyethylene glycol unit, methoxy proton in alkyl derived methacrylate, and the aromatic proton in the pyridine and found to be 3:5:2 (PEO:DecylMA:PDSEMA).

Synthesis of nanogels contaning DiI/DiO:

Polymers **P1-P6** (2 mg) and DiI or DiO (0.02 mg for 1 wt%, 0.04 mg for 2 wt% and 0.2 mg for 10 wt%) were dissolved in 200 µL of acetone and a calculated amount of DTT was added. The solution color changed to yellow, indicative of the production of pyridinethione byproduct of PDS cleavage. After stirring for 10 min, 1 mL of deionized water was added and the mixed solution was stirred overnight at room temperature,

open to the atmosphere to allow the organic solvent to evaporate. Insoluble DiI/DiO was removed by filtration and pyridinethione was removed from the nanogel solution by extensive dialysis using a membrane with a molecular weight cutoff of 10,000 g/mol.

DLS measurement:

Dynamic light scattering experiments were performed by using a Malvern Nanozetasizer. The light source was solid-state laser system, operating at 514 nm. The nanogels in deionized water (1mg/mL) were kept constant at 25 °C throughout the experiment. Dust was eliminated by filtering the solution through 0.45 μm filter. All the measurements were done at a correlation time of 30 seconds.

Nanogel encapsulated dye mixing:

A solution of nanogel containing DiI (100 μL) was mixed with a solution of nanogel containing DiO (100 μL), and milliQ water (800 μL) in a cuvette. The fluorescence intensity was recorded at 450 nm excitation wavelength.

Table 4.1: Leakage coefficient (Λ) in supramolecular nanoassemblies.

Nanogels-loading (wt%)	Leakage coefficient (Λ), h^{-1}
NG1-2 wt%	0.035
NG2-2 wt%	0.053
NG3-2 wt%	0.063
NG4-1 wt%	0.024
NG4-2 wt%	0.021
NG4-10 wt%	0.044
NG5-1 wt%	0.002
NG5-10 wt%	0.091
NG6-1 wt%	-0.001
NG6-10 wt%	0.107

4.5 References

1. Lipinski, C. A., Drug-link properties and the causes of poor solubility and poor permeability. *J. Pharmacol. Toxicol. Methods* **2000**, *44*, 235-249.

2. Torchilin, V. P., Targeted polymeric micelles for delivery of poorly soluble drugs. *Cell. Mol. Life Sci*. **2004**, *61*, 2549-2559.

3. Farokhzad, O. C.; Langer, R., Impact of nanotechnology on drug delivery. *ACS Nano* **2009**, *3*, 16-20.

4. Allen, T. M.; Culis, P. R., Drug discovery systems: Entering the mainstream. *Science* **2004**, *303*, 1818-1822.

5. Lipinski, C. A.; Lombardo, F.; W., D. B.; Feeney, P. J., Experimental and computational approaches to estimate solubility and permeability in drug discovery and development setting. *Adv. Drug Deliv. Rev*. **2001**, *46*, 3-26.

6. Savić, R.; Eisenberg, A.; Maysinger, D., Block copolymer micelles as delivery vehicles of hydrophobic drugs: Micelle–cell interactions. *J. Drug. Target.* **2006**, *14*, 343-355.

7. Kabanov, A. V.; Nazarova, I. R.; Astafieva, I. V.; Batrakova, E. V.; Alakhov, V. Y.; Yaroslavov, A. A.; Kabanov, V. A., Micelle formation and solubilization of fluorescent probes in poly(oxyethylene-b-oxypropylene-b-oxyethylene) solutions. *Macromolecules* **1995**, *28*, 2303-2314.

8. Kale, T. S.; Klaikherd, A.; Popere, B.; Thayumanavan, S., Supramolecular assemblies of amphiphilic homopolymers. *Langmuir* **2009**, *25*, 9660-9670.

9. Matsumura, Y., Polymeric micellar delivery systems in oncology. *Jpn. J. Clin. Oncol.* **2008**, *38*, 793-802.

10. Bae, Y. H.; Yin, H., Stability issues of polymeric micelles. *J. Controlled Release* **2008**, *131*, 2-4.

11. Jiwpanich, S.; Ryu, J.-H.; Bickerton, S.; Thayumanavan, S., Noncovalent encapsulation stabilities in supramolecular nanoassemblies. *J. Am. Chem. Soc*. **2010**, *132*, 10683-10685.

12. Kim, S. W.; Shi, Y.; Kim, J. Y.; Park, K.; Cheng, J.-X., Overcoming the barriers in micellar drug delivery: Loading efficiency, in vivo stability, and micelle-cell interaction. *Expert Opin. Drug Deliv*. **2010**, *7*, 49-62.

13. Chen, H.; Kim, S.; Li, L.; Wang, S.; Park, K.; Cheng, J.-X., Release of hydrophobic molecules from polymer micelles into cell membranes revealed by förster resonance energy transfer imaging. *Proc. Natl. Acad. Sci. U.S.A*. **2008**, *105*, 6596-6601.

14. Chen, H.; Kim, S.; He, W.; Wang, H.; Low, P. S.; Park, K.; Cheng, J.-X., Fast release of lipophilic agents from circulating PEG-PDLLA micelles revealed by *in vivo* förster resonance energy transfer imaging. *Langmuir* **2008**, *24*, 5213-5217.

15. Raemdonck, K.; Demeester, J.; Smedt, S. D., Advance nanogel engineering for drug delivery. *Soft Matter* **2009**, *5*, 707-715.

16. Oh, J. K.; Drumright, R.; Siegwart, D. J.; Matyjaszewski, K., The development of microgels/nanogels for drug delivery applications. *Prog. Polym. Sci*. **2008**, *33*, 448-477.

17. Ryu, J.-H.; Chacko, R. T.; Jiwpanich, S.; Bickerton, S.; Babu, R. P.; Thayumanavan, S., Self-cross-linked polymer nanogels: A versatile nanoscopic drug delivery platform. *J. Am. Chem. Soc*. **2010**, *132*, 17227-17235.

18. Kabanov, A. V.; Vinogradov, S., Nanogels as pharmaceutical carriers: Finite networks of infinite capabilities. *Angew. Chem. Int., Ed* **2009**, *48*, 5418-5429.

19. Hamidi, M.; Azadi, A.; Rafiei, P., Hydrogel nanoparticles in drug delivery. *Adv. Drug Deliv. Rev*. **2008**, *60*, 1638-1649.

20. Vinogradov, S., Nanogels in the race for drug delivery. *Nanomedicine* **2010**, *5*, 165-168.

21. Ryu, J.-H.; Jiwpanich, S.; Chacko, R.; Bickerton, S.; Thayumanavan, S., Surface-functionalizable polymer nanogels with facile hydrophobic guest encapsulation capabilities. *J. Am. Chem. Soc*. **2010**, *132*, 8246-8247.

22. Li, F.; Danquah, M.; Mahato, R., Synthesis and characterization of amphiphilic lipopolymers for micellar drug delivery. *Biomacromolecules* **2010**, *11*, 2610-2620.

23. Ghosh, S.; Basu, S.; Thayumanavan, S., Simultaneous and reversible functionalization of copolymers for biological applications. *Macromolecules* **2006**, *39*, 5595-5597.

24. Lai, J. t.; Filla, D.; Shea, R., Functional polymers from novel carboxyl-terminated trithiocarbonates as highly efficient RAFT agents. *Macromolecules* **2002**, *35*, 6754-6756.

CHAPTER 5

SUMMARY AND FUTURE DIRECTIONS

5.1 Introduction

This dissertation describes a new class of self-cross-linked polymer nanogels which provide a versatile platform for the development of novel nanoscopic drug delivery systems. The nanogels were synthesized by intra-/intermolecular disulfide cross-linking reaction and provide non-colvalent hydrophobic encapsulation capabilities with high encapsulation stability and controlled release of the payload. These cross-linked polymer nanogels are considered as potential carriers for use in drug delivery systems since thier cross-linked nature holds the polymer network together creating stable nanocontainers. In addition, the cross-linked polymer nanogels have no concentration dependent (CMC) or stability issues commonly observed with classical polymeric nanoassemble systems. It is important to note that polymer nanogels are of interest in the field of drug delivery and have been reported in the literature recently; however, the classical emulsion/inverse emulsion preparation method still faces certain complications described in Chapter 1.(Oh, Siegwart et al. 2007; Oh, Tang et al. 2007; Hamidi, Azadi et al. 2008; Oh, Drumright et al. 2008; Kabanov and Vinogradov 2009; Raemdonck, Demeester et al. 2009; Vinogradov 2010)

In this dissertation, we mainly focus on the development of a synthetic method for cross-linked polymer nanogels for drug delivery systems and utilizing this system for lipophilic drug delivery applications. In Chapter 2, we highlight our methodology development using intra-/intermolecular disulfide cross-linking with PDS containing

polymers. Through the use of a simple inter-/intramolecular self-cross-linking reaction, we have elaborated an emulsion-free method for the synthesis of well-defined, biocompatible nanogels.(Ryu, Chacko et al. 2010; Ryu, Jiwpanich et al. 2010) This cross-linking method is based on the presence of pyridyl disulfide (PDS) units in the precursor polymer chain. By addition of deficient amount of the reducing agent DTT, we are able to achieve nanogel formation through the formation of cross-linking disulfide bonds with hydrophobic encapsulation capabilities. The surface of self-cross-linked nanogels can be tailored with targeting ligands containing thiol through the remaining PDS groups.

As we mentioned above, the cross-linked nature of nanogels is of great interest for the potential drug delivery systems since it provides not only stable nanocarriers but also tunable encapsulation stability. In Chapter 3, we detailed a FRET based method as a tool to probe the encapsulation stability of non-covalently encapsulated lipophilic molecules in self-assembled nanocontainers.(Jiwpanich, Ryu et al. 2010) A FRET pair (DiI and DiO) was encapsulated into separate nanocontainers independently, and were then mixed. The evolution of FRET, readout for guest exchange dynamics, was monitored in the mixed solution. This simple method provides a useful starting point for evaluating viable drug delivery vehicles. Based on FRET-based studies, we have shown that our self-cross-linked polymer nanogels show high encapusltion stability and the release profile of stably encapsulated guest can be tuned by the cross-linking density.

In order to maximize loading capacity of lipophilic guest molecules in self-cross-linked polymer nanogels, in Chapter 4, we describe the use of a hydrophobic polymer to provide a hydrophobic pocket inside the nanogel network. The increased

hydrophobicity of the polymer backbone increases the lipophilic loading capabilities. Nonetheless, the maximum loading of lipophilic molecules into self-cross-linked polymer nanogels may cause leakage due to the surface bound lipophilic guest molecules. We highlight these issues so that the drug molecule leakage will be considered as a potential problem and due attention will be paid while designing novel nanoscopic carriers for drug delivery.

The newly developed self-cross-linked polymer nanogels described in this dissertation is based on disulfide self-cross-linking reaction and the initial findings of the cross-linked polymeric nanogels described here show great promise as therapeutic carrier scaffolds. In the following sections, we discuss the ongoing work in our research group.

5.2 Future Directions

5.2.1 Controlled Release inside Cells

The two key findings of the self-cross-linked polymer nanogels i.e., the stable drug encapsulation, and prevention of premature drug leakage render them great potential to carry lipophilic drugs into cancer cells. We are interested in testing the release of loaded cargo in the cross-linked polymer nanogels inside the cells having high glutathione (GSH) concentration, and also in delivering lipophilic cancer drugs into tumor cells. The preliminary results demonstrate that our cross-linked nanogels are able to transfer the loaded cargo inside the cells as shown in Figure 5.1. In this experiment, we co-encapsulate a FRET pair (DiI and DiO) in a nanogel and monitor the dye release inside MCF-7 cells which is known to have high levels of GSH. When the

FRET pair is stably encapsulated in the network interior, FRET (red color) will be observed, while the disappearance of FRET (more yellow) is an indication of dye release. As shown in Figure 5.1, both nanogels having 6% and 27% cross-linking display the ability to enter into cells and that the release kinetics are controlled by the cross-linking density. The 6% cross-linked nanogels release its cargo faster than 27% cross-linked nanogels.

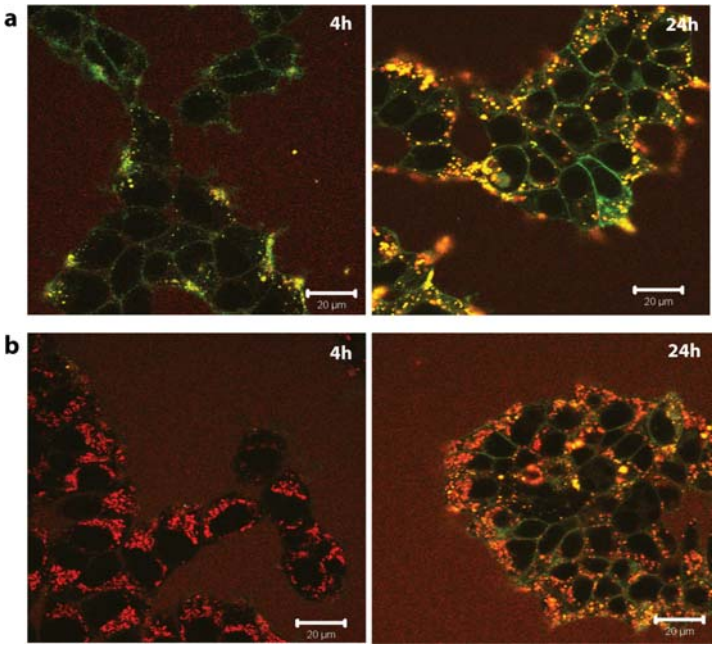

Figure 5.1: Confocal microscopy images of nanogels containing DiI and DiO at 4h and 24h incubation times: a) 6% cross-linked nanogels; b) 27% cross-linked nanogels.

Overall, the polymer nanogels developed by us hold great potential for drug delivery especially for chemotherapeutics. The *in vivo* delivery of cancer drugs such as doxorubicin to the breast cancer animal models is under investigation.

5.2.2 Cross-linked Nanogels with Cross-linker Modification

In this dissertation, we elaborate on the development of self-cross-linked polymer nanogels using disulfide self-cross-linking reaction by holding the amphiphilic polymer aggregation to create stable nanoparticles with hydrophobic encapsulation capabilities. Although, the nanogels based on disulfide cross-linker can be cleaved by biological reducing agents to release their loaded cargo in a controlled fashion, it is also interesting to explore other types of cross-linkers that repond to various external stimuli such as pH, enzymes, and proteins.

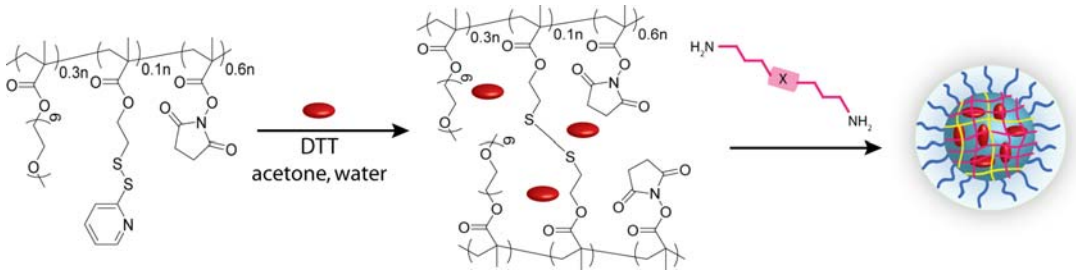

Figure 5.2: The polymer structures and cross-linked nanogels with modified cross-linkers.

To accomplish this, we hypothesize that if the cross-linking reaction occurs during the aggregation of amphiphilic polymers, then it would facilitate the nanogel formation and also provide lipophilic encapsulation in aqueous medium. To test this concept, the designed amphiphilic polymers will consist of the reactive ester groups that can be easily replaced by the cross-linker containing diamine functionalities. The cross-linking reaction will take place during the polymer aggregation. Using this concept, we can introduce various types of cross-linkers in the nanogel scaffolds. Two polymer systems are currently investigated in our research group.

In the first design, we chose *N*-hydroxysuccinimide (NHS) as the reactive esters to be incoported on the polymer pruecusors. We synthesized the amphiphilic ramdom copolymers containing 30% PEG, 60% NHS, and 10% of PDS groups. The polymer structure is shown in Figure 5.2. After initiating the nanogel formation with small amount of disulfide cross-linking reaction, the diamino cross-linker will be added to react with NHS groups to generate fully cross-linked polymer nanogels. By this methodology, we can incorporate various types of cross-linkers containing diamine functionalities for specific targeted external stimulus. We are currently optimizing this system with acetal cross-linker containing diamines to prepare cross-linked nanogels that respond to acidic condition.

In the second design, the pentafluorophenyl (PFP) ester will be used as an activated ester which is known to be replaced with amines with great fidelity. While the reactivity of PFP with amines is similar to the known NSH ester, it provides more hydrophobicity rendering the polymer precursors to form a stable aggregation without using initial disulfide bonds.

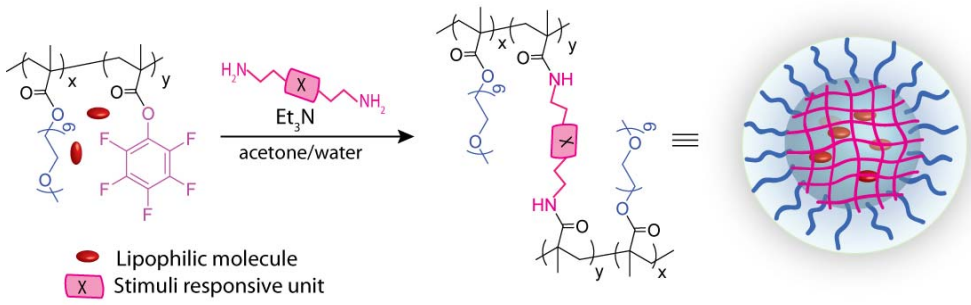

Figure 5.3: The PEG-PFP polymer structure and cystamine cross-linked nanogels.

In this design, we synthesize a random copolymer comprising PEG and PFP units as illustrated in Figure 5.3. While the PEG groups are charge neutral water soluble

units, PFPs are hydrophobic groups providing lipophilic encapsulation and are also reactive towards cross-linking amine groups. The addition of the cross-linker containing diamines to the stable polymer aggregation would result in stable cross-linked polymer nanogels. We are currently studying this system with cystamine and alkyldiamine cross-linkers. Initial findings indicate that the PEG-PFP polymers form stable self- assembies and provide lipophilic encapsulation. We are able to cross-link them with cystamine and alkyldiamine cross-linkers affording highly stable cross-linked polymer nanogels. We will ultilize this method to incorporate other cross-linker containing diamine units.

5.3 Summary

In this chapter, we summarize the key points detailed in each chapter and present the ongoing work in our laboratory on the self-cross-linked polymer nanogels. We hope that the findings of this dissertation on the new class of self-cross-linked polymer nanogels provide insights for the development of effective nanoscopic drug delivery vehicles with high stability of non-covalent lipophilic drug encapsulation.

5.4 References

1. Hamidi, M.; Azadi, A.; Rafiei, P., Hydrogel nanoparticles in drug delivery. *Adv. Drug Deliv. Rev.* **2008,** *60*, 1638-1649.

2. Kabanov, A. V.; Vinogradov, S., Nanogels as pharmaceutical carriers: Finite networks of infinite capabilities. *Angew. Chem. Int., Ed* **2009,** *48*, 5418-5429.

3. Oh, J. K.; Drumright, R.; Siegwart, D. J.; Matyjaszewski, K., The development of microgels/nanogels for drug delivery applications. *Prog. Polym. Sci.* **2008,** *33*, 448-477.

4. Oh, J. K.; Siegwart, D. J.; Lee, H.-I.; Sherwood, G.; Peteanu, L.; Hollinger, J. O.; Kataoka, K.; Matyjaszewski, K., Biodegradable nanogels prepared by atom transfer radical polymerization as potential drug delivery carriers: Synthesis, biodegradation, *in vitro* release, and bioconjugation. *J. Am. Chem. Soc.* **2007,** *129*, 5939-5945.

5. Raemdonck, K.; Demeester, J.; Smedt, S. D., Advance nanogel engineering for drug delivery. *Soft Matter* **2009,** *5*, 707-715.

6. Vinogradov, S., Nanogels in the race for drug delivery. *Nanomedicine* **2010,** *5*, 165-168.

7. Oh, J. K.; Tang, C.; Gao, H.; Tsarevsky, N.; Matyjaszewski, K., Inverse miniemulsion ATRP: A new Method for synthesis and functionalization of well-defined water-soluble/cross-linked polymeric particles. *J. Am. Chem. Soc.* **2007,** *128*, 5578-5584.

8. Ryu, J.-H.; Jiwpanich, S.; Chacko, R.; Bickerton, S.; Thayumanavan, S., Surface-functionalizable polymer nanogels with facile hydrophobic guest encapsulation capabilities. *J. Am. Chem. Soc.* **2010,** *132*, 8246-8247.

9. Ryu, J.-H.; Chacko, R. T.; Jiwpanich, S.; Bickerton, S.; Babu, R. P.; Thayumanavan, S., Self-cross-linked polymer nanogels: A versatile nanoscopic drug delivery platform. *J. Am. Chem. Soc.* **2010,** *132*, 17227-17235.

10. Jiwpanich, S.; Ryu, J.-H.; Bickerton, S.; Thayumanavan, S., Noncovalent encapsulation stabilities in supramolecular nanoassemblies. *J. Am. Chem. Soc.* **2010,** *132*, 10683-10685.

BIBLIOGRAPHY

Akiyoshi, K., deguchi, S., Moriguchi, N., Yamaguchi, S. and Sumamoto, J. (1993). "Self-aggregates of hydrophobized polysaccharides in water. Formation and characteristics of nanoparticles." Macromolecules **26**: 3062-3068.

Aliyar, H. A., Hamilton, P. D., Remsen, E. E. and Ravi, N. (2005). "Synthesis of polyacrylamide nanogels by intramolecular disulfide cross-linking." J. Bioactive Compat. Polym. **20**: 169-181.

Allen, T. M. and Chonn, A. (1987). "Large unilamellar liposomes with low uptake into the reticuloendothetial system." FEBS Lett. **223**: 42-46.

Allen, T. M. and Culis, P. R. (2004). "Drug discovery systems: Entering the mainstream." Science **303**: 1818-1822.

Amir, R. J., Pessah, N., Shamis, M. and Shabat, D. (2003). "Self-immolative dendrimers." Angew. Chem. Int., Ed. **42**: 4494-4499.

Arap, W., Pasqualini, R. and Ruoslahti, E. (1998). "Cancer treatment by targeted drug delivery to tumor vasculature in a mouse model." Science **279**: 377-380.

Baban, D. F. and Seymour, L. W. (1998). "Control of tumour vascular permeability." Adv. Drug Delivery Rev. **34**: 109-119.

Bachelder, E. M., Beaudette, T. T., Broaders, K. E., Dashe, J. and Fréchet, J. M. J. (2008). "Acetal-derivatized dextran: An acid-responsive biodegradable material for therapeutic applications." J. Am. Chem. Soc. **130**: 10494-10495.

Bae, K. H., Mok, H. and Park, T. G. (2008). "Synthesis, characterization, and intracellular delivery of reducible heparin nanogels for apoptotic cell death." Biomaterials **29**: 3376-3383.

Bae, Y. H. and Yin, H. (2008). "Stability issues of polymeric micelles " J. Control. Release **131**: 2-4.

Bae, Y. H. and Yin, H. (2008). "Stability issues of polymeric micelles." J. Controlled Release **131**: 2-4.

Bangham, A. D., Standish, M. M. and Watkins, J. C. (1965). "Diffusion of univalent ions across the lamellae of swollen phospholipids." J. Mol. Biol. **13**: 238-252.

Bao, A., Goin, B., Klipper, R., Negrete, G. and Phillips, W. T. (2004). "Direct 99m Tc labeling of pegylated liposomal doxorubicin (Doxil) for pharmacokinetic and non-invasive imageing studies." J. Pharcol. Exp. Ther. **308**: 419-425.

Bartlett, D. W., Su, H., Hildebrandt, I. J., Weber, W. A. and Davis, M. E. (2007). "Impact of tumor-specific targeting on the biodistribution and efficacy of siRNA nanoparticles measured by multimodality *in vivo* imaging." Proc. Natl. Acad. Sci. U.S.A. **104**: 15549-15554.

Batrakova, E. V. and Kabanov, A. V. (2008). "Pluronic block copolymers: Evaluation of drug delivery concept from inert nanocarriers to biological response modifiers." J. Controlled Release **130**: 98-106.

Bauhuber, S., Hozsa, C., Breunig, M. and Cöpferich, A. (2009). "Delivery of nucleic acids via disulfide-based carrier systems." Adv. Mater. **21**: 3286-3306.

Bernkop-Schnürch, A. (2005). "Thiomers: A new generation of mucoadhesive polymers." Adv. Drug Deliv. Rev. **57**: 1569-1582.

Buhleier, E., Wehner, W. and Vögtle, F. (1978). ""Cascade"-and-"nonskid-chain-like" syntheses of molecular cavity topologies." Synthesis (Mass.)(155-158).

Byrne, M. E., Park, K. and Peppas, N. A. (2002). "Molecular imprinting within hydrogels." Adv. Drug Deliv. Rev. **54**: 149-161.

Chan, Y., Wong, T., Byrne, F., Kavallaris, M. and Bulmus, V. (2008). "Acid-labile core cross-linked micelles for pH-rriggered release of antitumor drugs." Biomacromolecules **9**: 1826-1836.

Chen, H., Kim, S., He, W., Wang, H., Low, P. S., Park, K. and Cheng, J.-X. (2008). "Fast release of lipophilic agents from circulating PEG-PDLLA micelles revealed by *in vivo* förster resonance energy transfer imaging." Langmuir **24**: 5213-5217.

Chen, H., Kim, S., He, W., Wang, H., Low, P. S., Park, K. and Cheng, J.-X. (2008). "Fast release of lipophilic agents from circulating PEG-PDLLA micelles revealed by *in vivo* förster resonance energy transfer imaging." Langmuir **24**: 5213-5217.

Chen, H., Kim, S., Li, L., Wang, S., Park, K. and Cheng, J.-X. (2008). "Release of hydrophobic molecules from polymer micelles into cell membranes revealed by förster resonance energy transfer imaging." Proc. Natl. Acad. Sci. U.S.A. **105**(18): 6596-6601.

Chong, S.-F., Chandrawati, R., Städler, B., Park, J., Cho, J., Wang, Y., Jia, Z., Bulmus, V., Davis, T. P., Zelikin, A. N. and Caruso, F. (2009). "Stabilization of polymer-hydrogel capsules via thiol–disulfide exchange." Small **5**: 2601-2610.

Davis, F. F. (2002). "The origin of pegnology." Adv. Drug Deliv. Rev. **54**: 457-458.

Davis, M. E., Chen, Z. and Shin, D. M. (2008). "Nanoparticle therapeutics: An emerging treatment modality for cancer." Nat. Rev. Drug Discovery **7**: 771-782.

de Brabander-van den Berg, E. M. M. and Meijer, E. W. (1993). "Poly(propylene imine) dendrimers: Large-scale synthesis by hetereogeneously catalyzed hydrogenations." Angew. Chem. Int. Ed. **32**: 1308-1311.

de Groot, F. M. H., Albrecht, C., Koekkoek, R., Beusker, P. H. and Scheeren, H. W. (2003). "“Cascade-release dendrimers” Liberate all end groups upon a single triggering event in the dendritic core." Angew. Chem. Int., Ed. **42**: 4490-4494.

Duncan, B. "Drug polymer conjugates-Potential for improved chemotherapy." Anticancer Drugs **3**: 175-210.

Duncan, B., Kim, C. and Rotello, V. M. (2010). "Gold nanoparticle platforms as drug and biomacromolecule delivery systems." J. Controlled Release **148**: 122-127.

Duncan, R. (2003). "The dawning era of polymer therapeutics." Nat. Rev. Drug Discovery **2**: 347-360.

Duncan, R. (2006). "Polymer conjugates as anticancer nanomedicines." Nat. Rev. Cancer **6**: 688-701.

Duncan, R. and Kopecek, J. (1984). "Soluble synthetic-polymers as potential-drug carriers." Adv. Polym. Sci. **57**: 51-101.

Fang, H., Zhang, K., Shen, G., Wooley, K. L. and Taylor, J. A. (2009). "Cationic shell-cross-linked knedel-like (cSCK) nanoparticles for highly efficient PNA delivery." Mol. Pharmaceutics **6**: 615-626.

Farokhzad, O. C. and Langer, R. (2009). "Impact of nanotechnology on drug delivery." ACS Nano **3**: 16-20.

Ferrari, M. (2005). "Cancer nanotechnology: Opportunities and challenges." Nat. Rev. Cancer **5**: 161-171.

Fréchet, J. M. J. and Tomalia, D. A. (2001). Dendrimers and other dendritic polymers. chichester, New York, USA, John Wiley & Sons.

Gabizon, A. A. (2001). "Pegylated liposomal doxorubicin: Metamorphosis of an old drug into a new form of chemotherapy." Cancer Invest. **19**: 424-436.

Gabizon, A. A. (2001). "Stealth liposomes and tumor targeting: One step further in the quest for the magic bullet." Clin. Cancer Res. **7**: 223-225.

Ghosh, S., Basu, S. and Thayumanavan, S. (2006). "Simultaneous and Reversible Functionalization of Copolymers for Biological Applications." Macromolecules **39**: 5595-5597.

Gillies, E. R. and Fréchet, J. M. J. (2005). "Dendrimers and dendritic polymers in drug delivery." Drug Discovery Today **10**: 35-43.

Gillies, E. R., Goodwin, A. P. and Fréchet, J. M. J. (2004). "Acetals as pH-sensitive linkages for drug delivery." Bioconjug. Chem. **15**: 1254-1263.

Goren, D., Horowitz, A. T., Tzemach, D., Tarshish, M., Zalipsky, S. and Gabizon, A. (2000). "Nuclear delivery of doxorubicin via folate-targeted liposomes with bypass of multidrug-resistance efflux pump." Clin. Cancer Res. **6**: 1949-1957.

Gottesman, M. M., Fojo, T. and Bates, S. E. (2002). "Multidrug resistance in cancer: Role of ATP–dependent transporters." Nat. Rev. Cancer **2**: 48-58.

Gu, F., Zhang, L., Teply, B. A., Mann, N., Wang, A., Rodovic-Moreno, A. F., Langer, R. and Farokhzad, O. C. (2008). "Precise engineering of targeted nanoparticles by using self-assembled biointegrated block copolymers." Proc. Natl. Acad. Sci. U.S.A. **105**: 2586-2591.

Haag, R. (2004). "Supramolecular drug-delivery systems based on polymeric core–shell architectures." Angew. Chem., Int. Ed. **43**: 278-282.

Hamidi, M., Azadi, A. and Rafiei, P. (2008). "Hydrogel nanoparticles in drug delivery." Adv. Drug Deliv. Rev. **60**: 1638-1649.

Harris, J. M. and Chess, R. B. (2003). "Effect of pegylation on pharmaceuticals." Nat. Rev. Drug Discovery **2**: 214-221.

Hawker, C. J. and Fréchet, J. M. J. (1990). "Preparation of polymers with controlled molecular architecture. A new convergent approach to dendritic macromolecules." J. Am. Chem. Soc. **112**: 7638-7647.

Heffernan, M. J. and Murthy, N. (2009). "Disulfide-crosslinked polyion micelles for delivery of protein therapeutics." Ann. Biomed. Eng. **37**: 1993-2002.

Hong, s., Leroueil, P. R., Majoros, I. J., Orr, B. G., Baker, J. R. and Banaszak Holl, M. M. (2007). "The binding avidity of a nanoparticle-based multivalent targeted drug delivery platform " **14**: 107-115.

Iwai, K., Meada, H. and Konno, T. (1984). "Use of oily contrast medium for selective drug targeting to tumour: Enhanced therapeutic effect and x-ray image." Cancer Res. **44**: 2114-2121.

Jeong, B., Bae, Y. H., Lee, D. S. and Kim, S. W. (1997). "Biodegradable block copolymers as injectable drug-delivery systems." Nature **388**: 860-862.

Jia, Z., Wong, L., Davis, T. P. and Bulmus, V. (2008). "One-pot conversion of RAFT-generated multifunctional block copolymers of HPMA to doxorubicin conjugated acid- and reductant-sensitive crosslinked micelles." Biomacromolecules **9**: 3106-3113.

Jiang, J., Qi, B., Lepage, M. and Zhao, Y. (2007). "Polymer micelles stabilization on demand through reversible photo-cross-linking." Macromolecules **40**: 790-792.

Jiang, J. and Thayumanavan, S. (2005). "Synthesis and characterization of amine-functionalized polystyrene nanoparticles." Macromolecules **38**: 5886-5891.

Jiwpanich, S., Ryu, J.-H., Bickerton, S. and Thayumanavan, S. (2010). "Noncovalent encapsulation stabilities in supramolecular nanoassemblies." J. Am. Chem. Soc. **132**: 10683-10685.

Kabanov, A. V., Batrakova, E. V. and Alakhov, Y. (2002). "Pluronic® block copolymers for overcoming drug resistance in cancer " Adv. Drug Deliv. Rev. **54**: 759-779.

Kabanov, A. V., Nazarova, I. R., Astafieva, I. V., Batrakova, E. V., Alakhov, V. Y., Yaroslavov, A. A. and Kabanov, V. A. (1995). "Micelle formation and solubilization of fluorescent probes in poly(oxyethylene-*b*-oxypropylene-*b*-oxyethylene) solutions." Macromolecules **28**: 2303-2314.

Kabanov, A. V. and Vinogradov, S. (2009). "Nanogels as pharmaceutical carriers: Finite networks of infinite capabilities." Angew. Chem. Int., Ed **48**: 5418-5429.

Kadlubowski, S., Grobelny, J., Olejniczak, W., Cichomski, M. and Ulanski, P. (2003). "Pulses of fast electrons as a tool to synthesize poly(acrylic acid) nanogels. Intramolecular cross-Linking of linear polymer chains in additive-free aqueous solution." Macromolecules **36**: 2484-2492.

Kakizawa, Y., Harada, A. and Kataoka, K. (1999). "Environment-sensitive stabilization of core−shell structured polyion complex micelle by reversible cross-linking of the core through disulfide Bond." J. Am. Chem. Soc. **121**: 11247-11248.

Kale, T. S., Klaikherd, A., Popere, B. and Thayumanavan, S. (2009). "Supramolecular assemblies of amphiphilic homopolymers." Langmuir **25**: 9660-9670.

Kataoka, K., Harada, A. and Nagasaki, Y. (2001). "Block copolymer micelles for drug delivery: Design, characterization and biological significance." Adv. Drug Deliv. Rev. **47**: 113-131.

Kim, C. K., Ghosh, P., Pagliuca, C., Xhu, Z.-J., Menichetti, S. and Rotello, V. M. (2009). "Entrapment of hydrophobic drugs in nanoparticles monolayers with efficient release into cancer cells." J. Am. Chem. Soc. **131**: 1360-1361.

Kim, S. W., Shi, Y., Kim, J. Y., Park, K. and Cheng, J.-X. (2010). "Overcoming the barriers in micellar drug delivery: Loading efficiency, *in vivo* stability, and micelle-cell interaction." Expert Opin. Drug Deliv. **7**: 49-62.

Kim, Y. S., Gil, E. S. and Lowe, T. L. (2006). "Synthesis and characterization of thermoresponsive-co-biodegradable linear−dendritic copolymers." Macromolecules **39**: 7805-7811.

Klibanov, A. L., Maruyama, K., Torchilin, V. P. and Huang, L. (1990). "Amphipathic polyethyleneglycols effectively prolong the circulation time of liposomes." FEBS Lett. **268**: 235-237.

Koo, O. M., Rubinstein, I. and Onyuksel, H. (2005). "Role of nanotechnology in targeted drug delivery and imaging: A concise review." Nanomedicine: NBM **1**: 193-212.

Kopeček, J. (2002). "Polymer chemistry: Swell gels." Nature **417**: 388-391.

Kukowska-Latallo, J. F., Candido, K. A., Cao, Z., Nigavekar, S. S., Majoros, I. J., Thomas, T. P., Balogh, L. P., Khan, M. K. and Baker, J. R. (2005). "Nanoparticle targeting of anticancer drug improves therapeutic response in animal model of human epithelial cancer." Cancer Res. **65**: 5317-5324.

Lai, J. t., Filla, D. and Shea, R. (2002). "Functional polymers from novel carboxyl-terminated trithiocarbonates as highly efficient RAFT agents." Macromolecules **35**: 6754-6756.

Lee, C. C., MacKay, J. A., Fréchet, J. M. J. and Szoka, F. C. (2005). "Designing dendrimers for biological applications." Nat. Biotechnol. **23**: 1517-1526.

Lee, S.-M., Song, Y., Hong, B. J., MacRenaris, K. W., Mastarone, D. J., O'Halloran, T. V., Meade, T. J. and Nguyen, S. T. (2010). "Modular polymer-caged nanobins as a theranostic platform with enhanced magnetic resonance relaxivity and pH-responsive drug release." Angew. Chem. Int. Ed **49**: 9960-9964.

Leserman, L. D., Barbet, J., Kourilsky, F. and Weinstein, J. N. (1980). "Targeting to cells of fluorescent liposomes covalently coupled with monoclonal antibody or protein A." Nature **288**: 602-604.

Li, C. and wallace, S. (2008). "Polymer-drug conjugates: Recent development in clinical oncology." Adv. Drug Deliv. Rev. **60**: 886-898.

Li, F., Danquah, M. and Mahato, R. (2010). "Synthesis and characterization of amphiphilic lipopolymers for micellar drug delivery." Biomacromolecules **11**: 2610-2620.

Li, S., Szalai, M. L., Kevwitch, R. M. and McGrath, D. V. (2003). "Dendrimer disassembly by benzyl ether depolymerization." J. Am. Chem. Soc. **125**: 10516-10517.

Li, Y.-L., Zhu, L., Liu, Z., Cheng, R., Meng, F., Cui, J.-H., Ji, S.-J. and Zhong, Z. (2009). "Reversibly stabilized multifunctional dextran nanoparticles efficiently deliver doxorubicin into the nuclei of cancer cells." Angew. Chem. Int., Ed **48**: 9914-9918.

Li, Y., Lokitz, B. S., Armes, S. P. and McCormick, C. L. (2006). "Synthesis of reversible shell cross-linked micelles for controlled release of bioactive agents." Macromolecules **39**: 2726-2728.

Lipinski, C. A. (2000). "Drug-link properties and the causes of poor solubility and poor permeability." J. Pharmacol. Toxicol. Methods **44**: 235-249.

Lipinski, C. A., Lombardo, F., W., D. B. and Feeney, P. J. (2001). "Experimental and computational approaches to estimate solubility and permeability in drug discovery and development setting." Adv. Drug Deliv. Rev. **46**: 3-26.

Liu, S., Maheshwari, R. and Kiick, K. (2009). "Polymer-based therapeutics." Macromolecules **42**: 3-13.

Maeda, H., Wu, J., Sawa, T., Matsumura, Y. and Hori, K. (2000). "Tumor vascular permeability and the EPR effect in macromolecular therapeutics: A review." J. Controlled Release **65**: 271-284.

Malik, N., Evagorou, E. G. and Duncan, R. (1999). "Dendrimer-platinate: A novel approach to cancer chemotherapy." Anticancer Drugs **10**: 767-776.

Matsumura, Y. (2008). "Polymeric micellar delivery systems in oncology." Jpn. J. Clin. Oncol. **38**: 793-802.

Matsumura, Y. and Maeda, H. (1986). "A new concept of macromolecular therapies in cancer chemotherapy: Mechanism of tumortropic accumulation of proteins and the antitumor agent SMANCS." Cancer Res **6**: 6387-6392.

Miller, K., Erez, R., Segal, E., Shabat, D. and Satchi-Fainaro, R. (2009). "Targeting bone metastases with a bispecific anticancer and antiangiogenic polymer-alendronate-taxane conjugate." Angew. Chem. Int., Ed **48**: 2949-2954.

Moskaug, J. O., Sandvig, K. and Olsnes, S. (1987). "Cell-mediated reduction of the interfragment disulfide in nicked diphtheria toxin." J. Biol. Chem. **262**: 10339-10345.

Murthy, N., Thng, Y. X., Schuck, S., Xu, M. C. and Fréchet, J. M. J. (2002). "A novel strategy for encapsulation and release of proteins: Hydrogels and microgels with acid-labile acetal cross-linkers." J. Am. Chem. Soc. **124**: 12398-12399.

Newkome, G. R., Yao, Z., Baker, G. R. and Gupta, V. K. (1985). "Micelles. Part 1. Cascade molecules: A new approach to micelles. A [27]-arborol." J. Org. Chem. **50**: 2003-2004.

Oerlemans, C., Bult, W., Bos, M., Storm, G., nijsen, J. F. W. and Hennink, W. E. (2010). "Polymeric micelles in anticancer therapy: Targeting, imaging and triggered release." Pharm. Res. **27**: 2569-2589.

Oh, J. K., Bencherif, S. A. and Matyjaszewski, K. (2009). "Atom transfer radical polymerization in inverse miniemulsion: A versatile route toward preparation and functionalization of microgels/nanogels for targetd drug delivery applications." Polymer **50**: 4407-4423.

Oh, J. K., Drumright, R., Siegwart, D. J. and Matyjaszewski, K. (2008). "The development of microgels/nanogels for drug delivery applications." Prog. Polym. Sci. **33**: 448-477.

Oh, J. K., Siegwart, D. J., Lee, H.-I., Sherwood, G., Peteanu, L., Hollinger, J. O., Kataoka, K. and Matyjaszewski, K. (2007). "Biodegradable nanogels prepared by atom transfer radical polymerization as potential drug delivery carriers: Synthesis, biodegradation, *in vitro* release, and bioconjugation." J. Am. Chem. Soc. **129**: 5939-5945.

Oh, J. K., Siegwart, D. J. and Matyjaszewski, K. (2007). "Synthesis and biodegradation of nanogels as delivery carriers for carbohydrate drugs." Biomacromolecules **8**: 3326-3331.

Oh, J. K., Tang, C., Gao, H., Tsarevsky, N. and Matyjaszewski, K. (2007). "Inverse miniemulsion ATRP: A new method for synthesis and functionalization of well-defined water-soluble/cross-linked polymeric particles." J. Am. Chem. Soc. **128**: 5578-5584.

Peer, D., Karp, J. M., Hong, S., Farokhzad, O. C., Margalit, R. and Langer, R. (2007). "Nanocarriers as an emerging platform for cancer therapy." Nat. Nanotechnol **2**: 751-760.

Peer, D. and Margalit, R. (2006). "Fluoxetine and reversal of multidrug resistance." Cancer Lett. **237**: 180-187.

Raemdonck, K., Demeester, J. and Smedt, S. D. (2009). "Advance nanogel engineering for drug delivery." Soft Matter **5**: 707-715.

Ringsdorf, H. (1975). "Structure and properties of pharmacologically active polymers." J. Polym. Sci. Symp. **51**: 135-153.

Rodrigues, P. C. A., Beyer, U., Schumacher, P., Roth, T., Fiebig, H. H., Unger, C., Messori, L., Orioli, P., Paper, D. H., Mulhaupt, R. and Kratz, F. (1999). "Acid-sensitive polyethylene glycol conjugates of doxorubicin: Preparation, *in vitro* efficacy and intracellular distribution." Bioorg. Med. Chem. **7**: 2517-7524.

Ryu, J.-H., Chacko, R. T., Jiwpanich, S., Bickerton, S., Babu, R. P. and Thayumanavan, S. (2010). "Self-cross-linked polymer nanogels: A versatile nanoscopic drug delivery platform." J. Am. Chem. Soc. **132**: 17227-17235.

Ryu, J.-H., Jiwpanich, S., Chacko, R., Bickerton, S. and Thayumanavan, S. (2010). "Surface-functionalizable polymer nanogels with facile hydrophobic guest encapsulation capabilities." J. Am. Chem. Soc.(ASAP).

Ryu, J.-H., Roy, R., Ventura, J. and Thayumanavan, S. (2010). "Redox-sensitive diassembly of amphiphilic copolymer based micelles." Langmuir **26**: 7086-7092.

Safra, T., Muggia, F., Jeffers, S., Tsao-Wei, D. D., Groshen, S., Lyass, O., Henderson, R., Berry, G. and Gabizon, A. (2000). "Pegylated liposomal doxorubicin (doxil): Reduced clinical cardiotoxicity in patients reaching or exceeding cumulative doses of 500 mg/m^2." Ann. Oncol. **11**: 1029-1033.

Sanchis, J., Canal, F., Lucas, R. and Vicent, M. J. (2010). "Polymer-drug conjugates for novel melecular targets." Nanomedicine **5**: 915-935.

Satchi-Fainaro, R., Puder, M., Davies, J. W., Tran, H. T., Sampson, D. A., Greene, A. K., Corfas, G. and Folkman, J. (2004). "Targeting angiogenesis with a conjugate of HPMA copolymer and TNP-470." Nat. Med. **10**: 255-261.

Savić, R., Eisenberg, A. and Maysinger, D. (2006). "Block copolymer micelles as delivery vehicles of hydrophobic drugs: Micelle–cell interactions." J. Drug. Target., 14.

Savriar, E. N., Ghosh, S., González, D. C. and Thayumanavan, S. (2008). "Disassembly of noncovalent amphiphilic polymers with proteins and utility in pattern sensing." J. Am. Chem. Soc. **130**: 5416-5417.

Schmid, B., Chung, D.-E., Warnecke, A., Fichtner, I. and Kratz, F. (2007). "Albumin-binding prodrugs of camptothecin and doxorubicin with an Ala-Leu-Ala-Leu-linker that are cleaved by cathepsin B: Synthesis and antitumor efficacy." Bioconjug. Chem. **18**: 702-716.

Schraa, A. J., Kok, R. J., Moorlag, H. E., Bos, E. J., Proost, J. H., Meijer, D. K. F., De Leu, L. F. M. H. and Molema, G. (2002). "Targeting of RGD-modified proteins to tumor vasculature: A pharmacokinetic and cellular distribution study." Int. J. Cancer **102**: 469-475.

Sharma, P. K. and Bhatia, S. R. (2004). "Effect of anti-inflammatories on pluronic® F127: Micellar assembly, gelation and partitioning " Int. J. Pharm. **278**: 361-377.

Sisson, A. L., Steinhiber, D., Rossow, T., Welker, P., Licha, K. and Haag, R. (2009). "Biocompatible functionalized polyglycerol microgels with cell penetrating properties." Angew. Chem. Int., Ed **48**: 7540-7545.

Sivakumar, S., Bansal, V., Cortez, C., Chong, S.-F., Zelikin, A. N. and Caruso, F. (2009). "Degradable, surfactant-free, monodisperse polymer-encapsulated emulsions as anticancer drug carriers." Adv. Mater. **21**: 1820-1824.

Soni, s., Babber, A. K., Sharma, R. K. and Maitra, A. (2006). "Delivery of hydrophobised 5-fluorouracil derivative to brain tissue through intravenous route using surface modified nanogels." J. Drug. Target. **14**: 87-95.

Sutton, D., Nasongkla, N., Blanco, E. and Gao, J. (2007). "Functionalized micellar systems for cancer targeted drug delivery." Pharm. Res. **24**: 1209-1046.

Szalai, M. L., Kevwitch, R. M. and McGrath, D. V. (2003). "Geometric disassembly of dendrimers: Dendritic amplification." J. Am. Chem. Soc. **125**: 15688-15689.

Talsma, S. S., Eabensee, J., Murthy, N. and Williams, I. R. (2006). "Development and *in vitro* validation of a targeted delivery vehicle for DNA vaccines." J. Controlled Release **112**: 271-279.

Tomalia, D. A., Dewald, J., Hall, J., Kallos, G., Martin, S., Roeck, J., Ryder, J. and Smith, P. (1985). "A new class of polymers: Starburst-dendritic macromolecules." Polym. J. **17**: 117-132.

Torchilin, V. P. (2004). "Targeted polymeric micelles for delivery of poorly soluble drugs." Cell. Mol. Life Sci. **61**: 2549-2559.

Torchilin, V. P. (2005). "Recent advances with liposomes as pharmaceutical carriers." Nat. Rev. Drug Discovery **4**: 145-160.

Tyagi, R., Lala, S., Verma, A. K., Nandy, A. K., Mahto, S. B., Maitra, A. and Basu, M. K. (2005). "Targeted delivery of arjunglucoside I using surface hydrophilic and hydrophobic nanocarriers to combat experimental leishmaniasis." J. Drug. Target. **13**: 161-171.

Vinogradov, S. (2010). "Nanogels in the race for drug delivery." Nanomedicine **5**: 165-168.

Vinogradov, S., Bronich, T. K. and Kabanov, A. V. (2002). "Nanosized cationic hydrogels for drug delivery: Preparation, properties and interactions with cells." Adv. Drug Deliv. Rev. **54**: 135-147.

Wagner, V., Dullaart, A., Bock, A.-K. and Zweck, A. (2006). "The emerging nanomedicine landscape." Nat. Biotechnol. **24**: 1211-1217.

Wu, A. M. and Senter, P. D. (2005). "Arming antibodies: Prospects and challenges for immunoconjugates." Nat. Biotechnol. **23**: 1137-1146.

Yang, J., Chen, H., Vlahov, I. R., Cheng, J.-X. and Low, P. S. (2006). "Evaluation of disulfide reduction during receptor-mediated endocytosis by using FRET imaging." Prog. Polym. Sci. **103**: 13872-13877.

York, A. W., Kirkland, S. E. and McCormick, C. L. (2008). "Advances in the synthesis of amphiphilic block copolymers via RAFT polymerization: Stimuli-responsive drug and gene delivery." Adv. Drug Deliv. Rev. **60**: 1018-1036.

Zhang, L., Liu, W., Lin, L., Chen, D. and Stenzel, M. H. (2008). "Degradable disulfide core-cross-linked micelles as a drug delivery system prepared from vinyl functionalized nucleosides via the RAFT process." Biomacromolecules **9**: 3321-3331.